

P. J. DAVIDSON

PHD

2004





2004

PHD

P. J. DAVESON





This is to certify that the
dissertation entitled

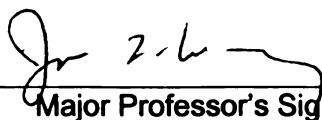
SHUTTLING OF GALECTIN-3 BETWEEN THE NUCLEUS
AND CYTOPLASM

presented by

PETER JOSEPH DAVIDSON

has been accepted towards fulfillment
of the requirements for the

Ph.D. degree in Cell and Molecular Biology



Major Professor's Signature

09/24/04

Date

PLACE IN RETURN BOX to remove this checkout from your record.
TO AVOID FINES return on or before date due.
MAY BE RECALLED with earlier due date if requested.

DATE DUE	DATE DUE	DATE DUE

SHUTTLING OF GALECTIN-3 BETWEEN THE NUCLEUS AND CYTOPLASM

By

Peter Joseph Davidson

A DISSERTATION

**Submitted to
Michigan State University
in partial fulfillment of the requirements
for the degree of**

DOCTOR OF PHILOSOPHY

Cell and Molecular Biology Program

2004

ABSTRACT

SHUTTLING OF GALECTIN-3 BETWEEN THE NUCLEUS AND CYTOPLASM

By

Peter Joseph Davidson

Galectin-3 (Gal3, Mr ~ 30 kDa) is a β -galactoside-specific lectin and a pre-mRNA splicing factor. To test if Gal3 might shuttle between the nucleus and cytoplasm, human fibroblasts (LG-1) were fused with mouse fibroblasts (3T3). The antibody NCL-GAL3, which specifically recognizes human Gal3, was used to monitor human Gal3 localization in heterodikaryons. Human Gal3 localized to both nuclei of a large percentage of heterodikaryons. Addition of leptomycin B decreased the percentage of heterodikaryons showing human Gal3 in both nuclei. In parallel, mouse 3T3 fibroblasts, expressing Gal3 were fused with fibroblasts from a Gal3-null mouse. The results from both assays suggested that galectin-3 can shuttle from one nucleus into another.

We engineered a vector that expressed a fusion protein containing Green Fluorescent Protein (GFP); bacterial maltose-binding protein (MalE); and Gal3. Analysis of fluorescence in mouse 3T3 fibroblasts transfected with this construct showed that the GFP-MalE-Gal3(1-263) fusion protein localized predominantly in the nucleus. Carboxyl-terminal truncations of the Gal3 polypeptide upstream of residue 259 showed loss of nuclear localization. Amino-terminal truncations of the same construct retained nuclear localization, and residues 228-263 of the Gal3 sequence were sufficient to direct the fusion protein into the nucleus. These results suggest that residues 228-258 of the Gal3 polypeptide are important for nuclear localization.

Incubation of fibroblasts with leptomycin B resulted in nuclear accumulation of Gal3, suggesting that nuclear export of Gal3 was mediated by the CRM1 receptor. A candidate leucine-rich nuclear export signal (NES) can be found between residues 240 and 255 of the murine Gal3 sequence. This sequence was engineered into the pRev(1.4)-GFP reporter system. Residues 240-255 of the Gal3 polypeptide exhibited nuclear export activity when tested in this system, and nuclear export of the fusion protein was sensitive to leptomycin B. Site-directed mutagenesis of Leu247 and Ile249 in the Gal3 NES decreased nuclear export activity, consistent with the notion that these two positions correspond to critical residues identified in a prototype leucine-rich NES. These results indicate that residues 240-255 of the galectin-3 polypeptide are important for nuclear export.

To my parents, to Yu-Wen,
and to all my friends and family.
Their support has made this possible.

ACKNOWLEDGEMENTS

I must first thank Dr. John Wang for his excellence as a mentor. Through him I learned a great deal about science. Moreover, Dr. Wang is a true intellectual, and this quality shined through in lab meetings and lunch discussions. These discussions were not only entertaining in their own right, but they proved to be excellent opportunities to refine the core elements of a scientific mind: critical reasoning, synthesis, and spirited debate.

I also wish to thank the members of my guidance committee for their advice and suggestions, particularly with respect to this thesis: Drs. Sue Conrad, Donna Koslowsky, and Ronald Patterson. Thanks also to Dr. Mel Schindler and Sharon Grabski for assistance and training on the InSight microscope.

Heartfelt thanks are also due to the other members of Dr. Wang's laboratory, both past and present. Dr. Eric Arnoys provided guidance and advice in the early stages of my project, but as time went on our relationship became more one of camaraderie and friendship. Eric has been an excellent example of a young faculty member for a graduate student to emulate. Thanks also to Patty Voss, who has provided advice and encouragement on many levels throughout my tour in Dr. Wang's laboratory. I also owe a great debt of thanks to Richard Gray, who has been a far better companion than I could have asked for.

The greatest thanks are due to my parents and to Yu-Wen, who have supported and encouraged me through this long process. Without them, I'd have quit long ago.

TABLE OF CONTENTS

LIST OF TABLES.....	x
LIST OF FIGURES.....	xi
LIST OF ABBREVIATIONS.....	xiii
CHAPTER 1. LITERATURE REVIEW.....	1
I. Galectins and Galectin-3.....	2
II. Nuclear Transport.....	8
Overview.....	8
Nuclear Import.....	13
Nuclear Export.....	20
Proteins.....	20
U snRNAs.....	27
tRNA.....	27
Ribosomal subunits.....	28
mRNA.....	28
Conclusions.....	30
References.....	31
CHAPTER 2. SHUTTLING OF GALECTIN-3 BETWEEN THE NUCLEUS AND CYOTPLASM.....	36
Title Page.....	37
Abstract.....	38
Introduction.....	38

Results.....	40
The monoclonal antibody NCL-GAL3 recognizes human galectin-3 but not the mouse homologue.....	40
Bead-tagging distinguishes heterodikaryons from homodikaryons.....	48
Localization of human galectin-3 to both nuclei of human-mouse heterodikaryons was partially dependent upon <i>de novo</i> protein synthesis.....	51
Localization of human galectin-3 to both nuclei of human-mouse heterodikaryons was dependent upon nuclear export.....	54
Mouse galectin-3 shuttles in 3T3-MEF Gal-3 ^{-/-} heterodikaryons.....	55
Discussion.....	63
Materials and Methods.....	66
Cell Culture and reagents.....	66
Bead-tagging and polyethylene glycol-mediated cell fusion.....	67
Immunostaining and fluorescence microscopy.....	68
Preparation of cell lysates and immunoblotting.....	69
Acknowledgements.....	71
References.....	72
CHAPTER 3. TRANSPORT OF GALECTIN-3 BETWEEN THE NUCLEUS AND CYTOPLASM I. CONDITIONS AND SIGNALS FOR NUCLEAR IMPORT.....	74
Title Page.....	75
Abstract.....	76
Introduction.....	76

Experimental Procedures.....	78
Preparation of the pEGFP-c1 vector for expression of the fusion protein GFP-MalE-Gal3.....	78
Cell culture and transfection.....	82
Fluorescence Microscopy.....	83
SDS-PAGE and immunoblotting.....	84
Results.....	85
A GFP reporter construct for the localization of Gal3.....	85
Comparison of the subcellular distribution of GFP-MalE-Gal3(1-263) and endogenous galectin-3.....	91
Effects of truncation from the carboxyl terminus on the localization of the GFP-MalE-Gal3 fusion protein.....	94
Effects of truncation of the amino-terminal domain.....	97
Discussion.....	100
References.....	107
CHAPTER 4. TRANSPORT OF GALECTIN-3 BETWEEN THE NUCLEUS AND CYTOPLASM II. IDENTIFICATION OF THE SIGNAL FOR NUCLEAR EXPORT.....	109
Title Page.....	110
Abstract.....	111
Introduction.....	112
Experimental Procedures.....	112
Site-directed mutagenesis of the putative NES sequence in the GFP-MalE-Gal3 fusion protein.....	112
The pRev(1.4)-GFP vector and variants.....	113
Cell culture and transfection.....	116

Fluorescence Microscopy.....	117
Statistical Analysis.....	117
SDS-PAGE and immunoblotting.....	117
Results.....	118
An attempt to identify the NES using the GFP-MalE-Gal3 reporter.....	118
The Rev(1.4)-GFP vector for the analysis of a functional NES.....	121
Analysis of the Gal NES in the Rev(1.4)-GFP vector.....	127
The effect of LMB on the fluorescence distribution.....	128
Site-directed mutagenesis of the Gal3 NES.....	129
Discussion.....	133
References.....	138
CHAPTER 5. CONCLUDING STATEMENTS.....	140
Concluding Statements.....	141

LIST OF TABLES

CHAPTER 1.

Table 1. Nuclear Import: Receptors & Signals.....	16
---	----

Table 2. Nuclear Export: Receptors and Signals.....	23
---	----

CHAPTER 2.

Table 1. Percent of heterodikaryons showing staining for galectin-3 in both nuclei.....	60
--	----

LIST OF FIGURES

CHAPTER 1.

Figure 1. Polypeptide architecture of the galectins.....	4
Figure 2. Schematic diagram depicting the architecture of the nuclear pore complex.....	11

CHAPTER 2.

Figure 1. Schematic illustrating the use of heterokaryons to study shuttling.....	42
Figure 2. Western blotting for galectin-3 in lysates of human HeLa cells, human LG-1 fibroblasts, and mouse 3T3 fibroblasts.....	45
Figure 3. Immunofluorescence staining for galectin-3 in fixed and permeabilized human HeLa cells and mouse 3T3 fibroblasts.....	47
Figure 4. Bead-tagged homodikaryons and heterodikaryons immunostained for human galectin-3.....	50
Figure 5. Effect of cycloheximide and leptomycin B on localization of human galectin-3 in human-mouse heterodikaryons.....	53
Figure 6. (A) Western blotting for galectin-3 in lysates of MEF Gal-3 -/- fibroblasts, MEF Gal-1 -/- fibroblasts, MEF WT fibroblasts, and mouse 3T3 fibroblasts. (B) Immunofluorescence staining for galectin-3 in fixed and permeabilized mouse 3T3 fibroblasts and MEF Gal-3 -/- fibroblasts.....	57
Figure 7. Effect of cycloheximide and leptomycin B on localization of galectin-3 in mouse 3T3-MEF Gal-3 -/- heterodikaryons.....	62

CHAPTER 3.

Figure 1. Schematic diagram illustrating the construction of the vector for the expression of the fusion protein GFP-MalE-Gal3 in mammalian cells.....	80
Figure 2. Analysis of the fusion proteins expressed from the GFP reporter vector by Western blotting.....	88

Figure 3. Representative fluorescence micrographs illustrating the N, N>C, N~C, N<C, and C labeling patterns.....	90
Figure 4. Comparison of the histograms of fluorescence patterns obtained with GFP-MalE-Gal3(1-263) with endogenous Gal3 in 3T3 fibroblasts.....	93
Figure 5. Comparison of the histograms of fluorescence distribution for GFP-MalE-Gal3(1-263) and mutants that are truncated from the carboxyl terminus.....	96
Figure 6. Comparison of the histograms of fluorescence distributions for GFP-MalE-Gal3(1-263) and mutants that are truncated from the amino terminus.....	99
Figure 7. (A) The amino acid sequence of the carboxyl-terminal 40 residues of the Gal3 polypeptide. (B) Ribbon diagram showing the three-dimensional structure of the polypeptide backbone of the CRD of Gal3.....	102

CHAPTER 4.

Figure 1. The Rev(1.4)-GFP vector.....	115
Figure 2. Comparison of the properties of GFP-MalE-Gal3 (1-263) and GFP-MalE-Gal3(1-263; L247A; I249A).....	120
Figure 3. Representative fluorescence micrographs illustrating the GFP localization patterns obtained with various test NES sequences in the pRev(1.4)-GFP vector.....	124
Figure 4. Histograms showing the distribution of the percent of cells with fluorescence patterns N, N>C, N~C, N<C, and C.....	126
Figure 5. A comparison of the histogram distributions of the percent of cells with various fluorescence patterns for Gal3 NES (WT), Gal3 NES (I244A; L247A), and Gal3 NES (L247A; I249A).....	131

LIST OF ABBREVIATIONS

ActD	actinomycin D
CD	Carboxy-terminal domain
CHX	cycloheximide
CRD	Carbohydrate Recognition Domain
DME	Dulbecco's modified Eagle's medium
FITC	fluorescein isothiocyanate
Gal1	galectin-1
Gal3	galectin-3
GFP	green fluorescent protein
GST	glutathione S-transferase
hnRNP	heterogeneous ribonucleoprotein
IBB	importin-beta binding
IgG	immunoglobulin G
L-rich NES	leucine-rich nuclear export signal
LMB	leptomycin B
MEF	mouse embryo fibroblasts
mRNA	messenger ribonucleic acid
ND	Amino-terminal domain
NES	nuclear export signal
NLS	nuclear localization signal
NPC	nuclear pore complex
PBS	phosphate-buffered saline
PCR	polymerase chain reaction
PI	propidium iodide
PKI	inhibitor of cAMP-dependent protein kinase
RNA	ribonucleic acid
RNP	ribonucleoprotein complex
rRNA	ribosomal ribonucleic acid
SMN	survival of motor neuron
snRNP	small nuclear ribonucleoprotein
TTF-1	thyroid-specific transcription factor
T-TBS	Tris-buffered saline containing 0.05% Tween 20
tRNA	transfer ribonucleic acid
WT	wild-type

Chapter 1
Literature Review

I. Galectins

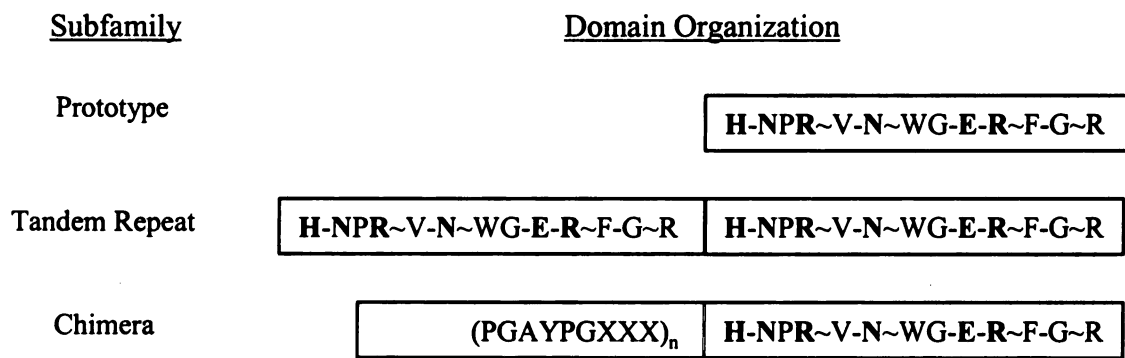
The galectin family of proteins, currently containing 14 members, is characterized by: (a) an affinity for β -galactosides; and (b) the presence of at least one conserved carbohydrate recognition domain (CRD), which is responsible for ligand binding (1; 2). The galectins are widely distributed phylogenetically, and analysis of genomic DNA sequence banks has yielded additional candidates for inclusion in the mammalian galectin family, as well as galectin candidates in plants and viruses (3). The galectins have been classified into three subfamilies based on the number and organization of their carbohydrate binding domains. The prototype subfamily contains one CRD, the chimera subfamily contains a unique proline- and glycine-rich domain fused to the amino terminus of the CRD, and the tandem repeat subfamily contains two CRDs fused in tandem (Figure 1) (4).

Galectin-3 ($M_r \sim 30$ kDa) is the sole member of the chimera subfamily (4), and consists of two domains. The amino-terminal domain (ND) of galectin-3 is unique, and contains multiple repeats of a nine-residue consensus sequence P-G-A-Y-P-G-X-X-X (1; 5). The carboxy-terminal domain (CD) of galectin-3 contains the conserved CRD. Physical-chemical studies of the galectin-3 polypeptide, as well as the two domains individually, have indicated that the ND and CD are structurally and functionally distinct (5). Differential scanning calorimetry revealed that the ND possesses a lower transition temperature than the CD (6). Accordingly, the ND exists in an unfolded, random coil state (7), while the CD exists as five-stranded and six-stranded β -sheets arranged

Figure 1. Polypeptide architecture of the galectins.

Members of the galectin family are organized into three subfamilies based upon their domain organization. Residues which are critical for carbohydrate binding are indicated in bold.

Figure 1



in a β -sandwich (8). Residues critical for carbohydrate binding lie in three strands of the six-stranded sheet (8).

Although the galectin family was so named because the minimal monosaccharide ligand is galactose, most members of the family, including galectin-3, have a much higher affinity for lactose and N-acetyllactosamine disaccharides. Galectin-3 also binds larger, multivalent oligosaccharides such as poly-N-acetyl-lactosaminoglycan, a saccharide polymer common in extracellular matrix (1; 8). Indeed, while free galectin-3 is typically monomeric (7; 9), binding to multivalent ligands induces galectin-3 to form oligomers (10). Self-association of individual ND and CRD fragments was also observed, indicating that oligomerization of galectin-3 may occur through either ND-ND or CRD-CRD association (7).

Galectin-3 is primarily intracellular, and has been documented in the nuclear and cytoplasmic compartments (11; 12; 13; 14). The subcellular distribution of galectin-3 in cultured fibroblasts is dependent upon the proliferative status of the culture. Galectin-3 in quiescent cultures is predominantly cytoplasmic, but proliferating cultures from the same cell type show predominantly nuclear localization (15). Moreover, human diploid fibroblasts have a finite replicative capacity in culture. Galectin-3 in low passage-number cultures (high replicative capacity) exhibited nuclear and cytoplasmic localization, but cultures monitored many passages later (at a low replicative capacity) exhibited primarily cytoplasmic galectin-3 (16; 17).

Several lines of evidence indicate that nuclear galectin-3 is associated with ribonucleoprotein (RNP) complexes (12). Treatment of unfixed, permeabilized fibroblasts with ribonuclease A eliminated galectin-3 staining in the nucleus, but

treatment in parallel with deoxyribonuclease I produced no such effect (12; 13). Moreover, separation of nucleoplasm by cesium sulfate centrifugation yielded galectin-3 in fractions with densities matching those reported for heterogeneous nuclear RNPs (hnRNPs) and small nuclear ribonucleoproteins (snRNPs). This observation prompted the use of depletion and reconstitution experiments to document that galectin-3 was a required factor for splicing of pre-mRNA (18).

The yeast two-hybrid system was employed to search for ligands of galectin-1, a relative of galectin-3. This assay revealed an interaction between galectin-1 and the carboxy-terminal 50 amino acids of the protein Gemin4 [Gemin4(C50)]. This interaction was confirmed using purified GST-Gemin4(C50), and in parallel galectin-3 was also shown to interact directly with GST-Gemin4(C50) (19). Gemin4 is a component of a macromolecular complex designated as the SMN (survival of motor neuron) complex (20). The SMN complex functions in both the nucleus and the cytoplasm. In the cytoplasm, the SMN complex mediates assembly of snRNP particles; in the nucleus, it delivers the snRNPs to the pre-mRNA during the early stages of spliceosome formation (21; 22). The association of galectin-3 with the SMN complex raises the possibility that galectin-3 might perform related functions in both the nucleus and the cytoplasm in the context of its role as a factor in pre-mRNA splicing.

In addition to members of the SMN complex, galectin-3 interacts with a variety of other ligands in both the nuclear and cytoplasmic compartments (5; references therein). In the nucleus, galectin-3 interacts directly with the homeodomain of the thyroid-specific transcription factor (TTF-1), stimulating the DNA-binding activity of the latter protein. This in turn increases the transcriptional activity of TTF-1, leading to increased

proliferation of thyroid cells (23). A second nuclear ligand for galectin-3 is CBP70, a lectin with affinity for glucose/N-acetylglucosamine (GlcNAc) saccharides (24). Galectin-3 was co-purified with CBP70 from HL60 cell nuclei. Interaction of the two proteins was inhibited by lactose, suggesting that lactose induces a conformational change in galectin-3 that disrupts the interaction with CBP70 (24; 25).

Galectin-3 interacts in the cytoplasm with Bcl-2 (26; 27) and synexin (28), in both cases producing an anti-apoptotic effect. Galectin-3 and Bcl-2 share two aspects of sequence similarity: the amino-terminal regions of both proteins are rich in proline, glycine, and alanine residues; and both proteins contain a motif of NWGR residues in their carboxyl termini. Mutation of the NWGR motif in galectin-3 abolished its anti-apoptotic activity. Moreover, galectin-3 binds to Bcl-2 *in vitro*, mimicking the heterodimerization of Bcl-2 family members (26; 27). Studies of apoptosis in human breast carcinoma induced by cisplatin revealed that galectin-3 translocation to the mitochondrial membranes prevented mitochondrial damage and apoptosis (28). Translocation of galectin-3 to the mitochondrial membranes was mediated by synexin, and reduction of synexin levels abrogated galectin-3 translocation and anti-apoptotic activity.

The studies reviewed here illustrate a variety of intracellular ligands and functions for galectin-3, both in the nuclear and cytoplasmic compartments. Concomitantly, they also suggest several important questions for future research on galectin-3. The interactions of galectin-3 with many of its intracellular ligands occur through protein-protein interactions rather than carbohydrate recognition (1). Therefore, one key topic for future work is to determine the significance of galectin-3 carbohydrate-binding activity

with respect to its intracellular function. Are there intracellular functions of galectin-3 which can be definitively linked to its carbohydrate-binding activity? In a related vein, it will be important to distinguish between activities which are either facilitated or inhibited by carbohydrate-binding *per se*, and activities which are facilitated or inhibited through the course of a conformational change in galectin-3 arising from carbohydrate-binding.

A second and more general point for future research is to rationalize how galectin-3 is involved in such a number and variety of activities. Is galectin-3 so multifunctional as to be involved, for example, in RNA processing, transcriptional regulation, and anti-apoptotic signaling? Alternately, might galectin-3 participate in one critical underlying process (e.g. RNA processing), through which other effects are mediated, either directly or indirectly (29)? Answers to such questions are important not only to the study of galectin-3, but in the broader context of understanding how multiple (and apparently disparate) processes in a cell might be coordinated.

II. Nuclear Transport

II.A. Overview

A defining feature of eukaryotic cells is the isolation of the nucleus as a distinct subcellular compartment by the nuclear envelope, a double-membrane system that is contiguous with the endoplasmic reticulum (30; 31). This separation necessitates a mechanism of regulated communication and transport between the nuclear and cytoplasmic compartments in order to coordinate fundamental cellular processes such as signal transduction, transcription and translation, and cell division (32; 33; 34).

Substrates for transport into (nuclear import) or out of (nuclear export) the nucleus include proteins, tRNA molecules, U snRNA molecules, and mRNA molecules (the latter two being transported as ribonucleoprotein complexes or RNPs) (30; 31; 33; 35).

Traffic between the nucleus and cytoplasm occurs through the nuclear pore complex (NPC), a large multi-protein complex which spans the nuclear envelope and provides an aqueous channel between the nuclear and cytoplasmic compartments (30; 33; 35; 36).

The vertebrate NPC is composed of approximately 30 distinct proteins termed nucleoporins (36; 37). The nucleoporins are present and arranged in groups of eight, and structural analysis has revealed that the NPC exhibits eight-fold symmetry (34; 36; 37).

As depicted in Figure 2 (34), the central feature of the NPC is the cylindrical central framework. The central framework is composed of eight spoke-like structures which form the aqueous channel through which cargo-receptor complexes traffic (33; 34; 37).

The central framework is sandwiched between the cytoplasmic and nuclear ring structures, each of which contains eight protruding filaments. The filaments of the cytoplasmic ring extend into the cytoplasm, whereas the filaments of the nuclear ring extend into the nucleoplasm but are joined at a distal ring (33; 34; 37).

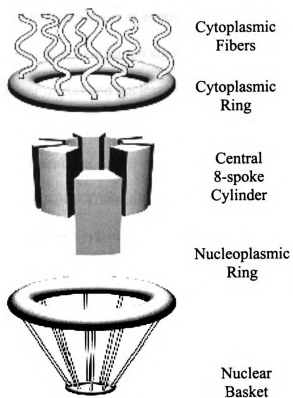
Recent evidence indicates that interactions between nucleoporins and transport receptors play a significant role in moving cargo through the NPC (33; 37; 38). These interactions occur predominantly between phenylalanine and glycine residues (so-called FG-repeats) of the nucleoporins and hydrophobic residues of transport receptors (37). Nucleoporins in the cytoplasmic fibrils bind importin-cargo complexes, possibly serving as “loading platforms” for entry to the NPC (37).

Figure 2. Schematic diagram depicting the architecture of the nuclear pore complex.

The central framework is depicted as a complex of eight cylindrical subunits located in the center of the nuclear pore. The cytoplasmic ring is depicted as a thick ring above the central framework, and cytoplasmic fibers are indicated as wavy structures. The nucleoplasmic ring is depicted as a thick ring below the central framework.

Nucleoplasmic filaments are depicted as rod-like structures extending conically from the nucleoplasmic ring, and are joined in a smaller ring at the distal end to form the nuclear basket. This figure is reproduced from reference 34.

Figure 2



Moreover, the import receptor importin- β (see below) exhibits progressively increasing affinities for nucleoporins in the cytoplasmic fibrils, the central core, and the nuclear basket, indicating that its interaction with these nucleoporins may augment the directionality of transport imposed by Ran. Conversely, the export receptor CRM1 (see below) has high affinity for a nucleoporin in the cytoplasmic fibril (33).

Most cargo destined for nuclear import or export bear signals specifying their fate. These have been dubbed nuclear localization signals (NLS) and nuclear export signals (NES), specifying nuclear import and nuclear export, respectively (34; 35). Cargo destined for transport through the NPC is first bound by at least one soluble receptor which recognizes the presence of a NLS or NES in the cargo, and mediates transport of the cargo through the NPC. Transport receptors that recognize the NES of nuclear cargo and mediate export to the cytoplasm have been termed exportins, while receptors that bind the NLS of cytoplasmic cargo and mediate import to the nucleus have been termed importins (32; 34; 39).

Implicit in this system is the principle of directionality: cargo is transported in the proper direction and released in the proper compartment. Directionality of nuclear transport is imposed by the GTPase Ran (30; 32; 34; 35; 39; 40), and is achieved by Ran mediating the interaction between cargo and receptor relative to its GTP/GDP state. In its GTP-bound state, Ran favors exportin-cargo interaction, but is antagonistic to importin-cargo interaction. Conversely, Ran in the GDP-bound state favors importin-cargo interaction, but is antagonistic to exportin-cargo interaction (41). A gradient of Ran-GTP is maintained across the nuclear envelope by the concerted action of several Ran-associated proteins. At the cytoplasmic face of the NPC, the GTPase activator

RanGAP and the coactivator Ran-binding protein 1 (RanBP1) promote GTP hydrolysis by Ran. Conversely, at the nuclear face of the NPC, exchange of GDP for GTP by Ran is promoted by the guanine exchange factor RanGEF1 (35). Through the coordinated activity of Ran, RanGAP/RanBP1, and RanGEF1, the nuclear compartment is enriched for RanGTP, while the cytoplasmic face of the NPC is enriched for RanGDP. Thus the formation of RanGDP-importin-cargo complexes is promoted at the cytoplasmic face of the NPC, while the formation of RanGTP-exportin-cargo complexes is favored at the nuclear face of the NPC (30; 35; 36; 40).

II.B Nuclear Import

Substrates destined for nuclear import are identified by the presence of a nuclear localization signal, or NLS, and include proteins and U snRNPs. In proteins, the NLS is a region of amino acids within the protein which is recognized by at least one receptor, most often referred to as importins or karyopherins (30; 31; 35; 39). Among the earliest identified NLSs (so-called “classical” NLSs) were those of the SV40 virus large T antigen (SV40 NLS) and nucleoplasmin (30). The SV40 NLS consists of the sequence **PKKKRKV** (42), and the nucleoplasmin NLS consists of the sequence **KRPAATKKAGQAKKKK** (43), where residues in bold are critical for nuclear import. Because the SV40 NLS contains one continuous stretch of basic residues, it has been dubbed a “simple” or “monopartite” NLS, while the nucleoplasmin NLS has been dubbed a “bipartite” NLS owing to the presence of two separated clusters of basic residues (35; 39).

Owing to their early identification, these “classical” motifs dominated early notions of what constituted an NLS. However, most proteins in which the NLS has been

identified do not bear a “classical” NLS, but rather variations on the theme, or even NLSs without apparent similarity to the “classical” examples (32; 35). As illustrated in Table 1, there is considerable variety among the characterized NLS motifs. For example, the HIV Rev protein NLS consists of an approximately 12-residue stretch rich in arginines, while the SR protein NLS is characterized by the presence of clustered serine and arginine residues. More divergent is the RGG domain (a 120-residue stretch of RGG repeats) of the yeast Npl3p, Nab2p, and Hrp1p proteins. Perhaps the most atypical NLSs characterized to date are the trimethyl-guanosine cap employed by the U snRNPs (see below), and the M9 signal (approximately 40 residues) identified in the hnRNP proteins A1, A2, and F, as well as the TAP protein (32; 35; references therein). The M9 signal deserves special mention because (a) it is almost entirely uncharged, and (b) it also acts as a nuclear export signal (see below). It is important to note that not only the apparent chemistry of these NLS motifs varies, but also the length of the NLS. Compare, for example, the short “classical” c-myc NLS (only three basic residues) with the 120-residue RG-rich NLS of Npl3p. Finally, many proteins which undergo nuclear import have no characterized NLS to date.

NLSs are recognized by soluble transport receptors known as importins (30; 32; 35). The prototype importins were identified as factors required for nuclear import of cargo bearing the SV40 NLS, and have been dubbed importin- α and importin- β (31; 44; 45; 46; 47; 48; 49; 50; 51). These studies revealed that importin- α binds directly to the NLS and acts as an adaptor protein to coordinate binding of importin- β , while importin- β mediates docking with and translocation through the NPC. In this scenario, importin- α and importin- β were deemed to function as a heterodimer (31; 39).

Table 1. Nuclear import receptors and the signals they recognize.

Nuclear import receptors are listed in the left column (Receptors), cargo is listed in the middle column (Cargo), and the signal recognized by each receptor is indicated in the right column (Signal Recognized). N/K, not known. Compiled from references 30, 32, 35 and references therein, except: ¹52; ²53.

Table 1
Nuclear Import: Receptors & Signals

Receptor(s)	Cargo	Signal Recognized
Importin-β/ Importin-α	SV40 T Ag nucleoplasmin c-myc	PKKKRKV KRPAATKKAGQAKKKKLD PAAKRVKLD
Importin-β	ribosomal proteins HIV Rev HTLV Rex HIV Tat histone core proteins	extended R-rich domains RQARRNRRRRWR R-rich domain R-rich domain BIB domain ¹
Transportin 1 (aka Importin-β2)	hnRNPA1, A2, F Nup153 histone core proteins	M9 (bi-directional signal) BIB domain
Transportin SR (aka Importin-β3)	SR proteins	S-, R- rich domains
Importin-β3	ribosomal proteins	N/K
Importin-5	ribosomal proteins histone core proteins	N/K BIB domain
Importin-7	ribosomal proteins histone core proteins	extended R-rich domains BIB domain
Importin-9 ¹	histone core, esp. H2B	BIB domain
Importin-11	UbcM2	N/K
Importin-β/ RIPα	replication protein A	N/K
Importin-β/ Snurportin	U snRNPs	m3G cap, Sm core proteins
Importin-β/ Importin-7	histone H1	extended basic-rich domain
NTF2	Ran	salt bridge between NTF2 and Ran ²

Soon after these seminal discoveries, a variety of importin- α (54) and importin- β (32; 35) relatives were characterized. Most importin- α relatives were characterized in humans and were identified based upon the presence of a short amino-terminal basic domain responsible for binding to importin- β (so-called importin- β binding or IBB domain), and a large domain containing Arm repeats (named for homology to the *Drosophila* protein Armadillo) responsible for NLS-binding (55; 56). All importin- α relatives function as adaptors to bridge “classical” NLS motifs with importin- β . However, nuclear import assays revealed that among the importin- α relatives, NLSs of different proteins were bound with varying efficiency, suggesting the possibility of NLS preference among the importin- α relatives (54).

Importin- β family members have been identified based upon the presence of an amino-terminal binding domain for Ran, and of 15 – 20 repeats of the HEAT motif (32; 33). In contrast to the prototype scenario of an importin- α/β heterodimer, most of the newly identified importin- β relatives mediate nuclear import without importin- α or other adaptor(s), and exhibit a wide range of cargo recognition (32; 35). Several cases of direct interaction between importin- β relatives and cargo are indicated in Table 1. Importin- β recognizes several cargos directly, including the HIV Rev and Tat proteins, ribosomal proteins, and the HTLV Rex protein, all of which appear to interact with importin- β via extended R-rich motifs. Transportin 1/importin- β 2 recognizes the M9 signal in hnRNP proteins to mediate their nuclear import, and Transportin SR/importin- β 3 recognizes serine- and arginine-rich domains in the SR proteins.

Import of histone core proteins by importin- β relatives (52) deserves special mention for two reasons. First, many importin- β relatives import histone core proteins in addition to other cargo. Importin- β , for example, imports a large variety of cargo. Second, interaction with the histone core proteins occurs through their BIB domain (52), an exceptionally basic motif distinct from the IBB domain of importin- α (57). The histone core proteins therefore highlight a trend among cargos that interact directly with importin- β family members: interaction occurs through motifs (NLS or BIB) of exceeding basic chemistry. Moreover, importin- β relatives possess different binding sites to accommodate different NLSs (52; 57), explaining how importin- β relatives (and importin- β in particular) can accommodate such a variety of cargo and signals. The question of whether importin- β relatives import multiple cargos simultaneously or if import occurs singly is still open, but evidence to date suggests that import is most efficient when cargo is handled singly (52; 57).

Two exceptions to the trend of direct interaction between importin- β relatives and cargo deserve mention. First, there are cases in which importin- β interacts with cargo through an adaptor distinct from importin- α . These include the importin- β /RIP α pathway for import of replication protein A, and the importin- β /snurportin pathway for import of U snRNPs. RIP α was identified as a required cofactor for nuclear import of the replication protein A, and is unrelated to importin- α (58). Similar to the histone core proteins, RIP α bears a domain rich in basic residues, which is likely to mediate interaction with importin- β . Snurportin was identified as a required cofactor for nuclear import of the U snRNPs (59; 60). While snurportin contains an IBB domain reminiscent

of importin- α , the two are dissimilar in all other respects. Snurportin recognizes the m3G cap structure of mature U snRNPs and represents the only case to date of an RNA structure being identified as an NLS.

The second variation is the importin- β /importin-7-mediated import of histone H1 (61). In this case, importin- β employs importin-7 as an adaptor to interact with H1. The exact mechanism of interaction is uncertain, but depends upon importin- β or importin-7 recognizing a BIB domain in H1. The likeliest scenario (61) is that importin- β and importin-7 form a loose heterodimer in the cytoplasm, which is greatly stabilized by the binding of H1, and the resulting trimeric complex is imported to the nucleus. The example of H1 import is particularly fascinating because importin-7 and importin- β function independently to import other cargo. Their cooperation represents the only case to date of two importin- β relatives acting together, with one in the role of adaptor.

As described above, directionality of nuclear transport is mediated by Ran. Ran at the cytoplasmic face of the NPC is GDP-bound, promoting importin-cargo association. However, Ran-GDP does not travel through the NPC with the importin-cargo complex, but remains associated with nucleoporins at the cytoplasmic side of the NPC (41; 53). Conversely, Ran at the nuclear face of the NPC is GTP-bound, promoting importin-cargo dissociation and subsequent exportin-cargo association. Critically, Ran-GTP associates with exportin-cargo complexes during export (see below), and upon reaching the cytoplasmic face of the NPC is acted upon by RanGAP. This results in GTP hydrolysis by Ran, leading to dissociation of the exportin-cargo complex. Since Ran-GDP is not carried back into the nucleus with importin-cargo complexes, an alternate mechanism must facilitate import of Ran back into the nucleus lest repeated rounds of nuclear import

and export deplete the nuclear pool of Ran and eventually “stall” nuclear transport. Indeed, the protein NTF2 (nuclear transport factor 2) binds cytoplasmic Ran-GDP and carries it through the NPC. At the nuclear face of the NPC, Ran-GDP is acted upon by RanGEF, effecting a replacement by Ran of GDP for GTP and resulting in dissociation of Ran-GTP from NTF2 (53). NTF2 is a small protein of approximately 15 kDa, highly conserved, and is unrelated to any of the importin family members (62; 63).

II.C Nuclear Export

Nuclear export proceeds in a manner that is analogous to import, but in many cases nuclear export is a much more complex process (30; 39). Substrates destined for nuclear export are recognized by receptors known as exportins, which together with Ran-GTP, mediate translocation of the exportin-cargo-Ran-GTP complex through the NPC. Cargos destined for nuclear export include proteins, immature U snRNAs, tRNA, ribosomal subunits, and mRNA (30; 39). Each of these cargo families proceeds through at least one unique export pathway, resulting in considerable diversity and complexity of nuclear export machinery. For the sake of simplicity, the pathway(s) responsible for export of each cargo type will be discussed individually.

II.C.1 Proteins

Most proteins identify themselves for export by the presence of a conserved nuclear export signal rich in leucine or isoleucine residues (30; 35; 39), dubbed the leucine-rich (L-rich) NES. The prototype examples of the L-rich NES were identified in the HIV Rev protein (64; 65) and the protein kinase inhibitor PKI (65). Since then, L-rich NESs have been identified in a wide variety of proteins (30; 66), and the consensus sequence of L-X_(2/3)-Z-X_(2/3)-L-X-L/I (where X represents any amino acid; Z represents

L, I, F, V, or M) has been accepted as typical of known L-rich NESs (39). The exportin responsible for conveying L-rich NES-bearing proteins out of the nucleus is CRM1 (also known as exportin-1) (67; 68), a relative of importin- β . Formation of a stable, “export competent” CRM1-mediated complex requires the presence of cargo bearing an L-rich NES, CRM1, and Ran-GTP. CRM1 is specifically inhibited by the fungal antibiotic leptomycin B, a property which figured prominently in early characterizations of CRM1 (67; 68), as well as subsequent identification of cargo exported by CRM1 (30).

As highlighted in Table 2, many proteins are exported by CRM1, and they cover a wide range of functions. One prime example is the HIV Rev protein, which functions as an adaptor to funnel HIV RNA transcripts bearing the Rev response element (RRE) into the CRM1 export pathway for transport to the cytoplasm (64). This represents a general trend of viruses in which cellular machinery is co-opted for the purpose of viral propagation. In this case, HIV benefits from “hijacking” a cellular export pathway to process its own transcripts.

Another prime example is PKI, the inhibitor of cyclic AMP-dependent protein kinase (PKA) (65). Upon stimulation by increased cAMP, the PKA holoenzyme dissociates, allowing the catalytic subunits of PKA to enter the nucleus and phosphorylate the cAMP response element binding (CREB) protein, thereby increasing transcription of genes bearing the cAMP response element (CRE) (69). To negate this effect, PKI enters the nucleus (apparently through simple diffusion, 70; 71), binds the catalytic subunits, and then funnels them into the CRM1 export pathway. In this case, the end result is a change in gene regulation by removal of a signaling kinase.

Table 2. Nuclear export receptors and the signals they recognize.

Nuclear export receptors are listed in the left column (Receptors), cargo is listed in the middle column (Cargo), and the signal recognized by each receptor is indicated in the right column (Signal Recognized). N/K, not known. Compiled from references 30, 32, 35, and references therein except: ¹72; ²67; ³73; ⁴74; ⁵75; ⁶76; ⁷77; ⁸60; ⁹66; ¹⁰78; ¹¹79; ¹²80; ¹³81; ¹⁴82; ¹⁵83.

**Table 2:
Nuclear Export: Receptors and Signals**

Proteins		
Receptor(s)	Cargo	Signal Recognized
CRM1 (aka exportin 1)	proteins containing L-rich NES Rev; PKI; IκBα; STAT1; c-Abl Snurportin	L-X _(2/3) -Z-X _(2/3) -L-X-L/I ~200 aa, regions similar to L-NES ^{1,2}
CAS (aka exportin 2)	Importin-α	~140 aa, acidic ^{3,4}
Exportin 4	eIF-5a	N/K ⁵
Transportin 2	HuR	HNS (M9-like) ⁶
Exportin 6	actin	N/K ⁷
N/K	proteins bearing M9 signal	N/K
RNA		
CRM1	immature U snRNA 43S rRNA 60S rRNA ARE-containing mRNA, via HuR assoc. w/pp32 and April	m7G cap binds CBC; CBC binds PHAX (L-NES) ⁸ N/K ⁹ subunit protein Rpl10 bound by Nmd3p (L-NES) ^{10,11} pp32/April bear L-NES
Exportin t	tRNA	Acceptor and TΨC arms, Mature 5' and 3' termini
TAP/NXF1 (aka Mex67p)	bulk mRNA via Aly/REF, SR proteins	N/K ^{9,12,13}
Transportin 2	ARE-containing mRNA, via HuR	HuR bears HNS ⁶
Exportin 5	miRNA precursor	N/K; proper end processing reqd ^{14,15}

The theme of regulating gene expression by controlling localization of signaling proteins or transcription factors has several other examples. Regulation of the NFκB/Rel family of transcription factors (84), as well as the STAT1 transcription factor (85) is accomplished through nuclear export. The inhibitor of κ B-α (IκBα) protein (84) binds NFκB/Rel proteins in the nucleus and acts as an adaptor for CRM1-mediated nuclear export. In the case of STAT1, binding to CRM1 is direct and occurs through an L-rich NES in STAT1 (85). Finally, activity of the c-Abl tyrosine kinase is also regulated by CRM1-mediated nuclear export. c-Abl contains an L-rich NES, and is exported from the nucleus in response to attachment of cells to fibronectin, indicating a shift in function of c-ABL from gene regulation in the nucleus to transduction of adhesion signals in the cytoplasm (86).

The snurportin protein, which functions as an adaptor for importin-β-mediated nuclear import of U snRNPs, is also exported from the nucleus by CRM1 (67; 72). The interaction between snurportin and CRM1 is unique because it does not occur through a typical L-rich NES, but rather through a region of approximately 200 amino acids in snurportin which contain regions of similarity to the L-rich NES. Moreover, despite its unusual mode, the interaction between snurportin and CRM1 is much stronger than that with cargos bearing the L-rich NES (72). The basis for the avidity of snurportin-CRM1 interaction compared to L-rich NES-CRM1 interaction is unclear, but one possibility is that several of the “imperfect” L-rich NES regions in snurportin might jointly interact with CRM1, resulting in an interaction that is stronger than a single “perfect” NES (72). This issue will likely be resolved only through improved structural knowledge of the interaction between snurportin and CRM1.

Importin- α is a prototype example of proteins that are exported by receptors other than CRM1 (30; 32; 35). Importin- α is the sole substrate of the CAS receptor, which behaves similarly to CRM1 and is also an importin- β relative (73; 74). Like CRM1, CAS requires Ran-GTP to mediate nuclear export of importin- α , but the mode of interaction between CAS and importin- α is unique and depends upon an acidic region of approximately 140 amino acids near the carboxyl terminus of importin- α . Intriguingly, importin- α bears a sequence of amino acids with homology to the L-rich NES, yet failed to interact with CRM1 either *in vitro* or *in vivo* (73). This highlights the critical point that “predicting” the presence of an L-rich NES in a protein based on sequence alone is error-prone (30). Indeed, both importin- α and importin- β bear sequences similar to the consensus L-rich NES, yet neither is exported by CRM1. Importin- β exits the nucleus in association with Ran-GTP and accesses the NPC directly, migrating through the pore by interacting with nucleoporins (30; references therein).

The eukaryotic translation initiation factor 5A (eIF-5A) is exported by exportin 4 (75), an importin- β relative. Like CRM1, exportin 4 requires Ran-GTP to form an export-competent complex with eIF-5A, but eIF-5A does not possess a typical L-rich NES. Instead, a unique modification of a lysine residue to hypusine (75; references therein) dramatically enhances the interaction between exportin 4 and eIF-5A. Moreover, the site of this modification is located in a highly exposed and flexible region of eIF-5A, suggesting that the hypusine modification makes direct contact with exportin 4. The biological significance of the exportin 4 pathway and the eIF-5A protein are not understood, but Lipowsky *et al.* have suggested that eIF-5A might function as an export adaptor or chaperone for RNA (75).

Nuclear export of actin is mediated by exportin 6 (77), an importin- β relative. Actin nuclear export requires Ran-GTP, as well as an interaction between actin and profilin, which binds actin monomers and suppresses spontaneous actin polymerization. Exportin 6 interacts with the actin-profilin complex much more avidly than it does with either component alone, suggesting that profilin acts as an adaptor between actin monomers and exportin 6. Entry of actin monomers into the nucleus is likely to occur following cell division, when they are packaged into daughter nuclei during regeneration of the nuclear envelope. Were the actin monomers to achieve sufficient concentration inside the nucleus, they would polymerize into cytotoxic aggregates. Exportin 6 therefore plays a key role in protecting cells from actin toxicity, and it is not surprising that exportin 6-mediated nuclear export of actin is conserved between vertebrates and insects (77).

Nuclear export of the protein HuR is more complex, in that it accesses two export pathways: one mediated by CRM1, and the other mediated by transportin 2, a relative of transportin 1 (76). HuR accesses these pathways by different mechanisms, and the pathways appear to be mutually exclusive. Access to the CRM1 export pathway occurs through HuR interaction with the nuclear phosphoproteins pp32 and April, both of which bear L-rich NESs (76). In this fashion, HuR “piggy-backs” into the CRM1 export pathway via its interactions with pp32 and April. Alternately, HuR can access the transportin 2 export pathway directly via its HuR nuclear shuttling (HNS) region (76; 87), a region which bears moderate sequence similarity to the M9 signal of hnRNPA1. As discussed below, HuR recognizes AU-rich elements (AREs) in the mRNAs of early

response genes, and participates in exporting ARE-bearing mRNAs from the nucleus (see below) (76).

II.C.2 U snRNAs

CRM1 mediates nuclear export of immature U snRNAs. U snRNAs are transcribed in the nucleus, and most U snRNAs require export to the cytoplasm where they associate with Sm core proteins and complete their maturation (60). Immature U transcripts are bound prior to export by the cap binding complex (CBC) which recognizes the monomethyl m7G cap at the 5' end of the transcript. The CBC is bound by the protein PHAX (phosphorylated adaptor for RNA export), which bears an L-rich NES. PHAX thus serves as an adaptor to facilitate interaction of the U-m7G-CBC complex with CRM1 (60).

II.C.3 tRNA

Export of tRNA is mediated by exportin-t, another relative of importin- β (88). All tRNAs are transcribed in the nucleus, and prior to export undergo a series of modifications including 5' and 3' end trimming. Exportin-t affinity for tRNA is vastly improved by the presence of proper 5' and 3' ends, correct tRNA folding, and base modifications (30; 35; 88), suggesting that Exportin-t acts not only as an export receptor, but also as a final checkpoint for proper maturation of the tRNA prior to export. Exportin-t is unique because it does not employ an adaptor to interact with tRNA, whereas all other export receptors that manage RNA cargos employ at least one adaptor (see Table 2).

II.C.4 Ribosomal subunits

Ribosomal subunits are assembled in the nucleolus, from which they are exported to the cytoplasm and assembled into functional ribosomes (66; 78; 79). The mechanism of export of ribosomal subunits to the cytoplasm remains incompletely understood, but recent experiments have indicated a role for CRM1 in export of the 60S subunit. 60s rRNA transcripts are bound in the nucleolus by the ribosomal subunit protein Rpl10p, which is in turn bound by the protein Nmd3p. Nmd3p bears two L-rich NESs, and apparently functions as an adaptor between the Rpl10p/60S transcript and CRM1 (78; 79). Export of the 43S ribosomal subunit requires the presence of Ran-GTP and is sensitive to mutations in CRM1, indicating that 43S subunits may be exported through the CRM1 pathway (66). How the 43S subunit might interact with CRM1 remains to be demonstrated.

II.C.5 mRNA

Most poly-adenylated transcripts (bulk mRNA) are exported by the protein TAP/NXF1 (Mex67p in yeast) (80; 81; 89). TAP was originally identified as a cellular factor responsible for binding the constitutive transport element in retroviral RNAs and exporting them to the cytoplasm (81; references therein). TAP is a member of the nuclear export factor (NXF) family of proteins, and is unrelated to importin- β (89). TAP acts as a heterodimer with the cofactor p15, and TAP/p15 heterodimers interact directly with nucleoporins in order to traverse the NPC. The interaction of TAP/p15 with mRNA occurs through RNA-binding proteins which serve as adaptors between the mRNA and TAP/p15 (80; 89).

Two examples of adaptor proteins for TAP/p15 have been characterized. The REF protein (also known in metazoans as Aly) is deposited upon pre-mRNAs during splicing as a member of a protein complex situated upstream of the junction between two exons (termed the exon-exon junction complex, EJC) (89; 90; references therein). REF can interact directly with TAP/p15, and has been proposed to act as an adaptor to link spliced mRNAs into the TAP/p15 export pathway (reviewed in 89).

The other adaptors for TAP/p15 are the shuttling serine/arginine-rich splicing factors (SR proteins) 9G8 and SRp20 (81). These SR proteins shuttle between the nucleus and cytoplasm, and interact directly with TAP. 9G8 and SRp20 bind a consensus 22-nucleotide export element present in many mRNAs (91), and once bound to the export element serve as adaptors to bridge their transcript to TAP/p15.

In contrast to TAP-mediated export of bulk mRNA, transcripts bearing AU-rich elements (AREs) are bound by the protein HuR and funneled into two pathways distinct from TAP/p15 (76). As described above, HuR bears the HNS signal, which is recognized by the export receptor transportin 2. Thus, HuR can function as an adaptor to funnel ARE-bearing transcripts into the transportin 2 export pathway. Alternately, HuR also interacts with the proteins pp32 and April, both of which bear L-rich NESs and are ligands for CRM1. By interacting with pp32 and April, HuR can funnel ARE-containing transcripts into the CRM1 pathway. AREs are commonly found in transcripts of early response genes, and access of HuR to two distinct export pathways might ensure rapid expression of these genes despite a variety of cellular conditions.

III. Conclusions

The field of nuclear transport has progressed considerably in terms of descriptive and mechanistic studies. Descriptive studies have documented nuclear import, export, or shuttling of many substrates, and in many cases mechanistic studies have identified the machinery responsible for these activities. However, the vast majority of studies to date have examined the trafficking of substrates individually. Thus, there is no notion of the “scale” of nuclear transport. How many substrates undergo nuclear import or export? How many import and export receptors are there? Questions such as these represent the next level of study for the field of nuclear transport: to understand the total number and identity of substrates that traffic between the nucleus and cytoplasm. Such knowledge will facilitate the placement of nuclear transport into the context of multiple biological pathways, and will illuminate the functional significance of nuclear transport at the level of a whole cell.

References

1. Krzeslak, A. and Lipinska, A. (2004) *Cell. Mol. Biol. Lett.* **9**(2), 305-328.
2. Barondes, S.H. *et al.* (1994) *Cell* **76**, 597-598.
3. Cooper, D.N.W., and Barondes, S.H. (1999) *Glycobiology* **9**, 979-984.
4. Hirabayashi, J., *et al.* (2002) *Biochim. Biophys. Acta.* **1572**, 232-254.
5. Wang, J.L., Gray, R.M., Haudek, K.C., and Patterson, R.J. (2004) *Biochim. Biophys. Acta.* **1673**, 75-93.
6. Agrwal, N., Sun, Q., Wang, S.-Y., and Wang, J.L. (1993) *J. Biol. Chem.* **268**(20), 14932-14939.
7. Birdsall, B., Feeney, J., Burdett, I.D.J., Bawumia, S., Barboni, E.A.M., and Hughes, R.C. (2001) *Biochemistry* **40**, 4859-4866.
8. Seetharaman, J., Kanigsberg, A., Slaaby, R., Leffler, H., Barondes, S.H., and Rini, J.M. (1998) *J. Biol. Chem.* **273**(21), 13047-13052.
9. Morris, S., Ahmad, N., Andre, S., Kaltner, H., Gabius, H.J., Brenowitz, M., and Brewer, C.F. (2004) *Glycobiology* **14**, 293-300.
10. Ahmad, N., *et al.* (2004) *J. Biol. Chem.* **279**, 10841-10847.
11. Moutsatsos, I.K., Davis, J.M., and Wang, J.L. (1986) *J. Cell Biol.* **102**, 477-483.
12. Laing, J.G. and Wang, J.L. (1988) *Biochemistry* **27**, 5329-5334.
13. Hubert, M. and Wang, S.Y. (1995) *Exp. Cell Res.* **220**, 397-406.
14. Craig, S.S., Krishnaswamy, P., Irani, A.M., Kepley, C.L., Liu, F.-T., and Schwartz, L.B. (1995) *Anat. Rec.* **242**, 211-219.
15. Moutsatsos, I.K., Wade, M., Schindler, M., and Wang, J.L. (1987) *Proc. Natl. Acad. Sci. U.S.A.* **84**, 6452.
16. Hamman, K.K., Cowles, E.A., Wang, J.L., and Anderson, R.L. (1991) *Exp. Cell Res.* **196**, 82-91.
17. Openo, K.P., Kadrofske, M.M., Patterson, R.J., and Wang, J.L. (2000) *Exp. Cell Res.* **255**, 278-290.

18. Dagher, S.F., Wang, J.L., and Patterson, R.J. (1995) *Proc. Natl. Acad. Sci. U.S.A.* **92**, 1213-1217.
19. Park, J.W., Voss, P.G., Grabski, S., Wang, J.L., and Patterson, R.J. (2001) *Nucleic Acids Res.* **29**, 3595-3602.
20. Charroux, B., Pellizzoni, L., Perkinson, R.A., Yong, J., Shevchenko, A., Mann, M., and Dreyfuss, G. (2000) *J. Cell Biol.* **148**, 1177-1186.
21. Fischer, U., Qing, L., and Dreyfuss, G. (1997) *Cell* **90**, 1023-1029.
22. Pellizzoni, L., Naoyuki, K., Charroux, B., and Dreyfuss, G. (1998) *Cell* **95**, 615-624.
23. Paron, I., *et al.* (2003) *Biochem. Biophys. Res. Commun.* **302**, 545-553.
24. Seve, A.P., Felin, M., Doyennette-Moyne, M.A., Sahraoui, T., Aubery, M., and Hubert, J. (1993) *Glycobiology* **3**, 23-30.
25. Rousseau, C., Muriel, M.-P., Musset, M., Botti, J., and Sève, A.-P. (2000) *J. Cell. Biochem.* **78**, 638-649.
26. Yang, R.-Y., Hsu, D.K., and Liu, F.-T. (1996) *Proc. Natl. Acad. Sci. U.S.A.* **93**, 6737-6742.
27. Akahani, S., Nangia-Makker, P., Inohara, H., Kim, H.R., and Raz, A. (1997) *Cancer Res.* **57**, 5272-5276.
28. Yu, F., Finley, R.L., Raz, A., and Kim, H.-R.C. (2002) *J. Biol. Chem.* **277**, 15819-15827.
29. Liu, F.-T., Patterson, R.J., and Wang, J.L. (2002) *Biochim. Biophys. Acta.* **1572**, 263-273.
30. Görlich, D. and Kutay, U. (1999) *Annu. Rev. Cell Dev. Biol.* **15**, 607-660.
31. Nigg, E.A. (1997) *Nature* **386**, 779-787.
32. Chook, Y.M. and Blobel, G. (2001) *Curr. Op. Struc. Biol.* **11**, 703-715.
33. Bednenko, J., Cingolani, G., and Gerace, L. (2003) *Traffic* **4**, 127-135.
34. Bayliss, R., Corbett, A.H., and Stewart, M. (2000) *Traffic* **1**, 448-456.
35. Nakielnny, S. and Dreyfuss, G. (1999) *Cell* **99**, 677-690.
36. Weis, K. (2002) *Curr. Op. Cell Biol.* **14**, 328-335.

37. Fahrenkrog, B., Koser, J., and Aeby, U. (2004) *Trends Biochem. Sci.* **29**(4), 175-182.
38. Powers, M.A. and Dasso M. (2004) *Nature Cell Biol.* **6**(2), 82-86.
39. Izaurralde, E. and Adam, S. (1998) *RNA* **4**, 351-364.
40. Adam, S.A. (1999) *Curr. Op. Cell Biol.* **11**, 402-406.
41. Görlich, D., Panté, N., Kutay, U., Aeby, U., and Bischoff, F.R. (1996) *EMBO J.* **15**(20), 5584-5594.
42. Kalderon, D., Roberts, B.L., Richardson, W.D., and Smith, A.E. (1984) *Cell* **39**, 499-509.
43. Dingwall, C., Sharnick, S.V., and Laskey, R.A. (1982) *Cell* **30**, 449-458.
44. Görlich, D., Prehn, S., Laskey, R.A., and Hartmann, E. (1994) *Cell* **79**, 767-778.
45. Görlich, D., Vogel, F., Mills, A.D., Hartmann, E., and Laskey, R.A. (1995) *Nature* **377**, 246-248.
46. Radu, A., Blobel, G, and Moore, M.S. (1995) *Proc. Natl. Acad. Sci. U.S.A.* **92**, 1769-1773.
47. Imamoto, N. *et al.* (1995) *EMBO J.* **14**, 3617-3626.
48. Imamoto, N., Tachibana, T., Matsubae, M. and Yoneda, Y.A. (1995) *J. Biol. Chem.* **270**, 8559-8565.
49. Görlich, D., *et al.* (1995) *Curr. Biol.* **5**, 383-392.
50. Weis, K., Mattaj, I.W., and Lamond, A.I. (1995) *Science* **268**, 1049-1053.
51. Chi, N.C., Adam, E.J., and Adam, S.A. (1995) *J. Cell Biol.* **130**, 265-274.
52. Mühlhäusser, P, Müller, E.C., Otta, A., and Kutay, U. (2001) *EMBO Rep.* **2**, 690-696.
53. Ribbeck, K., Lipowsky, G., Kent, H.M., Stewart, M., and Görlich, D. (1998) *EMBO J.* **17**(22), 6587-6598.
54. Kohler, M. *et al.* (1999) *Mol. Cell Biol.* **19**(11), 7782-7791.
55. Romanelli, M.G. and Morandi, C. (2002) *Eur. J. Biochem.* **269**, 2727-2734.
56. Dingwall, C. and Laskey, R.A. (1998) *Curr. Biol.* **8**, R922-R924.

57. Jäkel, S. and Görlich, D. (1998) *EMBO J.* **17**, 4491-4502.
58. 58, D., Görlich, D., Laemmli, U.K., and Adachi, Y. (1999) *EMBO J.* **18**, 4348-4358.
59. Huber, J., Cronshagen, U., Kadokura, M., Marshallsay, C., Wada, T., Sekine, M., and Luhrmann, R. (1998) *EMBO J.* **17**, 4114-4126.
60. Will, C.L. and Lührmann, R. (2001) *Curr. Op. Cell Biol.* **13**, 290-301.
61. Jäkel, S., Albig, W., Kutay, U., Bischoff, F.R., Schwamborn, K., Doenecke, D., and Görlich, D. (1999) *EMBO J.* **18**, 2411-2423.
62. Moore, M.S. and Blobel, G. (1994) *Proc. Natl. Acad. Sci. U.S.A.* **91**, 10212-10216.
63. Paschal, B.M. and Gerace, L. (1995) *J. Cell Biol.* **129**, 925-937.
64. Fischer, U., Huber, J., Boelens, W.C., Mattaj, I.W., and Lührmann, R. (1995) *Cell* **82**, 475-483.
65. Wen, W., Meinkoth, J.L., Tsien, R.Y., and Taylor, S.S. (1995) *Cell* **82**, 463-473.
66. Lei, E.P and Silver, P.A. (2002) *Dev. Cell* **2**, 261-272.
67. Fornerod, M., Ohno, M., Yoshida, M., and Mattaj, I.W. (1997) *Cell* **90**, 1051-1060.
68. Ossareh-Nazari, B., Bachelierie, F., and Dargemont, C. (1997) *Science* **278**, 141-144.
69. Alberts, B., Bray, D., Lewis, J., Raff, M., Roberts, K., and Watson, J.D. (1994) *Molecular Biology of the Cell*. Garland Publishing, 740-741.
70. Fantozzi, D.A., Harootunian, A.T., Wen, W., Taylor, S.S., Feramisco, J.R., Tsien, R.Y., and Meinkoth, J.L. (1994) *J. Biol. Chem.* **269**(4), 2676-2686.
71. Wiley, J.C., Wailes, L.A., Idzerda, R.L., and McKnight, G.S. (1999) *J. Biol. Chem.* **274**(10), 6381-6387.
72. Paraskeva, E. *et al.* (1999) *J. Cell Biol.* **145**(2), 255-264.
73. Herold, A., Truant, R., Wiegand, H., and Cullen, B.R. (1998) *J. Cell Biol.* **143**(2), 309-318.
74. Kutay, U., Bischoff, F.R., Kostka, S., Kraft, R., and Görlich, D. (1997) *Cell* **90**, 1061-1071.
75. Lipowsky, G. *et al.* (2000) *EMBO J.* **19**(16), 4362-4371.

76. Gallouzi, I.-E. and Steitz, J.A. (2001) *Science* **294**, 1895-1901.
77. Stüven, T., Hartmann, E., and Görlich, D. (2003) *EMBO J.* **22**(21), 5928-5940.
78. Ho, J.H.-N., Kallstrom, G., and Johnson, A.W. (2000) *J. Cell Biol.* **151**(5), 1057-1066.
79. Gadai, O., Strauß, D., Kessl, J., Trumpower, B., Tollervey, D., and Hurt, E. (2001) *Mol. Cell. Biol.* **21**(10), 3405-3415.
80. Herold, A., Teizeira, L., and Izaurralde, E. (2003) *EMBO J.* **22**(10), 2472-2483.
81. Huang, Y., Gattoni, R., Stévenin, J., and Steitz, J.A. (2003) *Mol. Cell* **11**, 837-843.
82. Lund, E., Güttinger, S., Calado, A., Dahlberg, J.E., and Kutay, U. (2004) *Science* **303**, 95-98.
83. Yi, R., Qin, Y., Macara, I.G., and Cullen, B.R. (2003) *Genes Dev.* **17**, 3011-3016.
84. Lee, S.-H. and Hannink, M. (2001) *J. Biol. Chem.* **276**(26), 23599-23606.
85. McBride, K., McDonald, C., and Reich, N.C. (2000) *EMBO J.* **19**(22), 6196-6206.
86. Taagepera, S., McDonald, D., Loeb, J.E., Whitaker, L.L., McElroy, A.K., Wang, J.Y.Y., and Hope, T.J. (1998) *Proc. Natl. Acad. Sci. U.S.A.* **95**, 7457-7462.
87. Fan, X.C. and Steitz, J.A. (1998) *EMBO J.* **17**, 3448-3460.
88. Kutay, U., Lipowsky, G., Izaurralde, E., Bischoff, F.R., Schwarzmaier, P., Hartmann, E., and Görlich, D. (1998) *Mol. Cell* **1**, 359-369.
89. Erkmann, J.A. and Kutay, U. (2004) *Exp. Cell Res.* **296**, 12-20.
90. Reed, R. and Hurt, E. (2002) *Cell* **108**, 523-531.
91. Huang, Y. and Steitz, J.A. (2001) *Mol. Cell* **7**, 899-905.

Chapter 2

Shuttling of Galectin-3 between the Nucleus and Cytoplasm

Shuttling of Galectin-3 between the Nucleus and Cytoplasm

**Peter J. Davidson¹, Michael J. Davis², Ronald J. Patterson²,
Marie-Anne Ripoche³, Françoise Poirier⁴, and John L. Wang^{5*}**

¹Cell and Molecular Biology Program, ²Department of Microbiology, ⁵Department of Biochemistry, Michigan State University, East Lansing, MI 48824 USA;

³INSERM 257, ICGM, Paris, France, ⁴Institut Jacques Monod, 75251 Paris Cedex 05, France.

Peter Davidson was responsible for all aspects of the experimental work reported in the figures and tables of this chapter. This included the design of the experiments, data collection, and interpretation. Michael Davis, an undergraduate at Michigan State, carried out the experiments using cells derived from the galectin-null mutant mice. This was done under the direct supervision of Peter Davidson. Drs. M.-A. Ripoche and F. Poirier generated the original galectin-null mice and provided the fibroblasts used in the present experiments. Drs. Ron Patterson and John Wang are faculty members in whose laboratories the experiments were performed.

Abstract

In previous studies, we documented that galectin-3 ($M_r \sim 30,000$) is a pre-mRNA splicing factor. Recently, galectin-3 was identified as a component of a nuclear and cytoplasmic complex, the SMN complex, through its interaction with Gemin4. To test the possibility that galectin-3 may shuttle between the nucleus and the cytoplasm, human fibroblasts (LG-1) were fused with mouse fibroblasts (3T3). The monoclonal antibody NCL-GAL3, which recognizes human galectin-3 but not the mouse homologue, was used to monitor the localization of human galectin-3 in heterodikaryons. Human galectin-3 localized to both nuclei of a large percentage of heterodikaryons. Addition of the antibiotic leptomycin B, which inhibits nuclear export of galectin-3, decreased the percentage of heterodikaryons showing human galectin-3 in both nuclei. In a parallel experiment, mouse 3T3 fibroblasts, which express galectin-3, were fused with fibroblasts derived from a mouse in which the galectin-3 gene was inactivated. Mouse galectin-3 localized to both nuclei of a large percentage of heterodikaryons. Again, addition of leptomycin B restricted the presence of galectin-3 to one nucleus of a heterodikaryons. The results from both heterodikaryon assays suggest that galectin-3 can exit one nucleus, travel through the cytoplasm, and enter the second nucleus, matching the definition of shuttling.

Introduction

Galectin-3 is a member of a family of proteins, defined on the basis of structural analysis and binding specificity studies, that: (a) bind β -galactosides; and (b) share significant sequence similarity in the carbohydrate-binding site (1). On the basis of

immunofluorescence and immunoelectron microscopy, as well as quantitative immunoblotting of subcellular fractions, it has been documented that galectin-3 was localized in the nucleus and cytoplasm of cells (2; 3; 4). Using a cell-free assay for the splicing of pre-mRNA, we have previously shown that galectin-3 is a required splicing factor (5). More recently, we have found that galectin-3 interacts with Gemin4 (6), a component of a macromolecular complex designated as the SMN (survival of motor neuron) complex (7). Moreover, co-immunoprecipitation experiments demonstrated that galectin-3 is a *bona fide* member of the SMN complex. The SMN complex functions in both the nucleus and the cytoplasm. In the cytoplasm, the SMN complex mediates assembly of small nuclear ribonucleoprotein (snRNP) particles; in the nucleus, it delivers the snRNPs to the pre-mRNA during the early stages of spliceosome formation (8; 9).

Nucleocytoplasmic shuttling is typically defined as the repeated bi-directional movement of a protein across the nuclear membranes (10). The association of galectin-3 with the SMN complex raises the possibility that galectin-3 might perform related functions in both the nucleus and the cytoplasm and that it might shuttle between the two compartments. To test directly whether galectin-3 can shuttle, we monitored the localization of galectin-3 in two different types of heterokaryon systems: (a) human-mouse heterodikaryons; and (b) mouse-mouse heterodikaryons, in which one of the cell types contained a null mutation in the galectin-3 gene (11). In the human-mouse heterodikaryons, we monitored the localization of human galectin-3 using a mouse monoclonal antibody that recognized human galectin-3 but not the mouse homologue. In the mouse-mouse heterodikaryons, we monitored the localization of mouse galectin-3

using a rat monoclonal antibody directed against galectin-3. The results obtained from both systems suggest that galectin-3 does shuttle between the nucleus and the cytoplasm.

Results

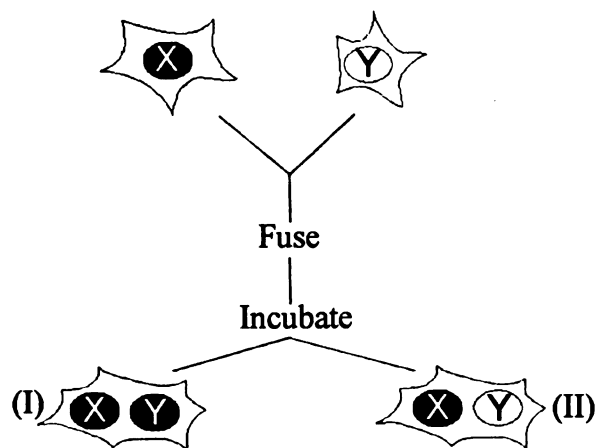
The monoclonal antibody NCL-GAL3 recognizes human galectin-3 but not the mouse homologue

The experimental strategy used to test for shuttling of galectin-3 is depicted in Figure 1. Heterokaryons were generated through fusion of two cell types: human LG-1 fibroblasts (cell X) and mouse 3T3 fibroblasts (cell Y). The presence of human galectin-3 in both nuclei of a heterodikaryon (path I) could arise due to nuclear import from three sources: (a) human galectin-3 in the cytoplasm; (b) newly synthesized human galectin-3; and (c) human galectin-3 from the human nucleus. The last of these three mechanisms requires export of human galectin-3 from the human nucleus into the cytoplasm of the heterodikaryon and subsequent import into the mouse nucleus. Therefore, if shuttling makes a significant contribution to the percentage of heterodikaryons exhibiting human galectin-3 staining in both nuclei, it should be sensitive to inhibition of nuclear export. On this basis, we expected the percentage of heterodikaryons showing human galectin-3 in both nuclei to be decreased and, correspondingly, the percentage of heterodikaryons showing galectin-3 in only one nucleus (path II) to be increased by inhibitors of nuclear export. This experimental scheme has two key requirements. First, we needed to be able

Figure 1. Schematic illustrating the use of heterokaryons to study shuttling.

Heterokaryons were generated through fusion of two cell types, for example: human LG-1 (cell X) and mouse 3T3 fibroblasts (cell Y). The presence of human galectin-3 in both nuclei of a heterodikaryon (path I) could be due to three mechanisms: (a) human galectin-3 originally in the cytoplasm of LG-1 cells; (b) newly synthesized human galectin-3; and (c) galectin-3 originally from the human nucleus. Mechanism (c) requires that human galectin-3 first gets exported from the human nucleus into the cytoplasm of the heterodikaryon and subsequently gets imported into the mouse nucleus. Path II depicts a heterodikaryon in which only one of the nuclei contains human galectin-3. This general scheme was also applied to the second cell pair in our test of galectin-3 shuttling: mouse 3T3 fibroblasts expressing galectin-3 (cell X) and MEF Gal-3 ^{-/-} cells not expressing galectin-3 (cell Y).

Figure 1



to distinguish heterodikaryons (human-mouse cell hybrids) from homodikaryons (human-human and mouse-mouse cell hybrids). This was accomplished by tagging the two cell types with distinguishable microsphere beads prior to fusion (see below). Second, we needed to be able to immunostain for human galectin-3 with an antibody that fails to recognize mouse galectin-3.

When lysates of human cells were subjected to immunoblotting with the mouse monoclonal antibody NCL-GAL3, a single polypeptide ($M_r \sim 29,000$) corresponding to the mobility of human galectin-3 was observed (Figure 2, panel A, lanes 1 and 2). In contrast, no polypeptide band could be detected when NCL-GAL3 was used to blot a corresponding lysate derived from mouse 3T3 fibroblasts (Figure 2, panel A, lane 3). The presence of galectin-3 in the mouse cell lysate was ascertained by blotting with anti-Mac-2, a rat monoclonal antibody directed against galectin-3 (Figure 2, panel B, lane 3). The appearance of mouse galectin-3 at a higher molecular weight than human galectin-3 (Figure 2, panel B, lanes 1 – 3) is consistent with the difference in the lengths of the respective polypeptide chains, as verified by cDNA sequencing. These results suggest that the mouse monoclonal antibody NCL-GAL3 recognizes human galectin-3 but not the mouse homologue.

This conclusion was substantiated by immunofluorescence staining of fixed and permeabilized cells. NCL-GAL3 yielded strong staining in HeLa cells but not in 3T3 cells (Figure 3, panels A and C). Again, the presence of galectin-3 in both cell types was verified by staining with anti-Mac-2 (Figure 3, panels E and G). In these experiments, we also ascertained that the secondary antibodies used for these and all subsequent immunofluorescence studies, FITC-conjugated goat anti-mouse IgG and FITC-

Figure 2. Western blotting for galectin-3 in lysates of human HeLa cells, human LG-1 fibroblasts, and mouse 3T3 fibroblasts.

Lane 1: human HeLa lysate. Lane 2: human LG-1 lysate. Lane 3: mouse 3T3 lysate. 50 μ g of total protein was loaded in each lane. Panel A: galectin-3 was detected using the mouse monoclonal antibody NCL-GAL3 (21 ng/ml) plus HRP-goat anti-mouse immunoglobulin. Panel B: galectin-3 was detected using the rat monoclonal antibody anti-Mac-2 (125 ng/ml) plus HRP-goat anti-rat immunoglobulin. The mobilities of molecular weight standards are indicated.

Figure 2

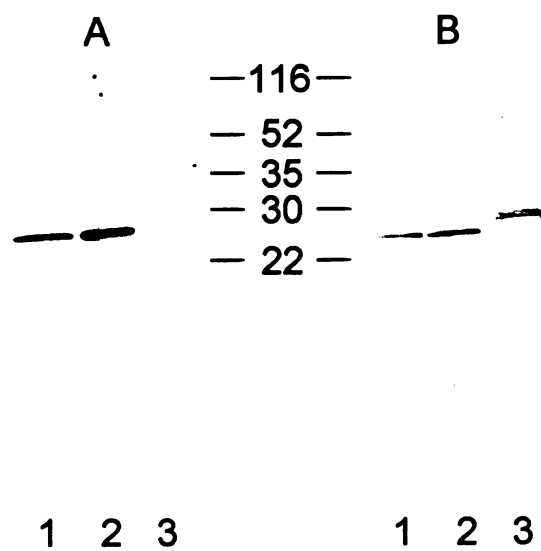
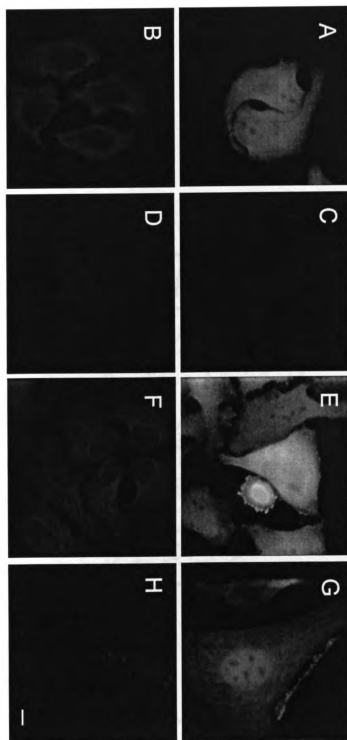


Figure 3. Immunofluorescence staining for galectin-3 in fixed and permeabilized human HeLa cells and mouse 3T3 fibroblasts.

Cells were fixed with paraformaldehyde (4%, room temperature, 20 min) and permeabilized with Triton X-100 (0.2%, 4°C, 5 min). Panels A, B, E, and F: human HeLa cells. Panels C, D, G, and H: mouse 3T3 cells. Panels A and C: galectin-3 was detected with NCL-GAL3 (2.1 µg/ml) plus FITC-goat anti-mouse immunoglobulin. Panels B and D: FITC-goat anti-mouse immunoglobulin. Panels E and G: galectin-3 was detected with anti-Mac-2 (25 µg/ml) plus FITC-goat anti-rat immunoglobulin. Panels F and H: FITC-goat anti-rat immunoglobulin. Bar, 10 µm.

Figure 3



conjugated goat anti-rat IgG, yielded negligible staining in human and mouse cells when used in the absence of any primary antibodies (Figure 3, panels B, D, F, and H).

Bead-tagging distinguishes heterodikaryons from homodikaryons

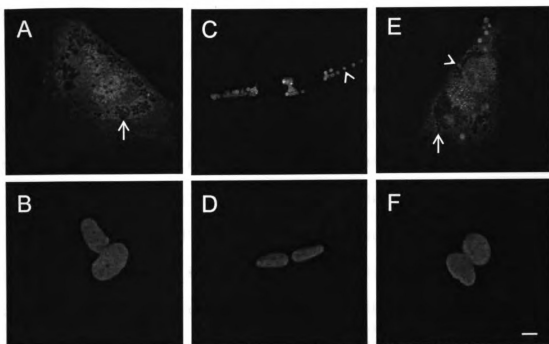
Fusion of human and mouse cells was expected to produce three types of cell hybrids: human-human, mouse-mouse, and human-mouse. In order to distinguish the three types and focus only on human-mouse fusions, we tagged our cells with microsphere styrene beads (~ 2 μm in diameter) prior to fusion. Human LG-1 fibroblasts were tagged with non-fluorescent (black) beads, whereas mouse 3T3 fibroblasts were tagged with green fluorescent beads. Tagged cells were then co-cultured and fused as depicted in Figure 1. Several hours post fusion, the cells were fixed and immunostained with NCL-GAL3 and FITC-goat anti-mouse IgG to determine the localization of human galectin-3 and the nuclei were stained with PI.

Monokaryons were immediately distinguished from di- or polykaryons by the number of nuclei as observed by PI fluorescence (not shown). As shown in Figure 4, panels A – C, human-human homodikaryons were indicated by the presence of only non-fluorescent beads in the cytoplasm. Similarly, mouse-mouse homodikaryons were indicated by the presence of only fluorescent beads in the cytoplasm (Figure 4, panels D – F). In contrast, the presence of both fluorescent and non-fluorescent beads within a dinucleated cell indicated a human-mouse heterodikaryon (Figure 4, panels G – I). Thus, the bead-tagging method proved to be a reliable technique for recognizing heterodikaryons.

Figure 4. Bead-tagged homodikaryons and heterodikaryons immunostained for human galectin-3.

Human LG-1 fibroblasts were tagged with non-fluorescent (black) beads, and mouse 3T3 fibroblasts were tagged with green fluorescent beads. Following bead-tagging, both cell types were co-cultured and fused. Fused cells were then fixed, permeabilized, and immunostained for human galectin-3 using NCL-GAL3 (2.1 $\mu\text{g/ml}$) and FITC-conjugated goat anti-mouse immunoglobulin. Panels A – B: a human-human homodikaryon. Note the presence of only non-fluorescent (black) beads in the cytoplasm. A cluster of black beads is indicated by the arrow. Panels C – D: a mouse-mouse homodikaryon. Note the presence of only green fluorescent beads in the cytoplasm. A single green fluorescent bead is indicated by the arrow head. Panels E – F: a human-mouse heterodikaryon. Note the presence of both black and green beads in the cytoplasm. The arrow indicates a single black bead, while the arrow head indicates a single green bead. Panels A, C, and E: FITC fluorescence showing localization of human galectin-3. Note the prominent nuclear and lesser cytoplasmic staining of human galectin-3 in panels A and E. Panels B, D, and F: PI fluorescence showing the location of both nuclei in each fusion. Bar, 10 μm .

Figure 4



Localization of human galectin-3 to both nuclei of human-mouse heterodikaryons was partially dependent upon de novo protein synthesis

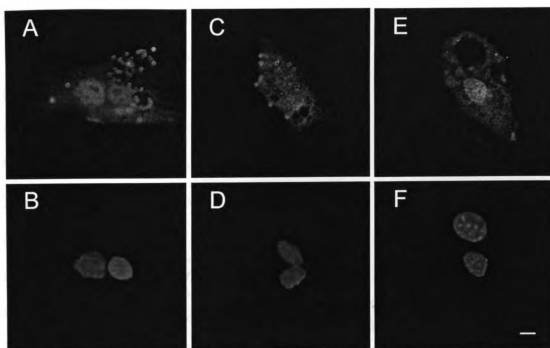
Figure 4 also serves to illustrate how an individual nucleus was scored for the presence of human galectin-3. In the mouse 3T3 homodikaryon (Figure 4, panel E), both nuclei yielded fluorescence intensity values of less than 250. Based on our quantitative scoring criteria (detailed in Materials and Methods), these nuclei would be negative in terms of reactivity with the NCL-GAL3 antibody (i.e. no human galectin-3). In the human LG-1 homodikaryon (Figure 4, panel B), the two nuclei yielded fluorescence intensity values of 1700 and 1800, far surpassing our threshold value of 300 for scoring positive in terms of human galectin-3. In the human-mouse heterodikaryon (Figure 4, panel H), the two nuclei yielded values of 760 and 900. Thus, human galectin-3 was observed in both nuclei of this heterodikaryon (Figure 4, panel H), indicating that it was redistributed into the mouse nucleus.

To assess the contribution of newly synthesized human galectin-3 in supplying the mouse nucleus, cycloheximide (CHX) was employed to block *de novo* protein synthesis (10; 12). CHX appeared to have two effects on the human-mouse heterodikaryons. First, it decreased the overall fluorescence intensity due to NCL-GAL3 staining, presumably because the drug inhibited *de novo* synthesis of human galectin-3. For example, in human-mouse heterodikaryons treated with CHX (Figure 5, panel E), the values of fluorescence intensity for the two nuclei were 450 and 530, reflecting a further decrease in fluorescence beyond the dilution of human galectin-3 into the two nuclei of the heterodikaryon (described for Figure 4, panel H above; Figure 5, panel B). Nevertheless, both of the nuclei of this heterodikaryon (Figure 5, panel E) were above the

Figure 5. Effect of cycloheximide and leptomycin B on localization of human galectin-3 in human-mouse heterodikaryons.

Heterodikaryons were generated and immunostained as described in the legend to Figure 4. Panels A – B: Human-mouse heterodikaryons incubated in the absence of CHX and LMB. Panels C – D: Human-mouse heterodikaryons incubated in the presence of CHX (10 µg/ml) prior to fusion. Panels E – F: Human-mouse heterodikaryons incubated in the presence of LMB (2 ng/ml; 3.8 nM) and CHX (10 µg/ml) prior to fusion. Panels A, C, and E: FITC fluorescence showing localization of human galectin-3. Note the staining for human galectin-3 in both nuclei in panels A and C. In contrast, note the absence of human galectin-3 staining in one of the nuclei in panel H and the accentuated staining in the other nucleus. Panels B, D, and F: PI fluorescence showing the location of both nuclei in each heterodikaryon. Bar, 10 µm.

Figure 5



threshold value of 300 and therefore, were scored positive for human galectin-3, indicating that there was still transport into the mouse nucleus.

Second, CHX also decreased the percentage of heterodikaryons exhibiting human galectin-3 in both nuclei. In the absence of CHX (Figure 5, panels A-C), the fraction of heterodikaryons exhibiting human galectin-3 in both nuclei nine hours post fusion was 72% (58 out of 81 heterodikaryons counted). In the presence of CHX (Figure 5, panels D-F), the corresponding value was 50% (59 out of 119 heterodikaryons counted). Thus, although *de novo* synthesized human galectin-3 contributed to the localization of the protein in both nuclei of human-mouse heterodikaryons, at least half of the heterodikaryons still exhibited human galectin-3 in both nuclei even in the presence of CHX. We interpret these results to indicate that newly synthesized human galectin-3 was not the only source for the mouse nucleus in the heterodikaryon. Rather, it appears that the majority of human galectin-3 supplying the mouse nucleus came from either the human nuclear pool or the human cytoplasmic pool.

Localization of human galectin-3 to both nuclei of human-mouse heterodikaryons was dependent upon nuclear export

Using digitonin-permeabilized 3T3 fibroblasts, we had previously shown that galectin-3 is rapidly and selectively exported from the nucleus and that this export was sensitive to inhibition by leptomycin B (LMB) (13). Therefore, to distinguish between the contributions of the nuclear pool and the cytoplasmic pool of human galectin-3, LMB was employed to block nuclear export of galectin-3. LMB binds and inactivates the CRM1 (chromosome region maintenance) nuclear export receptor (14), which recognizes

the leucine-rich nuclear export signal. In Figure 5, panels G and H show a representative human-mouse heterodikaryon treated with CHX and LMB.

Nine hours after fusion, approximately 50% of heterodikaryons treated with CHX alone exhibited human galectin-3 in both nuclei (59 out of 119 heterodikaryons counted, Table 1). In the presence of CHX and LMB, the corresponding value was 19% (23 out of 120 heterodikaryons counted, Table 1). These results suggest that the cytoplasmic pool of human galectin-3 was not the only source of the protein for the mouse nucleus.

Rather, human galectin-3 in the human nucleus must also contribute to supplying the mouse nucleus, since inhibition of export of human galectin-3 from the human nucleus concomitantly reduced the proportion of heterodikaryons exhibiting human galectin-3 in both nuclei. On this basis, we conclude that at least some of the human galectin-3 appearing in the mouse nucleus of a heterodikaryon had to first exit the human nucleus into the common cytoplasm followed by entry into the mouse nucleus, thus fulfilling the definition of shuttling.

Mouse galectin-3 shuttles in 3T3-MEF Gal-3 ^{-/-} heterodikaryons

In previous studies (11), the generation of mice carrying a null mutation of the galectin-3 gene was reported. This provided the opportunity to corroborate our test of galectin-3 shuttling in another system. We isolated fibroblasts from embryos of this strain of mice, designated MEF Gal-3 ^{-/-}.

To confirm the absence of the galectin-3 polypeptide in MEF Gal-3 ^{-/-} cells, we blotted cell lysate from MEF Gal-3 ^{-/-} cells with the anti-Mac-2 antibody. We did not detect any polypeptide in the lane containing MEF Gal-3 ^{-/-} lysate (Figure 6A, lane 2). In contrast, immunoblotting with anti-Mac-2 yielded a band of the same mobility as

Figure 6. Panel A: Western blotting for galectin-3 in lysates of MEF Gal-3 $-/-$ fibroblasts, MEF Gal-1 $-/-$ fibroblasts, MEF WT fibroblasts, and mouse 3T3 fibroblasts.

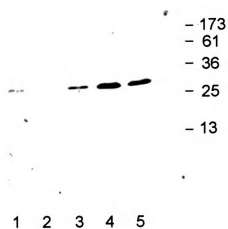
Galectin-3 was detected using anti-Mac-2 (125 ng/ml) and HRP-conjugated goat anti-rat immunoglobulin. Lane 1: recombinant mouse galectin-3, 50 ng. Lane 2: MEF Gal-3 $-/-$ lysate, 6.5 μ g total protein. Lane 3: MEF Gal-1 $-/-$ lysate, 6.5 μ g total protein. Lane 4: MEF WT lysate, 6.5 μ g total protein. Lane 5: mouse 3T3 lysate, 6.5 μ g total protein.

Panel B: Immunofluorescence staining for galectin-3 in fixed and permeabilized mouse 3T3 fibroblasts and MEF Gal-3 $-/-$ fibroblasts.

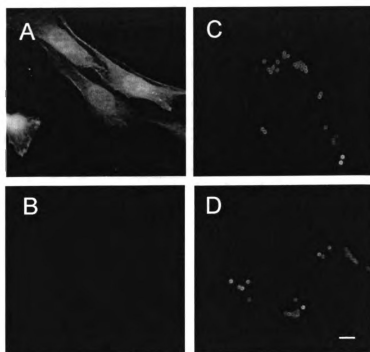
Cells were prepared as described in the legend to Figure 3. Galectin-3 was detected with anti-Mac-2 (25 μ g/ml) and FITC-conjugated goat anti-rat immunoglobulin. Panels A and B: mouse 3T3 cells. Panels C and D: bead-tagged MEF Gal-3 $-/-$ cells. Panels A and C: anti-Mac-2 and FITC-conjugated goat anti-rat immunoglobulin. Panels B and D: FITC-conjugated goat anti-rat immunoglobulin. Bar, 10 μ m.

Figure 6

A



B



recombinant galectin-3 (Figure 6A, lane 1) in lysates from MEF Gal-1 $-/-$ cells (MEF cells containing a null mutation in the Gal-1 gene) (15), MEF WT cells (MEF “wild-type” cells, without any mutations), and mouse 3T3 cells (Figure 6A, lanes 3 – 5).

These results indicated that the MEF Gal-3 $-/-$ cells did indeed lack the galectin-3 polypeptide. This conclusion is substantiated by immunofluorescence staining of fixed and permeabilized cells. Anti-Mac-2 stained mouse 3T3 cells but not MEF Gal-3 $-/-$ cells (Figure 6B, panels A and C). In these experiments, we also ascertained that the secondary antibody FITC-conjugated goat anti-rat IgG did not react non-specifically with fixed and permeabilized MEF Gal-3 $-/-$ cells (Figure 6B, panel D) when used in the absence of anti-Mac-2.

The experimental scheme of Figure 1 was used to study galectin-3 shuttling in 3T3-MEF Gal-3 $-/-$ heterodikaryons. In this case, 3T3 cells served as the source of galectin-3 (cell X) and were tagged with non-fluorescent (black) beads. The MEF Gal-3 $-/-$ cells served as the recipient of galectin-3 (cell Y) and were tagged with fluorescent green beads. The localization of galectin-3 in these heterodikaryons was monitored by immunofluorescence using anti-Mac-2. The results of shuttling assays conducted in 3T3-MEF Gal-3 $-/-$ heterodikaryons were generally similar to those obtained from the assays in human-mouse heterodikaryons. Four hours after fusion, 97% (47 out of 48) of heterodikaryons treated with CHX prior to fusion exhibited galectin-3 in both nuclei. In the presence of CHX and LMB, the corresponding value was 18% (16 out of 89 heterodikaryons counted, Table 1). In Figure 7, panels A – C show a typical 3T3-MEF Gal-3 $-/-$ heterodikaryon treated with CHX, while panels D – F show a typical 3T3-MEF Gal-3 $-/-$ heterodikaryon treated with CHX and LMB. These results suggest that the

Table 1. Percent of heterodikaryons showing staining for galectin-3 in both nuclei.

Experiment A: Human-mouse fusion. Mouse monoclonal antibody NCL-GAL3 used to detect human galectin-3. Experiment B: 3T3-MEF Gal3 ^{-/-} fusion. Rat monoclonal antibody anti-Mac-2 used to detect mouse galectin-3.

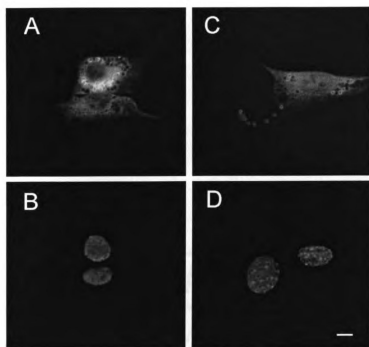
Table 1
Percent of heterodikaryons showing staining for galectin-3 in both nuclei.

<u>Experiment</u>	<u>Harvest Time</u>	<u>CHX</u>	<u>CHX + LMB</u>
A	9	50% (59/119)	19% (23/120)
B	4	97% (47/48)	18% (16/89)

Figure 7. Effect of cycloheximide and leptomycin B on localization of galectin-3 in mouse 3T3-MEF Gal-3 ^{-/-} heterodikaryons.

Mouse 3T3 fibroblasts were tagged with non-fluorescent (black) beads, and MEF Gal-3 ^{-/-} fibroblasts were tagged with green fluorescent beads. Following bead-tagging, both cell types were co-cultured and fused. Fused cells were then fixed, permeabilized, and immunostained for galectin-3 using anti-Mac-2 (25 µg/ml) and FITC-conjugated goat anti-rat immunoglobulin. Panels A – B: 3T3-MEF Gal-3 ^{-/-} heterodikaryons incubated in the presence of CHX (10 µg/ml) prior to fusion. Panels C – D: 3T3-MEF Gal-3 ^{-/-} heterodikaryons incubated in the presence of LMB (2 ng/ml; 3.8 nM) and CHX (10 µg/ml) prior to fusion. Panels A and C: FITC fluorescence showing localization of galectin-3. Note galectin-3 staining in both nuclei in panel A. In contrast, note the absence of galectin-3 staining in one of the nuclei in panel C. Panels B and D: PI fluorescence showing the location of both nuclei in each heterodikaryon. Bar, 10 µm.

Figure 7



localization of galectin-3 to both nuclei of 3T3-MEF Gal-3 ^{-/-} heterodikaryons was independent of protein synthesis, but dependent upon nuclear export of galectin-3.

Discussion

The key findings of this study include: (a) Human galectin-3 was observed in both nuclei of human-mouse heterodikaryons, and mouse galectin-3 was observed in both nuclei of 3T3-MEF Gal-3 ^{-/-} heterodikaryons. In both cases, galectin-3 had been imported into recipient nuclei that previously lacked it. (b) The addition of CHX caused a reduction of approximately 20% in the fraction of human-mouse heterodikaryons showing human galectin-3 in both nuclei. However, 50% of heterodikaryons still showed staining for human galectin-3 in both nuclei. (c) The addition of CHX and LMB caused a further reduction of approximately 30% in the fraction of human-mouse heterodikaryons showing human galectin-3 staining in both nuclei. In the 3T3-MEF Gal-3 ^{-/-} heterodikaryons, the addition of CHX and LMB caused a reduction of approximately 79% in the fraction of heterodikaryons showing galectin-3 staining in both nuclei. We conclude from these results that galectin-3 indeed undergoes nucleocytoplasmic shuttling. Our previous documentation of nuclear export of galectin-3, carried out in a permeabilized cell system, demonstrated that galectin-3 fulfilled a necessary condition for shuttling (13). We have now directly demonstrated shuttling of galectin-3 in an *in vivo* assay.

Interspecies heterokaryons have been used to demonstrate nucleocytoplasmic shuttling of several other proteins, including nucleolin and B23/No38 (10), hnRNP A1 (16), the hdm2 oncoprotein (17), and the 2A7 antigen (18). However, these proteins

differ from galectin-3 in that they are typically most prominent in the nucleus, whereas galectin-3 typically exhibits both nuclear and cytoplasmic localization. In the case of a predominantly nuclear protein, two pools of protein could supply a recipient nucleus in a heterokaryon assay: the nuclear pool and the newly synthesized pool. In contrast, when the protein is also present in the cytoplasm, as is the case for galectin-3, then the cytoplasmic pool represents a third pool that can also supply the recipient nucleus.

The presence of a cytoplasmic pool of galectin-3 complicated our analysis of galectin-3 shuttling, in that we had to differentiate between the contributions of cytoplasmic galectin-3 and galectin-3 that was exported from the nucleus. Therefore, we employed the antibiotic LMB to block nuclear export of galectin-3. By conducting shuttling assays in the presence of CHX (inhibiting protein synthesis), as well as in the presence of CHX and LMB (inhibiting protein synthesis and nuclear export), we were able to assess the contribution of each of the three pools of galectin-3 to the recipient nuclei in our heterokaryons. Indeed, our data from the human-mouse heterodikaryon assays suggest that all three pools did in fact contribute to supplying the mouse nucleus in roughly equal proportions.

The effect of LMB on the nuclear versus cytoplasmic distribution of galectin-3 has been documented for both of the cell types used in our human-mouse heterokaryon fusions. Incubation of live, intact mouse 3T3 fibroblasts in the presence of LMB (3.8 nM) resulted in the accumulation of galectin-3 in the nucleus, as revealed by accentuation of the nuclear staining (13). At a higher concentration of LMB (15.2 nM), galectin-3 was found predominantly, if not exclusively, in the nucleus. Similar results were obtained for human LG-1 cells; incubation with LMB (15.2 nM) resulted in the accumulation of

galectin-3 in the nucleus, as revealed by the almost exclusively nuclear staining (19).

These results indicate that the effect of LMB on decreasing the appearance of galectin-3 in both nuclei of heterokaryons must be due to its inhibitory effect on the export of galectin-3 from the donor nucleus, rather than any secondary effects of the drug on nuclear import.

Other shuttling proteins that appear to bear functional similarity to galectin-3 are nucleolin and hnRNP A1. Both of these proteins are associated with RNA processing, and both are believed to leave the nucleus in association with their substrate RNA molecule. Nucleolin imports ribosomal proteins from the cytoplasm into the nucleus and then coordinates binding of the ribosomal proteins to the nascent rRNA transcript (20; 21). The resulting complex may mediate processing of the transcript or stimulate cleavage reactions, after which nucleolin exports assembled ribosomal subunits out of the nucleus and deposits them in the cytoplasm (20). hnRNP A1 mediates nuclear export of mRNA from the nucleus (16). Pre-mRNAs are bound by hnRNP A1 in the nucleus, and upon completion of splicing, the nuclear export signal in hnRNP A1 directs the export of the hnRNP A1-mRNA complex to the cytoplasm (22; 23). Once in the cytoplasm, hnRNP A1 dissociates from the mRNA and returns to the nucleus to repeat the cycle.

The significance of trafficking of galectin-3 between the nuclear and cytoplasmic compartments is not fully understood. We have recently identified galectin-3 as a component of a macromolecular complex, designated as the SMN complex (6). Like previous immunofluorescence and ultrastructural studies on galectin-3 (2; 3), the SMN complex is found in both the cytoplasm and the nucleus (24; 25). In the cytoplasm, the SMN complex is associated with the core proteins of snRNPs and is involved in the

biogenesis of the snRNP particles (8; 26). In the nucleus, the SMN complex is found in discrete nuclear bodies called gems (gemini of coiled bodies) and it is required for supplying snRNPs to the H-complex during spliceosome assembly (9; 27). This H-complex juncture is also where galectin-3 appears to be required for splicing, as demonstrated by the effect of galectin depletion on the accumulation of intermediates during the assembly of splicing complexes (5).

We propose that galectin-3 might initially associate with Gemin4 in the cytoplasm, possibly during the course of snRNP biogenesis. When the SMN complex is imported into the nucleus, galectin-3 may be taken along by way of its interaction with Gemin4. Once in the nucleus, galectin-3 may participate with the SMN complex in the assembly of the spliceosome. Lastly, galectin-3 may be exported from the nucleus, in association with Gemin4 and possibly other members of the SMN complex, to repeat the cycle of snRNP biogenesis and delivery.

Materials and Methods

Cell Culture and reagents

NIH mouse 3T3 fibroblasts were obtained from the American Type Culture Collection and cultured in MEM-ASP (minimal essential Eagle's medium, supplemented with 0.2 mM L-aspartic acid, 0.2 mM L-serine, 1 mM sodium pyruvate, 100 U/ml penicillin, and 0.1 µg/ml streptomycin) plus 10 % calf serum at 37°C and 5% CO₂.

The human fibroblast strain, designated LG-1 (28), was a gift from Drs. J. J. McCormick and V. M. Maher at Michigan State University. LG-1 cells were used through passage 20, and were serially passaged at a split ratio of 1:4 as described

previously (19) in MEM-ASP supplemented with 10% fetal calf serum at 37°C and 5% CO₂.

Primary mouse embryonic fibroblasts (MEF) were derived from 129 wild type strain (MEF WT), galectin-1 null mutant strain (MEF Gal-1 ^{-/-}) (15) and galectin-3 null mutant strain (MEF Gal-3 ^{-/-}) (11) using the procedure described by Hogan *et al.* (29). MEF WT, MEF Gal-1 ^{-/-}, and MEF Gal-3 ^{-/-} cells were cultured in DME-HG (Dulbecco's Modified Eagle Medium with 4.5 g/l glucose, supplemented with 44 mM sodium bicarbonate, 100 U/ml penicillin, 0.1 µg/ml streptomycin, 50 µg/ml gentamicin sulfate) plus 10% calf serum at 37°C and 5% CO₂. Cells were passaged serially at split ratios of 1:5 or 1:10.

The rat monoclonal antibody anti-Mac-2 recognizes an epitope in the amino-terminus of galectin-3 (30). The mouse monoclonal antibody NCL-GAL3 was purchased from Novocastra Laboratories, Ltd., UK. Fluorescein isothiocyanate (FITC)-conjugated goat anti-rat IgG was obtained from Boehringer Mannheim, and FITC-conjugated goat anti-mouse IgG was obtained from Santa Cruz Biotech. Microsphere styrene beads were obtained from Polysciences.

Bead-tagging and polyethylene glycol-mediated cell fusion

Human LG-1 and mouse 3T3 fibroblasts were seeded separately in 100 X 20 mm tissue culture plates at 5×10^3 cells/cm², and allowed to attach for approximately six hours. Microsphere styrene beads were then added to the culture medium at a concentration of 250 beads/cell and incubated overnight. Plates were then rinsed with Versene (140 mM NaCl, 2.68 mM KCl, 10 mM Na₂HPO₄, 1.47 mM KH₂PO₄, 0.68 mM EDTA, 0.15% phenol red, pH 7.2), trypsinized, and resuspended separately. The

concentration of each cell suspension was determined, and both cell types were seeded together, each at a density of 3.9×10^3 cells/cm², into 35 mm dishes containing sterile glass coverslips. Co-cultured cells were then incubated overnight. Cycloheximide (Sigma) was added at 10 µg/ml in MEM-ASP one hour prior to fusion, removed during fusion, and returned after fusion. LMB was a gift from Dr. Minoru Yoshida (University of Tokyo), and was added at 2 ng/ml (3.8 nM) in MEM-ASP ten hours prior to fusion, removed during fusion, and returned after fusion.

Polyethylene glycol-1000 (Fluka Chemical Corp.) was melted and diluted to 45% (v/v) with warmed serum-free MEM-ASP media, then filtered through a 0.22 µm Millex syringe driven filter unit (Millipore). Co-cultured LG-1 and NIH 3T3 cells were rinsed in warmed phosphate-buffered saline (PBS, 140 mM NaCl, 2.68 mM KCl, 10 mM Na₂HPO₄, 1.47 mM KH₂PO₄, pH 7.4), and treated with 45% polyethylene glycol-1000 for 55 seconds. The medium was promptly removed and the cells were rinsed gently three times in warmed PBS. Cells were then incubated with MEM-ASP containing 10% fetal calf serum until immunostaining.

Immunostaining and fluorescence microscopy

Cells were prepared for fluorescence microscopy following fixation with 4% paraformaldehyde and permeabilization with 0.2% Triton X-100 (13). Human-mouse fusions were stained with NCL-GAL3 (2.1 µg/ml in PBS containing 0.2% gelatin) for one hour at room temperature, then washed three times with T-TBS (10 mM Tris, pH 7.5, 0.5 M NaCl, 0.05% Tween 20) on an orbital shaker at room temperature. The coverslips were then stained with FITC-goat anti-mouse IgG (in PBS containing 0.2% gelatin) for 30 minutes at room temperature. This and all subsequent steps were carried out in the

dimmiest light possible. The coverslips were washed with T-TBS, stained with propidium iodide (PI, 32 µg/ml in PBS containing 0.2% gelatin) for 30 minutes at room temperature, and rinsed again in T-TBS. The coverslips were then inverted onto clean microscope slides with a drop of Perma-Fluor (Lipshaw Immunon) and allowed to dry in a darkened environment overnight at room temperature. 3T3-MEF Gal-3 ^{-/-} fusions were treated similarly except they were stained with anti-Mac-2 (25 µg/ml), followed by FITC-conjugated goat anti-rat IgG.

Fluorescent cells were viewed using an Insight Plus laser scanning confocal microscope (Meridian Instruments). The maximum and minimum fluorescence intensities of each nucleus were determined using the image analysis subroutine. By viewing over one hundred images, including human and mouse monokaryons as well as homodikaryons and heterodikaryons, we found that a nucleus devoid of human galectin-3 (and therefore, not stained by NCL-GAL3) yielded a maximum fluorescence of 250 (arbitrary units). In contrast, a nucleus containing human galectin-3 always yielded a fluorescence intensity of 300 or greater. On this basis: (a) a nucleus whose maximum fluorescence intensity was 250 or less was scored negative for the presence of human galectin-3; and (b) a nucleus whose minimum fluorescence intensity was 300 or greater was scored positive for the presence of human galectin-3.

Preparation of cell lysates and immunoblotting

Cells were grown to near confluence in 100 X 20 mm tissue culture plates, rinsed once with ice-cold PBS, and scraped in four ml of PBS with a rubber policeman. Scraped cells were pooled into 15 ml tubes, centrifuged at 1470 X g for 10 minutes at 4°C, and the supernatant was decanted. The cells were resuspended in 1 ml ice-cold PBS, transferred

to Eppendorf tubes, and pelleted in a microfuge at 3406 X g for 2 minutes at 4°C. The supernatant was aspirated and the cells were resuspended in 150 µl of 10 mM Tris, pH 7.4, then incubated on ice for ten minutes. The cell suspension was then sonicated eight times (15 seconds each) and stored at -20°C.

The amount of protein in each sample was quantitated by the Bradford method (31) using Coomassie protein assay reagent (Pierce). Equal amounts of protein from each lysate were separated on a 12.5% SDS-polyacrylamide gel and then transferred electrophoretically to a nitrocellulose membrane in a buffer containing 25 mM Tris, 193 mM glycine, and 10% methanol (pH 8.3). The membrane was blocked overnight at room temperature in T-TBS containing 10% non-fat dehydrated milk, then rinsed three times briefly in T-TBS, and blocked with a 1:1000 dilution of goat anti-rabbit IgG in T-TBS containing 1% non-fat dehydrated milk. Following blocking, the membrane was rinsed with T-TBS.

In immunoblots employing NCL-GAL3, the membrane was incubated with NCL-GAL3 (21 ng/ml) in T-TBS containing 1% non-fat dehydrated milk for one hour at room temperature. Following incubation with NCL-GAL3, the membrane was rinsed with T-TBS, and incubated with horseradish peroxidase (HRP)-conjugated goat anti-mouse IgG in T-TBS containing 1% non-fat dehydrated milk for one hour at room temperature. The membrane was then rinsed with T-TBS, and the proteins were visualized using the Renaissance western blot chemiluminescence reagents (New England Nuclear Life Science Products, Boston, MA).

Immunoblots employing anti-Mac-2 were carried out in a similar fashion except that anti-Mac-2 was used at 125 ng/ml, and HRP-conjugated goat anti-rat IgG was used as the secondary antibody.

Acknowledgements

This work was supported by a grant (GM-38740) from the United States National Institutes of Health, a grant (MCB 97-23615) from the United States National Science Foundation, and a grant (number 5751) from Association de la Recherche contre le Cancer.

We thank Kyle Openo for his initial characterization of the specificity of the NCL-GAL3 antibody for human galectin-3. We thank Dr. Minoru Yoshida, University of Tokyo, for his generous gift of leptomycin B, and Drs. J. J. McCormick and V. M. Maher for their generous gift of LG-1 cells.

References

1. Barondes, S.H., *et al.* (1994) *Cell* **76**, 597-598.
2. Moutsatsos, I.K., Davis, J.M., and Wang, J.L. (1986) *J. Cell. Biol.* **102**, 477-483.
3. Hubert, M., Wang, S.-Y., Wang, J.L., Sève, A.-P., and Hubert, J. (1995) *Exp. Cell Res.* **220**, 397-406.
4. Craig, S.S., Krishnaswamy, P., Irani, A.-M.A., Kepley, C.L., Liu, F.-T., and Schwartz, L.B. (1995) *Anat. Rec.* **242**, 211-219.
5. Dagher, S.F., Wang, J.L., and Patterson, R.J. (1995) *Proc. Natl. Acad. Sci. U.S.A.* **92**, 1213-1217.
6. Park, J.W., Voss, P.G., Grabski, S., Wang, J.L., and Patterson, R.J. (2001) *Nucleic Acids Res.* **27**, 3595-3602.
7. Charroux, B., Pellizzoni, L., Perkinson, R.A., Yong, J., Shevchenko, A., Mann, M., and Dreyfuss, G. (2000) *J. Cell Biol.* **148**, 1177-1186.
8. Fischer, U., Qing, L., and Dreyfuss, G. (1997) *Cell* **90**, 1023-1029.
9. Pellizzoni, L., Naoyuki, K., Charroux, B., and Dreyfuss, G. (1998) *Cell* **95**, 615-624.
10. Borer, R.A., Lehner, C.F., Eppenberger, H.M., and Nigg, E.A. (1989) *Cell* **56**, 379-390.
11. Colnot, C., Fowlis, D., Ripoche, M.-A., Bouchaert, I., and Poirier, F. (1998) *Dev. Dyn.* **211**, 306-313.
12. Agrwal, N., Wang, J.L., and Voss, P. (1989) *J. Biol. Chem.* **264**, 17236-17242.
13. Tsay, Y.G., Lin, N.Y., Voss, P.G., Patterson, R.J., and Wang, J.L. (1999) *Exp. Cell Res.* **252**, 250-261.
14. Nishi, K., Yoshida, M., Fujiwara, D., Nishikawa, M., Horinuchi, S., and Beppu, T. (1994) *J. Biol. Chem.* **269**, 6320-6324.
15. Poirier, F. and Robertson, E.J. (1993) *Development* **119**, 1229-1236.
16. Piñol-Roma, S. and Dreyfuss, G. (1992) *Nature* **355**, 730-732.
17. Roth, J., Dobbstein, M., Freedman, D.A., Shenk, T., and Levine, A.J. (1998) *EMBO J.* **17**, 554-564.

18. Levasseur-Paulin, M., and Julien, M. (1999) *Exp. Cell Res.* **250**, 439-451.
19. Openo, K.P., Kadrofske, M.M., Patterson, R.J., and Wang, J.L. (2000) *Exp. Cell. Res.* **255**, 278-290.
20. Ghisolfi-Nieto, L., Joseph, G., Dutilleul, F.-P., Amalric, F., and Bouvet, P. (1996) *J. Mol. Biol.* **260**, 34-53.
21. Ginisty, H., Amalric, F., and Bouvet, P. (1998) *EMBO J.* **17**, 1476-1486.
22. Michael, W.M., Choi, M., and Dreyfuss, G. (1995) *Cell* **83**, 415-422.
23. Pollard, V.W., Michael, W.M., Nakielnny, S., Siomi, M.C., Wang, F., and Dreyfuss, G. (1996) *Cell* **86**, 985-994.
24. Dietz, H. (1998) *Nature Genet.* **20**, 321-322.
25. Matera, A.G. and Frey, M.R. (1998) *Am. J. Hum. Genet.* **63**, 317-321.
26. Mattaj, I.W. (1998) *Curr. Biol.* **8**, 93-95.
27. Meister, G., Bühler, D., Lagerbauer, B., Zobawa, M., Lottspeich, F., and Fischer, U. (2000) *Hum. Mol. Genet.* **9**, 1977-1986.
28. Morgan, T.L., Yang, D., Fry, D.G., Hurlin, P.F., Kohler, S.K., Maher, V.M., and McCormick, J.J. (1991) *Exp. Cell Res.* **197**, 125-136.
29. Hogan, B., Beddington, R., Costantini, F., and Lacy, E. (1994) *Manipulating the mouse embryo*. (2nd ed.) Cold Spring Harbor Laboratory Press.
30. Ho, M.K. and Springer, T.A. (1982) *J. Immunol.* **128**, 1221-1228.
31. Bradford, M.M. (1976) *Anal. Biochem.* **72**, 248-254.

Chapter 3

Transport of Galectin-3 between the Nucleus and Cytoplasm

I. Conditions and Signals for Nuclear Import

**Transport of Galectin-3 between the Nucleus and Cytoplasm.
I. Conditions and Signals for Nuclear Import***

Peter J. Davidson[§], Su-Yin Li[#], Rianna Vandergaast^Δ,
Ronald J. Patterson^Ψ, John L. Wang[#], and Eric J. Arnoys^{Δ*}

Cell and Molecular Biology Program[§], Departments of Biochemistry[#]
and Microbiology^Ψ, Michigan State University, East Lansing, MI 48824, USA

Department of Chemistry and Biochemistry^Δ, Calvin College
Grand Rapids, MI 49546, USA

Peter Davidson was responsible for collecting and interpreting the data reported in Figures 2 – 7 of this chapter. Su-Yin Li, a student in the M.S. program, designed and engineered the expression vector shown in Figure 1, from which all of the mutants reported in the present experiments were derived. This was done under the direct supervision of Dr. Eric Arnoys. Rianna Vandergaast, an undergraduate student with Dr. Eric Arnoys, carried out the site-directed mutagenesis to produce the mutants described in Figures 5 and 6. Drs. Ron Patterson, John Wang, and Eric Arnoys are faculty members in whose laboratories the reported experiments were performed.

ABSTRACT

Galectin-3 (Gal3), a factor involved in the splicing of pre-mRNA, shuttles between the nucleus and the cytoplasm. We have engineered a vector that expresses the fusion protein containing: (a) Green Fluorescent Protein (GFP) as a reporter of localization; (b) bacterial maltose-binding protein (MalE) to increase the size of the reporter polypeptide; and (c) Gal3 whose sequence we wish to dissect in search of a nuclear localization signal.

Analysis of the fluorescence in mouse 3T3 fibroblasts transfected with this expression construct showed that the GFP-MalE-Gal3(1-263) fusion protein was localized predominantly in the nucleus. Mutants of this construct, containing truncation of the Gal3 polypeptide from the carboxyl terminus, showed loss of nuclear localization: this effect was observed beginning with truncation at residue 259 and the full effect is seen with truncation at residue 232. Mutants of the same construct, containing truncation of the Gal3 polypeptide from the amino terminus, retained nuclear localization; residues 228-263 of the Gal3 sequence was sufficient to direct the fusion protein into the nucleus.

These results suggest that the carboxyl-terminal region of the murine Gal3 polypeptide, residues 228-258 in particular, is important for nuclear localization.

INTRODUCTION

Galectin-3 (Gal3¹) is a member of a family of galactose-specific carbohydrate-binding proteins found in a variety of cell types (1). It is predominantly an intracellular protein, being found in both the cytoplasm and nucleus of cells (2). The nuclear localization of Gal3 was sensitive to ribonuclease treatment of permeabilized cells, prior

to their fixation for analysis by immunofluorescence and immunoelectron microscopy (3, 4). Moreover, sedimentation of nucleoplasm over cesium sulfate density gradients identified Gal3 in fractions with densities corresponding to those reported for heterogeneous nuclear ribonucleoprotein complex (hnRNP) and small nuclear RNPs (snRNP). Because these RNPs play important roles in the nuclear processing of pre-mRNA, the possibility was raised that Gal3 was a splicing factor as well.

Indeed, using a cell-free assay, depletion and reconstitution experiments showed that Gal3 and another member of the galectin family, galectin-1 (Gal1), were redundant but required factors in the splicing of pre-mRNA (5, 6). More recently, it was documented (7) that Gal3, as well as Gal1, interacts with Gemin4, which has been characterized as one component of a macromolecular complex, designated as the SMN complex (8). The functional significance of this interaction appears to be in the early steps of spliceosome assembly. The addition of the NH₂-terminal domain of Gal3 or the COOH-terminal 50 amino acids of Gemin4 to splicing competent nuclear extracts inhibited splicing and blocked the conversion of early (H/E) complexes to active spliceosomes (7).

The SMN complex is found in both the nucleus and in the cytoplasm. In the cytoplasm, the SMN complex is involved in the biogenesis of snRNPs (9), prior to their entry into the nucleus to function as required components in the splicing of pre-mRNA. In the nucleus, the SMN complex is localized in discrete bodies called Gems (10) and appears to play a role in the "rejuvenation or recycling" of the snRNPs for supplying them to the intermediates (H/E complex) in spliceosome assembly (11). The association of Gal3 with the SMN complex raises the possibility that the protein might also perform

functions in both the nucleus and the cytoplasm and that it might shuttle between the two compartments. Indeed, analysis of Gal3 localization in both nuclei of heterodikaryons (e.g. derived from fusion of a Gal3-expressing cell with a Gal3-null cell) provided definitive evidence for nucleocytoplasmic shuttling (12).

In this chapter, we document the conditions and sequences required for nuclear import of the protein.

EXPERIMENTAL PROCEDURES

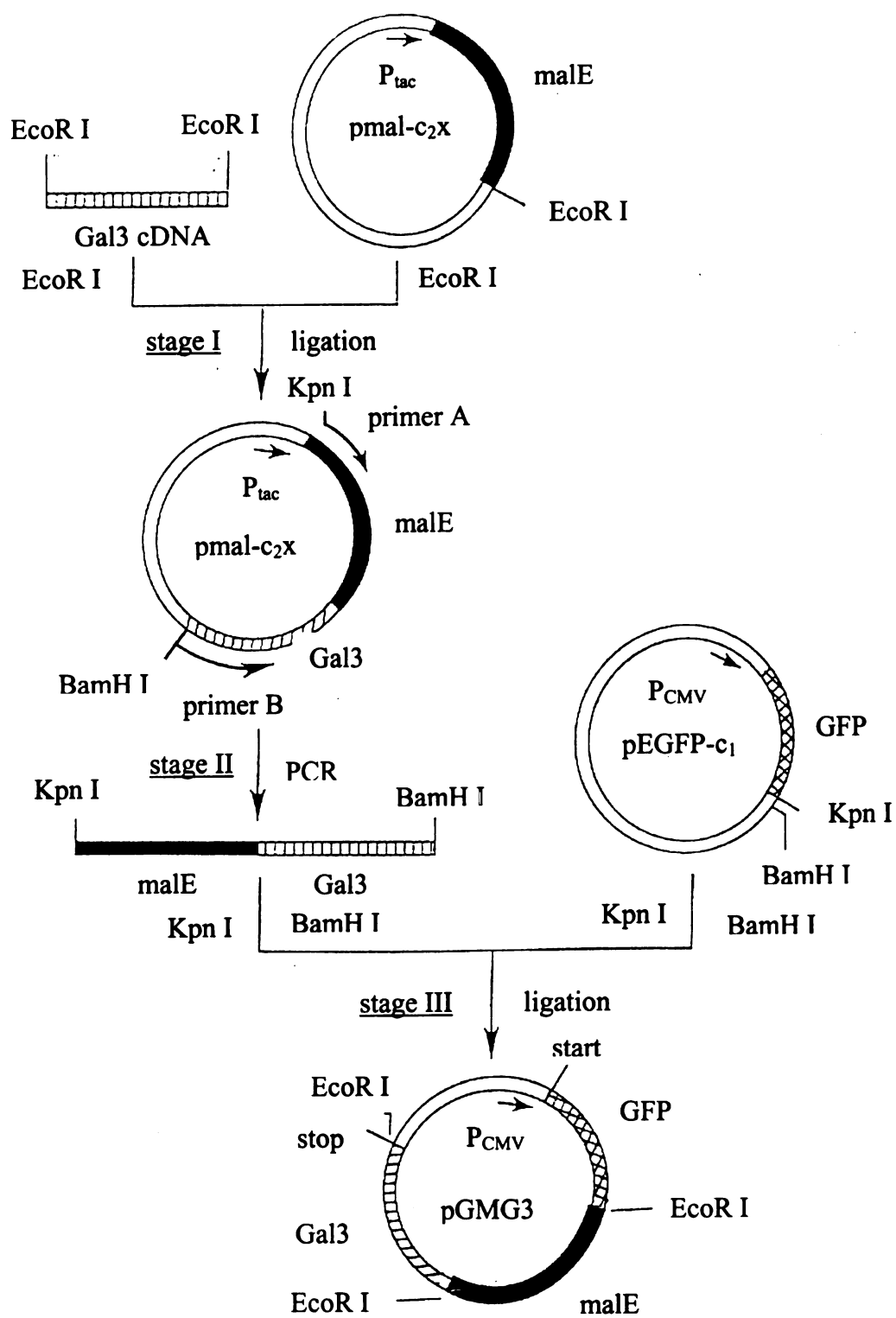
Preparation of the pEGFP-c₁ vector for expression of the fusion protein GFP-MalE-Gal3

In this study, the analysis of nuclear versus cytoplasmic localization was carried out using a fusion protein containing Gal3, Green Fluorescent Protein (GFP) and bacterial maltose-binding protein (MalE). The construction of the vector pGMG3 for expression of the fusion protein GFP-MalE-Gal3 in mammalian cells is summarized in Figure 1. In stage 1, the cDNA for Gal3 was excised from plasmid pWJ31 (13) by EcoRI digestion and then inserted into the corresponding restriction site of the bacterial expression vector pmal-c₂x (New England Biolabs, Beverly, MA). In stage II, this plasmid encoding the fusion protein MalE-Gal3 was used as the template for polymerase chain reaction (PCR) amplification, using primers: 5'-GGGGGTACCATGAAAATCGAAGAAGGTAAAC-3' (which generates the KpnI restriction site not on the template); 5'-AGGTCGACTCTAGAGGATC-3' (which reproduces the BamHI site on the template). In stage III, this PCR product was ligated into the mammalian expression vector, pEGFP-c₁ (Clontech, San Jose, CA). The expression of the fusion protein GFP-MalE-Gal3 from pGMG3 in transfected cells is driven by a cytomegalovirus

Figure 1. Schematic diagram illustrating the construction of the vector for the expression of the fusion protein GFP-MalE-Gal3 in mammalian cells.

In stage I, the cDNA for Gal3 was inserted into the EcoRI restriction site of the bacterial expression vector pmal-c₂x. After ascertaining that this vector expressed the desired fusion protein MalE-Gal3, it was used, in stage II, as template for PCR amplification of the fragment coding for MalE-Gal3, with a KpnI site at the 5'-end and BamHI site at the 3'-end. In stage III, this fragment was ligated into the mammalian expression vector, pEGFP-c₁. The expression of the fusion protein GFP-MalE-Gal3 from the pGMG3 vector in mammalian cells is driven by a cytomegalovirus promoter. The relative positions of the three EcoRI restriction sites in the pGMG3 vector are indicated.

Figure 1



promoter (Fig. 1). The vector for the production of GFP-Gal3 was prepared from the respective cDNAs in a similar fashion, using the same primers and taking advantage of the same restriction sites.

The strategy for generating mutants in which the Gal3 sequence was truncated from the carboxyl terminus was to introduce stop codons at specific positions in the pGMG3 plasmid (Fig. 1). Using the QuikChange Site-Directed Mutagenesis Kit (Stratagene, La Jolla, CA), this was carried out at amino acid residues 262, 261, 260, 259, 258, 253, and 232. For example, insertion of a stop codon at position 259 results in the fusion protein GFP-MalE-Gal3(1-258).

The pGMG3 plasmid contains three EcoRI restriction sites (Fig. 1): (a) between GFP and MalE; (b) at the start of the Gal3 coding sequence; and (c) at the end of the Gal3 sequence. Site-directed mutagenesis (5'-CATCCCGGACTTCGGATCCACC-3' and 5'-GTGGATCCGAAGTCCGGGATG-3') was carried out to remove the last of these EcoRI sites. The resulting plasmid was used as the template to remove the first EcoRI site, between the GFP and MalE sequences (5'-CGAGCTCAAGCTTCGACTTCTGCAGTCGACGG-3' and 5'-CCGTCGACTGCAGAAGTCGAAGCTTGAGCTCG-3'). This provided the starting material for the generation of mutants in which the Gal3 sequence was truncated from the amino terminus. Site-directed mutagenesis was carried out to insert EcoRI sites into specific positions of the Gal3 sequence. After digestion with the restriction enzyme, the isolated DNA was religated with T4 DNA ligase. The following forward and reverse primers were used to obtain the respective GFP-MalE-Gal3 mutants: (a) (74-263), 5'-CCTAGTGCCTACCCCGAATTCCTACTGCCCCTGGAGC-3' and 5'-GCTCCAGGGGCAGTGAATTCGGGGTAGGCACTAGG-3'; (b) (121-263), 5'-GC

TATCCTGCTGCTGGCGAATTCGGTGTCCCCGCTGGACC-3' and 5'-GGTCCAGC
GGGGACACCGAATTCGCCCCGAAGCAGGATAGC-3'; and (c) (131-263), 5'-GGT
GTCCCCGCTGGAGAATTCACGGTGCCCTATGAC-3' and 5'-GTCATAGGGCAC
CGTGAATTCTCCAGCGGGGACACC-3'.

Cell culture and transfection

NIH mouse 3T3 fibroblasts were obtained from the American Type Culture Collection (Rockville, MD). The cells were grown as monolayers in Dulbecco's modified Eagle's medium (DME) containing 10% calf serum, 100 U/ml penicillin, and 100 µg/ml streptomycin at 37 °C in a humidified atmosphere of 10% CO₂ (14). Cells were transfected with vectors expressing fusion proteins containing the GFP reporter group described above. For transfections to be analyzed by immunoblotting, the cells were cultured and transfected in 60 mm plates (29 cm² growth surface). For transfections to be analyzed by fluorescence, the cells were cultured on glass coverslips in 35 mm plates (10 cm² growth surface). The following describes the protocol used for transfection of a single 35 mm plate; for transfection of 60 mm plates, the amounts of reagents used are increased 3-fold.

Cells were seeded at a density of 1×10^4 cells/cm² and cultured overnight. A 100 µl solution of serum-free DME containing 1 µg of the DNA construct was mixed with 100 µl of serum-free DME containing 3 µl of lipofectamine (Invitrogen, Carlsbad, CA; 2 mg/ml). The cells in the culture plate were washed with serum-free DME and the 200 µl mixture containing DNA and lipofectamine was added, along with 0.8 ml of serum-free DME. The plate was placed in the CO₂ incubator for three hours, at which time 1 ml of

DME containing 20% calf serum was added. The plate was incubated for another six hours. The medium in the plate was then replaced with 2 ml of fresh DME containing 10% calf serum. In some experiments, cycloheximide (CHX; Boehringer Mannheim, Indianapolis, IN; 10 µg/ml final concentration) and leptomycin B (LMB; LC Laboratories, Woburn, MA; 5.4 ng/ml (10 nM) final concentration) were included during this medium change. The cells were incubated for an additional 5 hours, at which time they were processed for fluorescence analysis (see below). For immunoblotting analysis, the cells in 60 mm plates were incubated for 24 hours after the medium change before harvesting for preparation of lysates.

Fluorescence Microscopy

For examination of the transfected cells by fluorescence microscopy, the coverslips were first washed three times with ice-cold phosphate-buffered saline (PBS). The cells were then fixed by treating for 20 minutes in 2 ml of 4% paraformaldehyde in PBS at room temperature. The cells were washed twice (10 minutes each, 3 ml PBS) at room temperature. Finally, the coverslips were mounted on glass microscope slides using Perma-Fluor (Thermo Shandon, Pittsburgh, PA). In some early experiments, we had also transfected cells cultured in Lab-Tek Chamber slides (Nalge Nunc International, Naperville, IL) using the same conditions as described for the transfection of the cells cultured on coverslips in 35 mm plates. The results obtained with GFP fluorescence in the live cells in chamber slides and fixed cells on coverslips were essentially the same.

We also compared the localization of the GFP-MalE-Gal3 reporter against the localization of endogenous Gal3 in the 3T3 fibroblasts. Endogenous Gal3 was detected

using the rat monoclonal antibody, anti-Mac2 (25 µg/ml in PBS containing 0.2% gelatin) and fluorescein-conjugated goat anti-rat immunoglobulin (Sigma, St. Louis, MO; 1:500 dilution). The details of the indirect immunofluorescence protocol have been previously described (15).

Fluorescent cells were examined using a Meridian Instruments (Okemos, MI) Insight confocal laser scanning microscope. For each construct, we counted approximately 100 cells, scoring the fluorescence labeling pattern in each cell in one of five categories: (a) exclusively nuclear (N); (b) intensely nuclear over a cytoplasmic background ($N > C$); (c) equal distribution between the nucleus and cytoplasm ($N \sim C$); (d) less nuclear labeling than the cytoplasm ($N < C$); and (e) exclusively cytoplasmic (C). These distributions of fluorescence are expressed in the form of histograms. Representative cells were photographed at low (66X) magnification to show a field containing multiple cells and at high (200X) magnification to show a single cell.

SDS-PAGE and immunoblotting

Proteins were resolved on SDS-PAGE (10% acrylamide) as described by Laemmli (16). The procedures for immunoblotting after SDS-PAGE have also been described (15). The antibodies used for immunoblotting and their sources were: (a) polyclonal anti-GFP (Clontech); (b) anti-MalE (New England Biolabs); and (c) polyclonal anti-Gal3 (#32 and #33, see reference 17).

RESULTS

A GFP reporter construct for the localization of Gal3

In order to define the NLS and NES of Gal3, we developed a reporter construct expressing a fusion protein containing Gal3 (~33 kD) and GFP (~27 kD). This fusion protein also contains bacterial maltose-binding protein (MalE; ~40 kD) to serve as a "spacer" that increases the molecular weight of the reporter polypeptide. This was done to insure that the size of the reporter polypeptide would exceed the exclusion limit of nuclear pores (40-60 kD), even when the portion of the Gal3 polypeptide is decreased through truncation.

The cDNA for Gal3 was digested with EcoRI and ligated into the corresponding restriction site in the prokaryotic expression vector pMAL-c₂x (Fig. 1). The success of this step was indicated by: (a) the same MalE-Gal3 fusion protein (~74 kD) could be detected in bacterial lysates by immunoblotting with either anti-MalE or anti-Gal3; (b) the MalE-Gal3 fusion protein could be isolated on lactose affinity columns. This plasmid then served as the template for PCR amplification of the coding region corresponding to MalE-Gal3 and the product was ligated into the eukaryotic expression vector, pEGFP-c₁ (Fig. 1). This initial construct and its variants were used to transfect mouse 3T3 fibroblasts. The authenticity of each of the constructs was confirmed by DNA sequencing. In addition, extracts of transfected cultures were subjected to Western blotting with antibodies directed against the three parts of the expressed fusion protein: (a) anti-GFP; (b) anti-MalE; and (c) anti-Gal3. This was carried out to ascertain that the predominant polypeptide bearing the GFP reporter group corresponded to the expected

molecular weight of the fusion protein. Thus, the observed fluorescence signal can be ascribed to the localization of the construct under study.

Transfection of 3T3 cells with GFP resulted in the expression of a ~27 kD polypeptide (Fig. 2, lane 1) and fluorescence in both the nuclear and cytoplasmic compartments (data not shown). This observation is consistent both with the expectation that a ~30 kD polypeptide would be able to diffuse across the nuclear pores, as well as with previous reports on the localization of GFP (18, 19). Western blotting of cells transfected with GFP-MalE-Gal3 (1-263) yielded an ~100 kD polypeptide (Fig. 2, lane 4), consistent with the sum of the molecular weights of the three parts of the fusion protein. Some GFP-MalE-Gal3(1-263) transfected cells exhibit fluorescence exclusively in the nucleus (N) (Fig. 3, panel A) while other cells showed fluorescence intensely nuclear over a cytoplasmic background (N>C) (Fig. 3, panel B).

Transfection with GFP-Gal3 (1-263) yielded the expected ~60 kD polypeptide (Fig. 2, lane 2) and a predominantly N>C fluorescence pattern, similar to that shown in Figure 3, panel B. The N~C pattern (equal distribution between the nucleus and cytoplasm) was found in cells transfected with GFP-MalE (~67 kD) (Fig. 2, lane 3; Fig. 3, panel C). GFP-MalE-Gal3(1-252) (Fig. 2, lane 5), in which the Gal3 polypeptide is truncated at residue 253, yielded the N<C (less nuclear labeling than the cytoplasm) fluorescence pattern (Fig. 3, panel D). The exclusively cytoplasmic (C) labeling pattern was found in cells transfected with GFP-MalE-Gal3(1-231) (Fig. 3, panel E), which produced a ~96 kD polypeptide (Fig. 2, lane 6).

Figure 2. Analysis of the fusion proteins expressed from the GFP reporter vector by Western blotting.

Lane 1: GFP; lane 2: GFP-Gal3(1-263); lane 3: GFP-MalE; lane 4: GFP-MalE-Gal3(1-263); lane 5: GFP-MalE-Gal3(1-252); lane 6: GFP-MalE-Gal3(1-231). Mouse 3T3 fibroblasts were transfected with the various constructs. Extracts (~50 µg total protein) derived from each of the transfected cultures were subjected to SDS-PAGE and immunoblotting with antibodies directed against GFP.

Figure 2

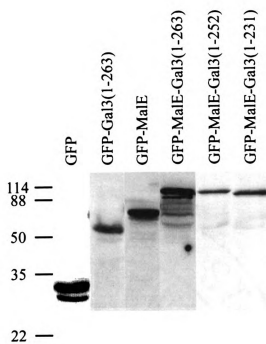
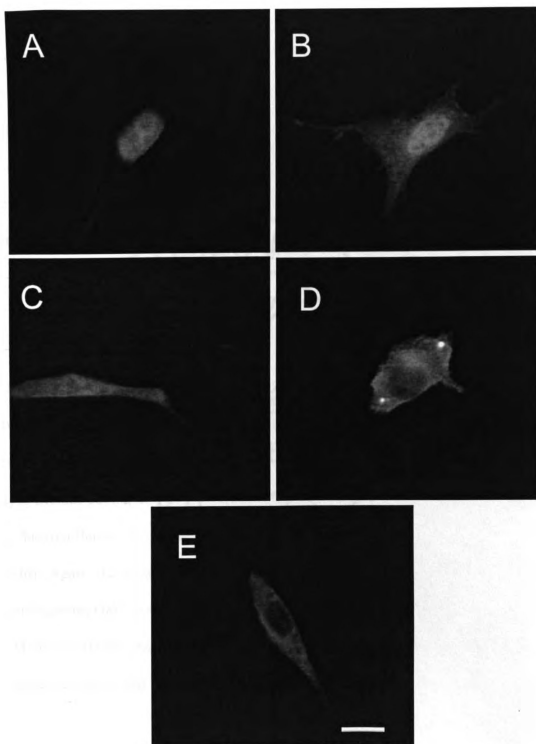


Figure 3. Representative fluorescence micrographs illustrating the N, N>C, N~C, N<C, and C labeling patterns.

(A) cells exhibiting the N pattern (exclusively nuclear fluorescence); (B) cells exhibiting the N>C pattern (intensely nuclear fluorescence over a cytoplasmic background); (C) cells exhibiting the N~C pattern (approximately equal fluorescence distribution between the nucleus and cytoplasm); (D) cells exhibiting the N<C pattern (weaker nuclear fluorescence than the cytoplasm); (E) cells exhibiting the C pattern (exclusively cytoplasmic fluorescence). Bar = 10 μ m.

Figure 3



Comparison of the subcellular distribution of GFP-MalE-Gal3(1-263) and endogenous galectin-3

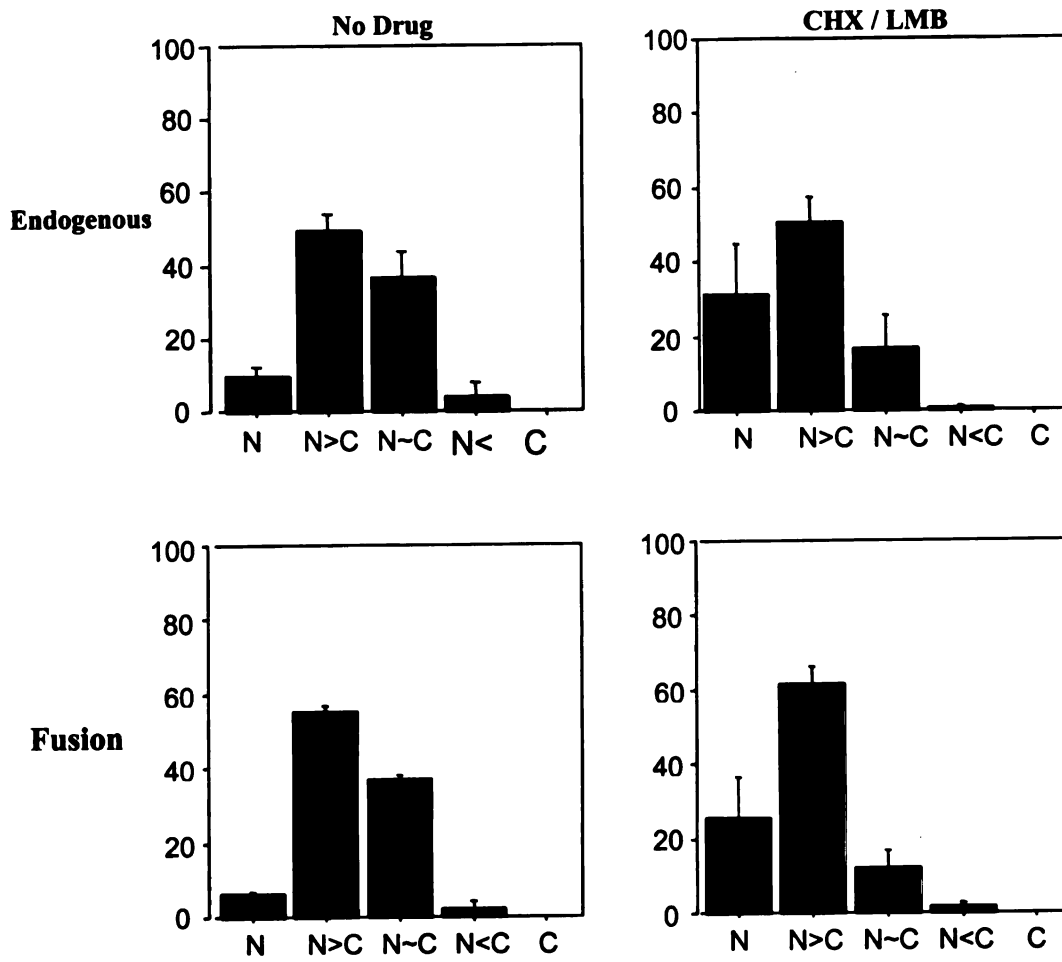
To ascertain that the subcellular distribution of the GFP-MalE-Gal3(1-263) reporter construct reflected that of the endogenous protein, we compared the GFP fluorescence pattern against the localization of Gal3 in 3T3 fibroblasts as revealed by indirect immunofluorescence using a rat monoclonal antibody directed against the protein. This comparison was carried out on a quantitative basis by scoring each cell in one of five categories: N, N>C, N~C, N<C, and C. The histograms of the fluorescence patterns for GFP-MalE-Gal3(1-263) and endogenous Gal3 were very similar, with ~10% N, ~50% N>C, ~40% N~C, and <5% N<C (Figure 4).

In previous studies, we had documented that treatment of mouse and human fibroblasts with LMB resulted in the accumulation of Gal3 in the nucleus, as revealed by an accentuation of the nuclear staining pattern (15, 20). LMB inhibits the interaction between the CRM1 export receptor and a leucine-rich NES on the cargo (21). In the present experiments, we included CHX (10 µg/ml) during the incubation with LMB (10 nM) to exclude complications that might be introduced by newly synthesized proteins (e.g. due to different rates of synthesis of the endogenous protein versus the fusion protein). Again, the histograms of the fluorescence patterns for GFP-MalE-Gal3(1-263) and endogenous Gal3 were very similar, with ~30% N, ~60% N>C, and ~15% N~C (Fig. 4). More importantly, the data clearly showed that treatment with LMB shifted the fluorescence distribution "to the left," in favor of the nucleus.

Figure 4. Comparison of the histograms of fluorescence patterns obtained with GFP-MalE-Gal3(1-263) with endogenous Gal3 in 3T3 fibroblasts.

The localization of GFP-MalE-Gal3(1-263) (Fusion) was monitored by GFP fluorescence; the localization of endogenous Gal3 (Endo) was determined by indirect immunofluorescence using a rat monoclonal antibody against Gal3, the anti-Mac2 antibody. The fluorescence distributions were compared both in the presence and absence of a combination of the drugs LMB (5.4 ng/ml) and CHX (10 µg/ml). Data were collected from three independent experiments in which at least 100 fluorescent cells were scored for the localization of GFP fluorescence. The average percentages of cells showing each localization was plotted. Error bars represent the standard deviation of the data within each localization category.

Figure 4



Effects of truncation from the carboxyl terminus on the localization of the GFP-MalE-Gal3 fusion protein

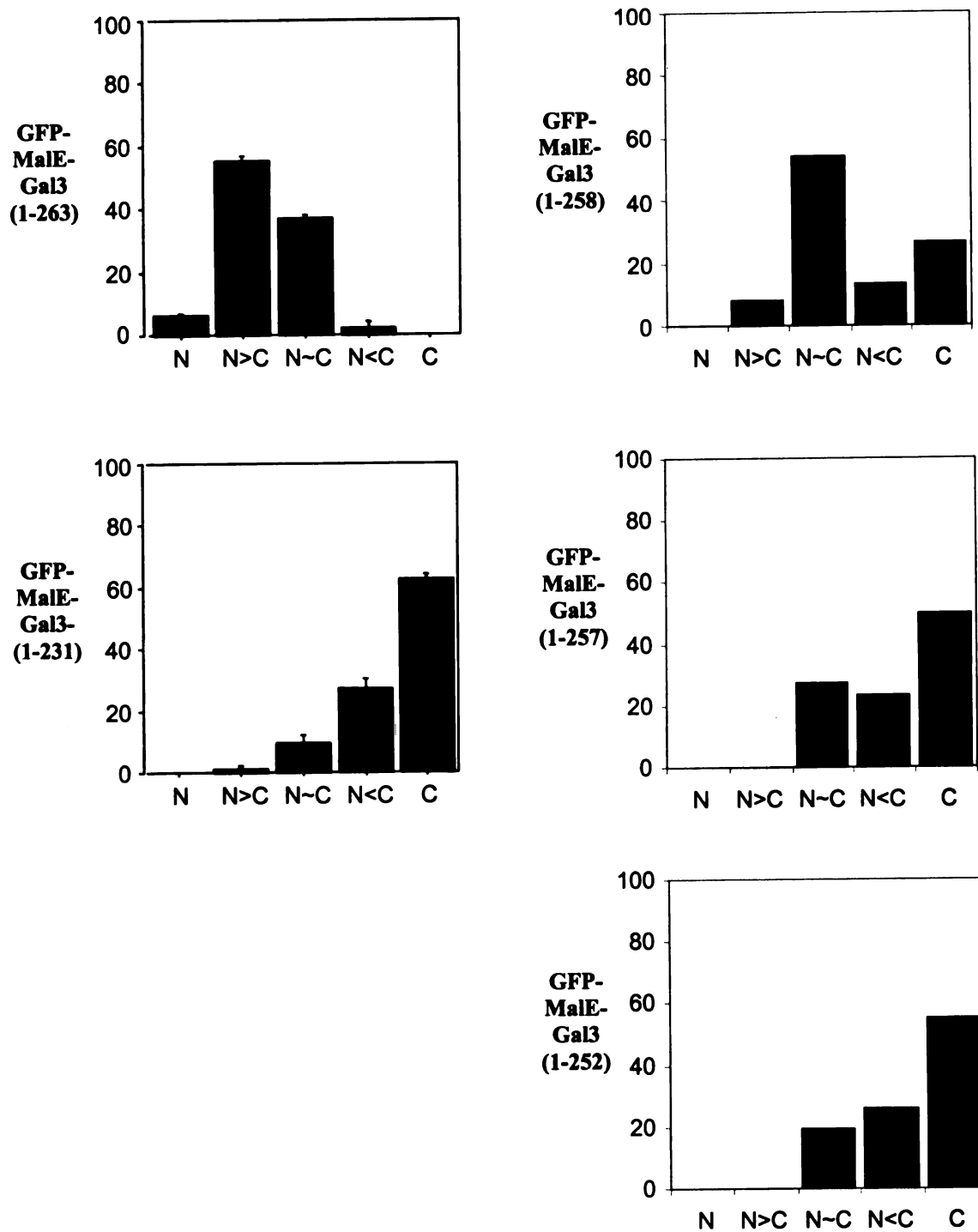
Transfection with the construct expressing the full-length Gal3 polypeptide, GFP-MalE-Gal3(1-263), resulted in nuclear localization of the fusion protein (Fig. 3, panel A). These qualitative observations of fluorescence patterns were confirmed by a more quantitative analysis in terms of the histogram distribution (Fig. 5). Approximately 10% of the transfected cells showed an exclusively nuclear localization while ~55% of the cells showed fluorescence intensely nuclear over a cytoplasmic background (N>C). The remaining 40% of the transfected cells exhibited fluorescence in both the nucleus and cytoplasm (N~C). Using site-directed mutagenesis to insert stop codons, we found that deletion of the last four amino acids of the Gal3 polypeptide did not alter the localization; for example, the histogram of fluorescence patterns for GFP-MalE-Gal3(1-259) was very similar to that of the parent protein, GFP-MalE-Gal3(1-263) (data not shown).

Truncation of residue 259 (i.e. GFP-MalE-Gal3(1-258)), however, resulted in a shift of the histogram "to the right," representing loss of nuclear localization in favor of the cytoplasm (Fig. 5). This shift became more pronounced as the analysis is carried out sequentially from residue 259 through residue 253. In GFP-MalE-Gal3(1-252) (~100 kD; Fig. 2, lane 5) transfected cells, ~50% of the cells exhibited an exclusively cytoplasmic (C) localization while ~20% of the cells showed the N~C fluorescence pattern.

Figure 5. Comparison of the histograms of fluorescence distribution for GFP-MalE-Gal3(1-263) and mutants that are truncated from the carboxyl terminus.

For GFP-MalE-Gal3(1-263) and GFP-MalE-Gal3(1-231), the data represent the averages of triplicate determinations with standard deviation.

Figure 5



When the truncation is made at residue 232 (GFP-MalE-Gal3(1-231, ~96 kD) (Fig. 2, lane 6), more than 60% of the transfected cells had an exclusively cytoplasmic localization, as evident by examining either the micrograph (Fig. 3, panel E) or the histogram (Fig. 5). These results strongly suggest that the carboxyl terminal portion of the Gal3 polypeptide, upstream of residue 259, was important for nuclear localization.

Effects of truncation of the amino-terminal domain

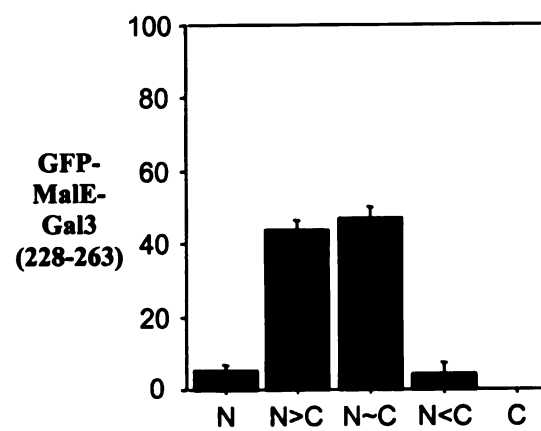
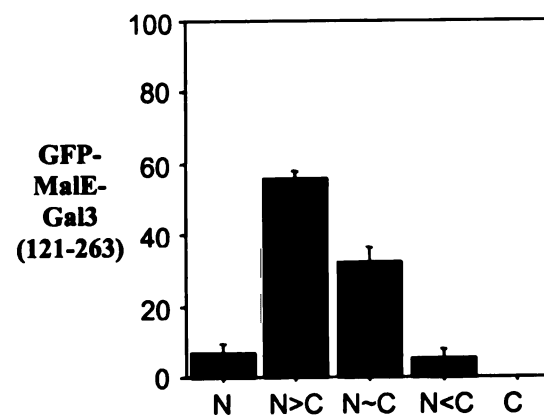
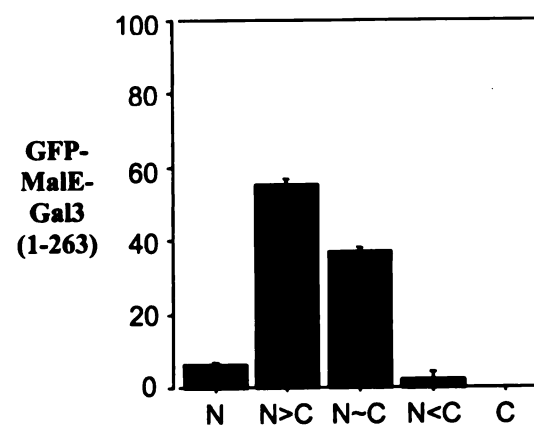
Using site-directed mutagenesis, EcoRI sites were inserted at various positions in the Gal3 polypeptide. Mutants with truncation from the amino terminus of various lengths were generated after restriction enzyme digestion and religation, and were then analyzed as GFP-MalE-Gal3 fusion proteins. The histogram of fluorescence patterns for GFP-MalE-Gal3(121-263) was essentially the same as that of the full-length protein, GFP-MalE-Gal3(1-263) (Fig. 6). Similar results were obtained with GFP-MalE-Gal3(74-263) and GFP-MalE-Gal3(131-263) (data not shown). Together, the data indicated that the amino-terminal domain of the Gal3 polypeptide is dispensable with respect to nuclear localization.

Of particular significance is the mutant GFP-MalE-Gal3(228-263), which showed that in practically all of the cells transfected with this construct, the fusion protein was able to localize to the nucleus. The interpretation of this result may be complicated by the fact that in transfections with GFP-MalE (lacking Gal3 sequence) we observed nuclear localization of the fluorescent reporter in a majority of the cells. Thus,

Figure 6. Comparison of the histograms of fluorescence distributions for GFP-MalE-Gal3(1-263) and mutants that are truncated from the amino terminus.

The data represent the averages of triplicate determinations with standard deviation.

Figure 6



the nuclear localization of GFP-MalE-Gal3(228-263) could simply reflect the behavior of GFP-MalE. Two lines evidence argue against this notion. First, preliminary evidence indicates that GFP-MalE-Gal3(228-252) yielded a cytoplasmic localization pattern, consistent with the conclusion that amino acids upstream of residue 259 was important for nuclear localization. Second, we also engineered the construct GFP-MalE-Gal3(1-159; 226-263) and preliminary evidence indicates that this was also localized to the nucleus. These results, coupled with the fact that over 90% of the cells expressing the GFP-MalE-Gal3(1-231) construct showed cytoplasmic localization, suggests that the amino acid sequence spanning the carboxyl- terminal 30 residues of the Gal3 polypeptide contains information which allowed the protein to localize to the nuclear compartment. This sequence is displayed in Figure 7A for the mouse protein as well as orthologs in other species.

DISCUSSION

The murine Gal3 polypeptide contains 263 amino acids (22). Measurements of the solution molecular weight of the purified protein by hydrodynamic (23) or by thermodynamic methods (24) yielded a value of ~30,000, suggesting that the polypeptide exists predominantly as a monomer. Although this is of a size that could be accommodated by the aqueous channel of the nuclear pore complex (exclusion limit of 40-60 kD; for reviews, see 25, 26), two lines of evidence argue against the notion that passive diffusion could account for the observed nuclear localization of Gal3.

Figure 7. (A) The amino acid sequence of the carboxyl-terminal 40 residues of the Gal3 polypeptide.

The murine polypeptide, subjected to mutagenesis in the present study, is shown at the top. The sequences of orthologs in other species are also shown for comparison. Residue numbers corresponding to the positions in the polypeptides of the respective species are shown on the left.

(B) Ribbon diagram showing the three-dimensional structure of the polypeptide backbone of the CRD of Gal3.

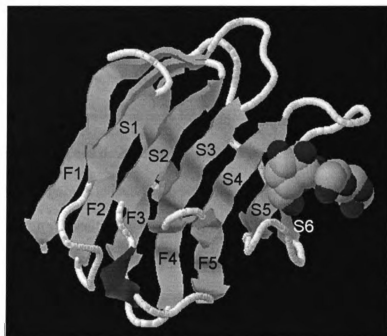
The thick ribbons highlight the strands of two β -pleated sheets that form the core of the structure. One β -sheet contains five strands (F1-F5); the other β -sheet contains six strands (S1-S6). The dark, twisted arrow at the lower left highlights the position of the solvent exposed helix (His 236 through Ser 245) that connects the two β -sheets. The balls at the right represent the position of the bound carbohydrate ligand.

Figure 7

A

MOUSE	224	VAV	ND	AH	LL	QYN	HR	MKN	LRE	IS	QL	GIS	GD	IT	LT	SA	NH	AM	I		
HAMSTER	206	VAV	ND	AH	LL	QYN	HR	MKN	LRE	IN	CM	ET	IS	GD	IT	LT	SA	AP	TM	I	
HUMAN	202	VAV	ND	AH	LL	QYN	HR	VKK	LNE	IR	KL	GIS	GD	IT	DL	LT	SA	NT	YM	I	
RAT	223	VAV	ND	AH	LL	QYN	HR	MKN	LRE	IS	QL	GII	GD	IT	LT	SA	SH	AM	I		
RABBIT	194	VAV	ND	AH	LL	QYN	HR	MKN	LKE	IN	KL	GIS	GD	IT	QL	LT	SA	SH	AM	I	
DOG	257	VAV	ND	AH	LL	QYN	HR	MKN	LPE	IS	KL	GIS	GD	IT	DL	LT	SA	SY	AM	I	
CHICKEN	223	VAV	ND	AH	LL	GF	NF	RE	KK	LNG	IT	KL	CI	A	GD	IT	LT	SV	LT	SM	I

B



First, analysis of Gal3 in cell fractions suggests that the protein is associated with high molecular weight complexes inside cells: (a) in ~40S particle when nuclear extracts are fractionated on a sucrose gradient (3); and (b) in a ~670 kD complex when the transported fraction of a nuclear export assay in permeabilized cells is fractionated by gel filtration (15). Second, there are reports in which an exclusively cytoplasmic localization of Gal3 in one cell type can be altered to yield a predominantly nuclear phenotype and vice versa. For example, the protein is cytoplasmic in quiescent cultures of 3T3 fibroblasts but it relocates to the nuclear compartment upon serum stimulation (27). In the LG1 strain of human diploid fibroblasts, Gal3 can be found in both the nucleus and the cytoplasm of young, proliferating cells; in contrast, the protein was predominantly cytoplasmic in senescent LG1 cells that have lost replicative competence through *in vitro* culture (20). In heterodikaryons derived from fusion of young and senescent LG1 cells, the predominant phenotype was galectin-3 in both nuclei, suggesting that the senescent cells might lack a factor(s) specifically required for Gal3 nuclear import. Conversely, Gal3 has been reported to be concentrated in the nuclei of differentiated colonic epithelial cells. The progression from normal mucosa to adenoma to carcinoma is characterized by a distinct absence of Gal3 in the nuclei of adenoma and carcinoma cells (28). Thus, the finding that Gal3 can show a uniquely nuclear localization under one set of conditions and an almost exclusively cytoplasmic localization under other conditions suggests specific and regulated mechanisms of balance between cytoplasmic anchorage, nuclear import, nuclear retention, and nuclear export.

The results of the present study indicate that the carboxyl terminal region of the murine Gal3 polypeptide is important for nuclear localization, as assayed using a GFP-

MalE-Gal3 reporter system. The critical residues appear to lie, at the least, within a region spanning His 230 and Ala 258. Mutants truncated from the amino-terminal end retained nuclear localization activity; in fact, GFP-MalE-Gal3(228-263) bearing the carboxyl-terminal 35 amino acids could still localize to the nucleus. Truncation from the carboxyl-terminal end, however, resulted in the loss of nuclear localization activity. Although truncation at residue 258 resulted in a shift from the nuclear to the cytoplasmic localization, the full effect is seen by truncation at residue 231, in which more than 60% of the cells exhibited an exclusively cytoplasmic localization.

Our results need to be compared with those reported by two other laboratories that have attempted to define the region of the Gal3 polypeptide important for nuclear localization. Gong *et al.* (29) reported that deletion of the amino-terminal 11 amino acids of human Gal3 resulted in a mutant exhibiting cytoplasmic (and no nuclear) localization in BT-549, a human breast carcinoma cell line. Moreover, when the sequence corresponding to the first 11 amino acids was fused to GFP, a predominantly nuclear distribution of the reporter was observed. On the basis of these and other data, the authors concluded that the 11 residues at the amino terminus are involved in Gal3 translocation to the nucleus (29). The nuclear localization of our mutants truncated from the amino-terminal end (e.g. GFP-MalE-Gal3 (121-263)) and the cytoplasmic localization of our mutants truncated from the carboxyl-terminal end (e.g. GFP-MalE-Gal3(1-231)) are clearly inconsistent with the results and conclusion of Gong *et al.* (29).

In contrast to the results of Gong *et al.* (29), Gaudin *et al.* (30) transfected Cos-7 (SV40 virus-transformed monkey kidney) cells and Rb-1 (rabbit smooth muscle) cells with cDNAs encoding mutants of hamster Gal3 containing amino-terminal or internal

deletions and showed that nuclear localization does not require the first 103 amino acid residues. Further deletion of residues 104-110 drastically reduced nuclear localization but the specific sequences between residues 104-110 were not obligatory (these residues could be substituted by unrelated sequences). Gaudin *et al.* (30) concluded that nuclear localization of Gal3 does not require determinants in the amino-terminal domain; rather, the carbohydrate-binding carboxyl-terminal domain was sufficient to allow nuclear localization. In this respect, our present results are at least consistent with their results and conclusions. The requirement noted by Gaudin *et al.* (30) that the carboxyl-terminal domain be extended by additional (and unrelated) peptide sequences could, in effect, be satisfied in our system by the GFP-MalE portion of the fusion protein.

The three-dimensional structure of the carbohydrate-binding carboxyl terminal domain of Gal3 has been determined by X-ray crystallography (31). Like the carbohydrate recognition domains of other members of the galectin family, the Gal3 structure is composed of two β -pleated sheets associating in a sandwich-like arrangement (see Fig. 7B). One of the β sheets contains five anti-parallel strands while the other sheet contains six anti-parallel strands. An α -helix (highlighted in Fig. 7B) connects the five-stranded sheet with the six-stranded sheet. The stretch of the Gal3 sequence identified in the present study to be important for nuclear localization (230-258) is found in this region of the three-dimensional structure. In particular, His 236 through Ser 245 forms the solvent exposed connector helix between the two β -pleated sheets. Within these ten residues (see Fig. 7A), there are three positively-charged residues (two arginines and one lysine), as well as a histidine residue which could potentially also bear a positive charge.

This appears to be similar to the NLS of the c-myc polypeptide (PAAKRVKLD), in which a nine-residue sequence contains one arginine and two lysines (32).

It should be emphasized that we do not know if the region of Gal3 important for nuclear localization represents a binding site for a nuclear import receptor (importin- β or relative). A direct interaction between Gal3 and a known importin remains to be documented. Once identified, the binding between the particular importin and a candidate NLS peptide (e.g. residues 236-245 of the Gal3 sequence) will also need to be tested. Alternatively, the region of Gal3 important for nuclear localization could simply represent a binding site to another nuclear protein which carries a *bona fide* NLS mediated by a well-characterized importin.

REFERENCES

1. Barondes, S.H., Castronovo, V., Cooper, D.N.W., Cummings, R.D., Drickamer, K., Feizi, T., Gitt, M.A., Hirabayashi, J., Hughes, C., Kasai, K., Leffler, H., Liu, F.-T., Lotan, R., Mercurio, A.M., Monsigny, M., Pillai, S., Poirier, F., Raz, A., Rigby, P.W.J., Rini, J.M., and Wang, J.L. (1994) *Cell* **76**: 597-598.
2. Liu, F.-T., Patterson, R.J., and Wang, J.L. (2002) *Biochim. Biophys. Acta* **1572**: 263-273.
3. Laing, J.G., and Wang, J.L. (1988) *Biochemistry* **27**: 5329-5334.
4. Hubert, M., Wang, S.-Y., Wang, J.L., Seve, A.-P., and Hubert, J. (1995) *Exp. Cell Res.* **220**: 397-406.
5. Dagher, S.F., Wang, J.L., and Patterson, R.J. (1995) *Proc. Natl. Acad. Sci., U.S.A.* **92**: 1213-1217.
6. Vyakarnam, A., Dagher, S.F., Wang, J.L., and Patterson, R.J. (1997) *Mol. Cell. Biol.* **17**: 4730-4737.
7. Park, J.W., Voss, P.G., Grabski, S., Wang, J.L., and Patterson, R.J. (2001) *Nucleic Acids Res.* **27**: 3595-3602.
8. Meister, G., Eggert, C., and Fischer, U. (2002) *Trends Cell Biol.* **12**: 472-478.
9. Fisher, U., Liu, Q., and Dreyfuss, G. (1997) *Cell* **90**: 1023-1029.
10. Liu, Q., and Dreyfuss, G. (1996) *EMBO J.* **15**: 3555-3565.
11. Pellizzoni, L., Kataoka, N., Charroux, B., and Dreyfuss, G. (1998) *Cell* **95**: 615-624.
12. Davidson, P.J., Davis, M.J., Patterson, R.J., Ripoche, M.-A., Poirier, F., and Wang, J.L. (2002) *Glycobiology* **12**: 329-337.
13. Agrwal, N., Wang, J.L., and Voss, P.G. (1989) *J. Biol. Chem.* **264**: 17236-17242.
14. Steck, P.A., Voss, P.G., and Wang, J.L. (1979) *J. Cell Biol.* **83**: 562-575.
15. Tsay, Y.-G., Lin, N.Y., Voss, P.G., Patterson, R.J., and Wang, J.L. (1999) *Exp. Cell Res.* **252**: 250-261.
16. Laemmli, U.K. (1970) *Nature* **227**: 680-685.
17. Agrwal, N., Sun, Q., Wang, S.-Y., and Wang, J.L. (1993) *J. Biol. Chem.* **268**: 14932-14939.

18. Sherman, M.P., de Noronha, C.M.C., Heusch, M.I., Greene, S., and Greene, W.C. (2001) *J. Virol.* **75**: 1522-1532.
19. Alefantis, T., Barmak, K., Harhaj, E.W., Grant, C., and Wigdahl, B. (2003) *J. Biol. Chem.* **278**: 21814-21822.
20. Openo, K.P., Kadrofske, M.M., Patterson, R.J., and Wang, J.L. (2000) *Exp. Cell Res.* **255**: 278-290.
21. Ossareh-Nazari, B., Bachelier, F., and Dargemont, C. (1997) *Science* **278**: 141-144.
22. Swiss-Prot: P16110 (<http://us.expasy.org/cgi-bin/niceprot.pl?P16110>)
23. Roff, C.F. and Wang, J.L. (1983) *J. Biol. Chem.* **258**: 10657-10663.
24. Morris, S., Ahmad, N., Andre, S., Kaltner, H., Gabius, H.-J., Brenowitz, M., Brewer, C.F. (2004) *Glycobiology* **14**: 293-300.
25. Nigg, E.A. (1997) *Nature* **386**: 779-787.
26. Gorlich, D. and Kutay, U. (1999) *Ann. Rev. Cell Dev. Biol.* **15**: 607-660.
27. Moutsatsos, I.K., Wade, M., Schindler, M., and Wang, J.L. (1987) *Proc. Natl. Acad. Sci. U.S.A.* **84**: 6452-6456.
28. Lotz, M.M., Andrews, C.W., Korzeliuss, C.A., Lee, E.C., Steele, G.D., Clarke, A. and Mercurio, A.M. (1993) *Proc. Natl. Acad. Sci. U.S.A.* **90**: 3466-3470.
29. Gong, H.C., Honjo, Y., Nangia-Makker, P., Hogan, V., Mazurak, N., Bresalier, R.S., and Raz, A. (1999) *Cancer Res.* **59**: 6239-6245.
30. Gaudin, J.-C., Mehul, B., and Hughes, R.C. (2000) *Biol. Cell* **92**: 49-58.
31. Seetharaman, J., Kanigsberg, A., Slaaby, R., Leffler, H., Barondes, S.H., and Rini, J.M. (1998) *J. Biol. Chem.* **273**: 13047-13052.
32. Dang, C.V. and Lee, W.H. (1988) *Mol. Cell. Biol.* **8**: 4048-4054.

Chapter 4

Transport of Galectin-3 between the Nucleus and Cytoplasm II. Identification of the Signal for Nuclear Export

**Transport of Galectin-3 between the Nucleus and Cytoplasm.
II. Identification of the Signal for Nuclear Export***

Su-Yin Li[#], Peter J. Davidson[§], Beric R. Henderson[⊕],
Ronald J. Patterson^ψ, John L. Wang[#], and Eric J. Arnoys^{Δ*}

Departments of Biochemistry[#] and Microbiology^ψ, the Cell and Molecular
Biology Program[§], Michigan State University, East Lansing, MI 48824, USA

Department of Chemistry and Biochemistry^Δ, Calvin College
Grand Rapids, MI 49546, USA

Westmead Institute for Cancer Research[⊕], Westmead Hospital,
University of Sydney, Westmead, New South Wales 2145, Australia

Dr. Beric Henderson engineered the original expression vector for testing nuclear export signals, as described in Figure 1. He provided this vector for our study. Su-Yin Li, a student in the M.S. program, generated the expression vectors containing the nuclear export signal of galectin-3, as well as the site-directed mutants. She also carried out most of the transfection experiments in testing the galectin-3 nuclear export signal (Figures 4 and 6). Peter Davidson was responsible for Figures 2, 3, and 5, as well as the analysis of the data shown in Figures 4 and 6. Drs Ron Patterson, John Wang, and Eric Arnoys are faculty members in whose laboratories the reported experiments were performed.

ABSTRACT

Galectin-3 (Gal3), a factor involved in the splicing of pre-mRNA, shuttles between the nucleus and the cytoplasm. Previous studies had shown that incubation of fibroblasts with leptomycin B resulted in the accumulation of Gal3 in the nucleus, suggesting that the export of Gal3 from the nucleus may be mediated by the CRM1 receptor. A candidate nuclear export signal (NES), containing the requisite spacing of leucine/isoleucine residues fitting the consensus sequence recognized by the CRM1 exportin, can be found between residues 240 and 255 of the murine Gal3 sequence. This sequence was engineered into the pRev(1.4)-GFP (Green Fluorescent Protein) reporter system, in which candidate sequences can be tested for nuclear export activity in terms of counteracting the nuclear localization signal present in the Rev(1.4) protein. We found that the sequence spanning residues 240-255 of the Gal3 polypeptide did exhibit nuclear export activity when tested in this system. The previously characterized NES sequences of PKI (inhibitor of cAMP-dependent protein kinase) and I κ B- α were also tested in the pRev(1.4)-GFP system as examples of "strong" and "weak" nuclear export activities, respectively. Compared in these terms, the NES of Gal3 was found to be "weak." Nevertheless, the nuclear export of Rev(1.4)-Gal3 NES-GFP fusion protein was sensitive to inhibition by leptomycin B, accumulating in the nucleus of drug-treated cells. Site-directed mutagenesis of Leu247 and Ile249 in the Gal3 NES decreased nuclear export activity, consistent with the notion that these two positions correspond to the critical residues identified on the NES of PKI. These results indicate that residues 240-255 of the Gal3 polypeptide contains a leucine-rich NES which overlaps with the region (residues 228-258) identified to be important for nuclear localization.

INTRODUCTION

Galectin-3 is a pre-mRNA splicing factor found in both the cytoplasm and in the nucleus of cells (1, 2). The protein shuttles between the two subcellular compartments (3). Using digitonin-permeabilized mouse 3T3 fibroblasts, we had previously documented that Gal3 is selectively exported from the nucleus (4). This export was temperature dependent and could be blocked by the addition of wheat germ agglutinin, which binds to the nuclear pore protein p62. In addition, we also showed that incubation of mouse and human fibroblasts with leptomycin B (LMB) resulted in the accumulation of Gal3 in the nuclei of the treated cells (4, 5). LMB binds to and inhibits the activity of the nuclear export receptor, CRM1, which recognizes a leucine-rich nuclear export signal (NES) on the cargo (6, 7). These results suggest that Gal3 is exported through the nuclear pore complex by a receptor-mediated pathway involving CRM1. Thus, the nuclear versus cytoplasmic distribution of the protein must represent some balance between nuclear import versus export as well as mechanism(s) of retention in either one of the compartments, cytoplasmic anchorage or binding to a nuclear component.

In this chapter we present evidence for a leucine-rich NES at the COOH-terminal portion of the protein.

EXPERIMENTAL PROCEDURES

Site-directed mutagenesis of the putative NES sequence in the GFP-MalE-Gal3 fusion protein

The construction of the vector for expression of the fusion protein GFP-MalE-Gal3 was described in Chapter 3. To generate the L247A and I249A mutant of GFP-

MalE-Gal3, site-directed mutagenesis was carried out with the QuikChange Site-Directed Mutagenesis Kit (Stratagene, La Jolla, CA), using the vector for GFP-MalE-Gal3 as template and primers: 5'-CGGGAAATCAGCCAAGCGGGGGCCAGTGGTGACATA ACC-3'; 5'-GGTTATGTCACCACTGGCCCCCGCTTGGCTGATTTCCTCG-3'.

The pRev(1.4)-GFP vector and variants

The pRev(1.4)-GFP vector (Fig. 1A) and its application for testing potential NES sequences were developed by Henderson and Eleftheriou (8). Two previously identified NES sequences were also used in our study as controls: (a) the NES of the inhibitor of cAMP-dependent protein kinase (PKI) was characterized as a strong NES (Fig. 1C, line 3); and (b) the NES of I κ B- α represented weak NES activity (Fig. 1C, line 4). Each of these sequences was cloned as short fragments between the BamHI and the AgeI sites of pRev(1.4)-GFP, sandwiched between the Rev and the GFP coding sequences.

The vector pRev(1.4)-GFP containing the putative NES sequence of Gal3 (residues 240-255) (Fig. 1C, line 5) was derived from the pRev(1.4)-GFP vector containing the NES of PKI by site-directed mutagenesis in five steps, each of which changed multiple amino acids. Finally, two mutants of the Gal3 NES, designated Gal3 NES (I244A; L247A) and Gal3 NES (L247A; I249A) were derived from the wild-type Gal3 NES in the pRev(1.4)-GFP vector by site-directed mutagenesis (Fig. 1C, lines 6 and 7). For Gal3 NES (I244A, L247A), the forward and reverse primers were, respectively: 5'-CCAAACCTTCGAGAGGCATCTCAGGCAGGTATCAGTGGG-3' and 5'-CCCCTGATACCTGCCTGAGATGCCTCTCGAAGGTTTGG-3'.

Figure 1. The Rev(1.4)-GFP vector.

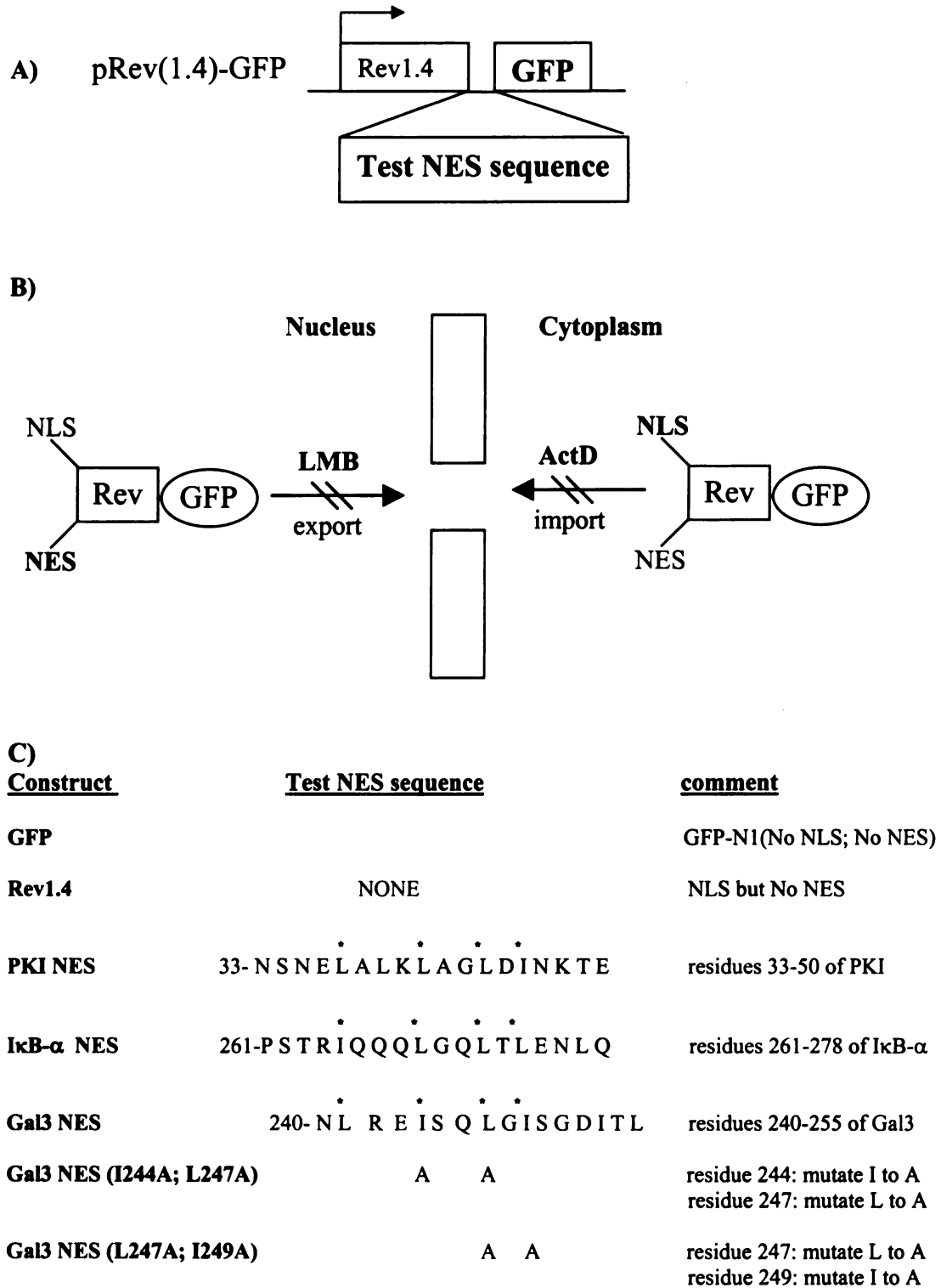
(A) Schematic diagram of the pRev(1.4)-GFP vector for testing potential nuclear export signals (NES). A potential NES is cloned into this vector for the expression of a fusion protein containing Rev(1.4)-test NES-GFP. Normal Rev has both a NLS and a NES; the Rev(1.4) variant is NES deficient. The expressed fusion protein uses the NLS of Rev to import the reporter into the nucleus. The activity of the potential NES to export the reporter is measured in terms of the nuclear vs. cytoplasmic distribution of the GFP fluorescence.

(B) Schematic diagram illustrating the basis of the assay to determine the nuclear export activity of a potential NES. The Rev NLS is highlighted by bold letters in the cytoplasm; Rev NLS-mediated import is reduced by treatment of cells with actinomycin D (ActD). The test NES is highlighted by bold letters in the nucleus; nuclear export mediated by leucine-rich NESs is reduced by leptomycin B (LMB).

(C) Summary of the contents of the fusion proteins expressed by various constructs.

The construct designated as GFP is simply the mammalian expression vector for the production of GFP. The construct designated as Rev1.4 expresses a NES-deficient variant of Rev as a fusion protein with GFP. The construct designated as PKI NES expresses the Rev(1.4)-GFP fusion protein containing the specific NES sequence shown, derived from PKI. Similarly, the other constructs express the Rev(1.4)-GFP fusion protein containing the specific test NES sequence shown.

Figure 1



For Gal3 NES (L247A, I249A), the primers were: 5'-CGAGAGATATCTCAGGCAGG TGCCAGTGGGGACATCACAC-3' and 5'-GTGTGATGTCCCCACTGGCACCTGCC TGAGATATCTCTCG-3'. All of these experiments used the QuikChange Site-Directed Mutagenesis Kit of Stratagene.

Cell culture and transfection

The conditions for the culture and transfection of NIH mouse 3T3 fibroblasts are detailed in Chapter 3. In the present experiments, the effects of various drugs on the nuclear versus cytoplasmic distribution of the reporter proteins were tested. At 9 hours post transfection, either actinomycin D (ActD) and cycloheximide (CHX) or leptomycin B (LMB) and CHX were added to the samples. The samples receiving no drugs served as controls. After 5 hours of treatment (14 hours post transfection), the cells were observed by fluorescence microscopy. ActD was purchased from Sigma (St. Louis, MO) and was dissolved in H₂O as a 1 mg/ml stock solution and stored at -20 °C. It was added to cultures at a final concentration of 5 µg/ml. CHX (Boehringer Mannheim, Indianapolis, IN) was dissolved directly in culture medium at a concentration of 200 µg/ml and was added to cultures at a final concentration of 10 µg/ml. LMB was purchased from LC Laboratories (Woburn, MA) as a 5.4 µg/ml stock solution in ethanol and was stored at -20 °C. It was diluted in culture medium and then added to cultures at a final concentration of 5.4 ng/ml (10 nM).

Fluorescence Microscopy

Transfected cells were examined by fluorescence microscopy as described in Chapter 3, using a Meridian Instruments (Okemos, MI) Insight confocal laser scanning microscope. Approximately 100 cells were scored for GFP localization: (a) N, fluorescence exclusively in the nucleus; (b) N>C, fluorescence intensely nuclear over a cytoplasmic background; (c) N~C, fluorescence in both the nucleus and cytoplasm; (d) N<C, less nuclear labeling than the cytoplasm; and (e) C, fluorescence exclusively in the cytoplasm. Representative cells were photographed at low (66X) magnification to show a field containing multiple cells and at high (200X) magnification to show a single cell.

Statistical Analysis

The number of cells scored into each localization category was tabulated from triplicate experiments. Chi-square analyses were carried out using the statistical analysis program StatView, version 5.0.1 (SAS Institute, Inc., Cary, NC 27513 USA). Analyses were performed using the “Contingency Table” function, selecting “Coded summary data” and deselecting “Fisher’s Exact Test”.

SDS-PAGE and immunoblotting

Proteins were resolved on SDS-PAGE (10% acrylamide) as described by Laemmli (9). The procedures for immunoblotting after SDS-PAGE have also been described (4). Polyclonal anti-GFP antibodies were obtained from Clontech (San Jose, CA); anti-MalE antibodies were from New England Biolabs (Beverly, MA); and polyclonal rabbit anti-Gal3 (#32 and #33) have been described previously (10).

RESULTS

An attempt to identify the NES using the GFP-MalE-Gal3 reporter

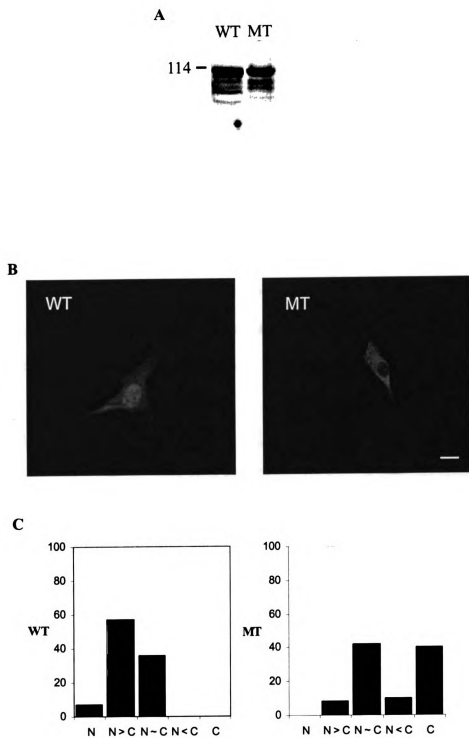
Previous studies had documented that treatment of mouse and human fibroblasts with LMB resulted in the accumulation of Gal3 in the nucleus, as revealed by accentuation of the nuclear staining (4, 5). Moreover, in the accompanying manuscript, we also showed that the GFP-MalE-Gal3(1-263) construct behaved in the same way as endogenous galectin-3 in terms of its response to LMB by accumulating in the nucleus. These results all suggest that LMB inhibited the export of Gal3 from the nucleus and that the latter process was mediated by the CRM1 exportin, which recognizes the leucine-rich NES (6). Indeed, a putative leucine-rich NES, with requisite spacing of leucine/isoleucine residues, can be identified between residues 241 and 249 of the murine Gal3 sequence (see Fig. 1C, line 5). Moreover, this putative NES motif appears to be conserved in the Gal3 homologs of various species.

On this basis, we wanted to make use of the availability of the GFP-MalE-Gal3(1-263) construct by testing the effect of mutating two key residues in the putative NES: leucine 247 to alanine (L247A) and isoleucine 249 to alanine (I249A). These two residues were chosen for mutagenesis because they occupy corresponding positions that had been shown to be critical for the functioning of the leucine-rich NES in PKI (11). If the putative NES was indeed functional in CRM1-mediated nuclear export, we would expect the fusion protein expressed by the mutant construct (GFP-MalE-Gal3(1-263; L247A; I249A) to exhibit a nuclear localization. Transfection of 3T3 cells with the mutant construct resulted, however, in a predominantly cytoplasmic fluorescence pattern (Fig. 2B). Whereas ~60% of the cells transfected with the wild-type construct (GFP- MalE-

Figure 2. Comparison of the properties of GFP-MalE-Gal3 (1-263) and GFP-MalE-Gal3(1-263; L247A; I249A).

(A) Western blots of lysates (~50 µg total protein) derived from cells transfected with the indicated constructs using antibodies directed against GFP. (B) Representative fluorescence micrographs illustrating the GFP localization patterns. Bar = 10 µm. (C) Histograms showing the distribution of the percent of cells with the indicated fluorescence patterns.

Figure 2



Gal3 (1-263)) showed nuclear localization, most of the cells transfected with the mutant showed cytoplasmic fluorescence (Fig. 2C).

DNA sequence analysis confirmed that the mutations had been correctly carried out. Lysates derived from the transfected cultures were subjected to SDS-PAGE and immunoblotting. Antibodies directed against all three parts of the fusion protein (GFP, MalE, and Gal3) yielded the same results. The most prominent band was observed at ~100 kD, corresponding to the expected molecular weights of the wild-type and mutant polypeptides (Fig. 2A). We interpret the results to indicate that this stretch of the Gal3 sequence, containing the putative NES, was also important for a functional NLS and that our mutagenesis on residues 247 and 249 inactivated the nuclear import signal. This notion is consistent with the results of our analysis on the NLS, which implicated the carboxyl-terminal 30 amino acids as necessary for nuclear import (see Chapter 3).

The Rev(1.4)-GFP vector for the analysis of a functional NES

The apparent overlap of the NLS and NES in the Gal3 polypeptide precluded us from using the GFP-MalE-Gal3 reporter construct to define the NES. Mutations intended to inactivate the putative NES also inactivated the NLS and therefore, the properties of the NES cannot be studied in a polypeptide that fails to enter the nucleus. To circumvent these difficulties, we have taken advantage of the pRev(1.4)-GFP vector (8). Although the HIV-1 Rev protein normally contains both a NLS as well as a NES, the Rev(1.4) variant is NES-deficient. Instead, test sequences representing a putative NES can be cloned in frame between the Rev(1.4) segment and the GFP reporter (see schematic in Fig. 1A). The fusion protein expressed by this vector contains the NLS of Rev, whose

nuclear import activity could be decreased by treatment of cells with ActD (12, 13). This allows the activity of very weak NESs to be detected. Thus, the relative activity of different NESs can be distinguished by their ability to shift the fusion protein to the cytoplasm, both in the presence and absence of active nuclear import (i.e., in the absence and presence of ActD, respectively). If the test NES is recognized by the CRM1 exportin, then nuclear export is expected to be sensitive to LMB inhibition (6, 7).

On this basis, ActD and LMB will play critical roles in our dissection of the NLS-based nuclear import and the CRM1-mediated nuclear export of fusion proteins derived from the Rev(1.4)-GFP vector (Fig. 1B). In addition, in order to obviate any complications arising from newly synthesized proteins bearing the GFP reporter, the ActD and LMB experiments were always carried out in the presence of CHX. Therefore, we first tested the effects of the three drugs on the nuclear versus cytoplasmic distribution of endogenous galectin-3 as revealed by staining with anti-galectin-3 antibodies. Neither CHX (10 μ g/ml) nor ActD (5 μ g/ml), alone or in combination, altered the nuclear and cytoplasmic localization of galectin-3 in 3T3 cells. On the other hand, treatment of the same cells with LMB at a concentration as low as 5.4 ng/ml (10 nM) resulted in the accumulation of galectin-3 in the nucleus, as was reported previously (4). This effect of LMB was also observed in the presence of CHX (see Chapter 3) or a combination of CHX and ActD (data not shown).

Cultures of 3T3 cells were transfected with the construct expressing the Rev(1.4)-GFP fusion protein (~40 kD). In the absence of drugs, ~70% of the fluorescent cells exhibited the N labeling pattern (Fig. 3, panel A; Fig. 4). Addition of CHX and ActD shifted the histogram of fluorescence distributions to the right, at the expense of the N

Figure 3. Representative fluorescence micrographs illustrating the GFP localization patterns obtained with various test NES sequences in the pRev(1.4)-GFP vector.

(A) Cells expressing Rev(1.4)-GFP protein in the absence of drugs, ~70% of which yielded the N fluorescence pattern. (B) Cells expressing Rev(1.4)-GFP containing the NES of PKI in the absence of drugs, which yielded the C fluorescence pattern. (C) Cells expressing Rev(1.4)-GFP containing the NES of I κ B- α in the absence of drugs, which yielded the N-C and N~C fluorescence patterns. (D) Cells expressing Rev(1.4)-GFP containing the NES of I κ B- α and incubated in the presence of CHX (10 μ g/ml) and ActD (5 μ g/ml), many of which yielded the C fluorescence pattern. Bar = 50 μ m.

Figure 3

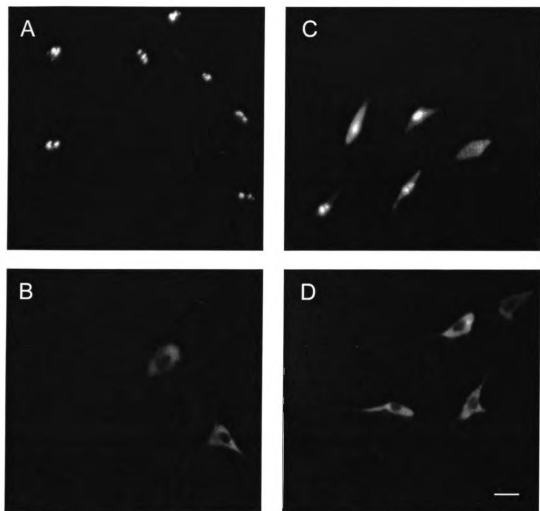
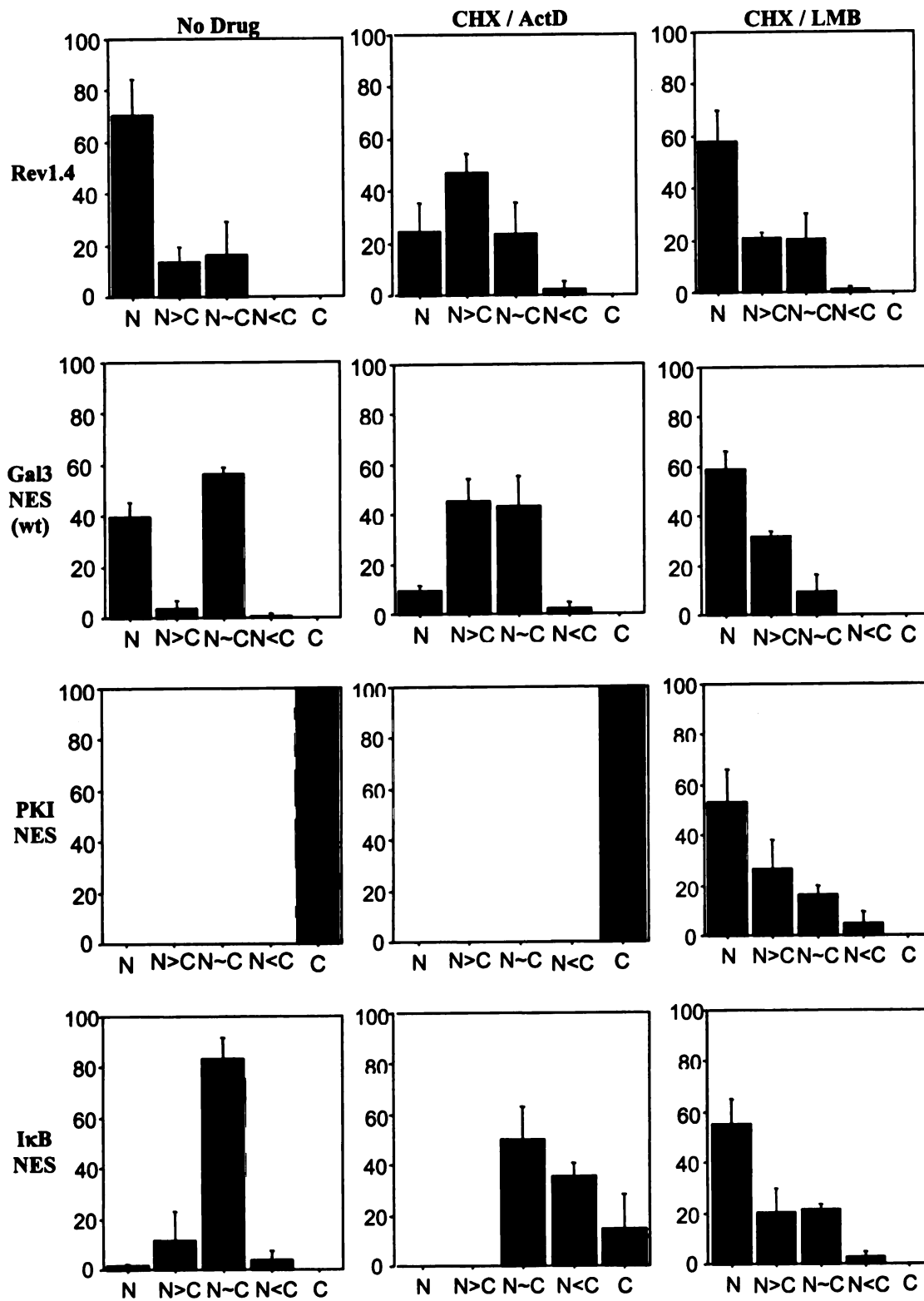


Figure 4. Histograms showing the distribution of the percent of cells with fluorescence patterns N, N>C, N~C, N<C, and C.

The constructs used for transfection are indicated on the left-hand side of each row.

Transfected cells were incubated in the absence of drugs (No Drug), the presence of CHX (10 µg/ml) and ActD (5 µg/ml) (CHX / ActD), or the presence of CHX (10 µg/ml) and LMB (5.4 ng/ml) (CHX / LMB). The data represent the averages of triplicate determinations with standard deviation.

Figure 4



labeling pattern (Fig. 4). This is consistent with the notion that the Rev(1.4)-GFP polypeptide contains a NLS whose activity could be decreased by ActD (Fig. 1B) (12, 13).

We also tested the effect of inserting test NES sequences whose strengths had been previously characterized (8). In 100% of the cells transfected with the Rev(1.4)-GFP vector containing the NES of PKI as the test sequence, the fluorescence labeling pattern was exclusively C, cytoplasmic (Fig. 3, panel B). This was true irrespective whether CHX and ActD were included in the cultures (Fig. 4). Thus, the PKI NES was sufficiently strong to overcome an active NLS (Fig. 1C, line3). The NES of I κ B- α (Fig. 1C, line 4) could neutralize an active NLS, resulting in a majority of the cells exhibiting the N~C labeling pattern in the absence of drugs (Fig. 3 panel C; Fig. 4). In the presence of CHX and ActD, the histogram shifts to the right, with ~50% of the cells showing either a N<C or an exclusively C fluorescence pattern (Fig. 3, panel D; Fig. 4) since the NLS activity has been decreased.

Analysis of the Gal NES in the Rev(1.4)-GFP vector

When the putative NES of Gal3 was inserted into the Rev(1.4)-GFP vector as the test sequence (Fig. 1C, line 5), about 40% of the transfected cells showed the N labeling pattern while ~55% of the cells showed the N~C fluorescence pattern (Fig. 4). This 40%-60% distribution between the N versus N~C labeling patterns was reproducible from experiment to experiment. This distribution should be compared to the corresponding distribution obtained in the transfection with the Rev(1.4)-GFP vector (Fig. 4). There

was a higher percentage of cells showing the N~C labeling pattern with the Gal3 NES than with no NES. Nevertheless, the activity of the Gal3 NES appeared weaker than that of the I κ B- α NES, neutralizing the effect of the active nuclear import in only half of the cells.

When nuclear import was reduced by addition of CHX and ActD, the majority of the cells transfected with Gal3 NES yielded either the N>C or the N~C fluorescence pattern (Fig. 4), and the fraction of cells with exclusively nuclear (N) fluorescence pattern dropped below 10%. Some 2% of the transfected cells showed a shift of the GFP fluorescence to the cytoplasm. Thus, the NES activity of the Gal3 sequence becomes more apparent when nuclear import is reduced.

The effect of LMB on the fluorescence distribution

The Gal3 NES activity, as reported by the pRev(1.4)-GFP vector, should be sensitive to LMB inhibition, as had been documented for endogenous Gal3 of mouse and human fibroblasts (4, 5). Indeed, incubation of transfected cells with CHX and LMB shifts the distribution in favor of the nucleus, with more than 90% of the cells showing an exclusively N or the N>C fluorescence pattern (Fig. 4). Although about 60% of the cells yielded the N labeling pattern, there was nevertheless ~10% that showed N~C (Fig. 4). When 3T3 cells were incubated with CHX and LMB, they accumulated endogenous Gal3 in the nucleus, as reflected by an accentuation of the nuclear staining (4); however, there was always some cytoplasmic fluorescence in these LMB-treated cells. This was also the case when the effect of LMB was studied using the GFP-MalE-Gal3(1-263) reporter (see Chapter 3).

Addition of CHX and LMB also affected the fluorescence of other test NES sequences, shifting the distribution in favor of the exclusively nuclear (N) pattern. In the presence of CHX and LMB, about 50% of the PKI NES showed the N labeling pattern; this should be compared with the exclusively cytoplasmic (C) pattern obtained in the absence of the export inhibitor (Fig. 4). Similarly, CHX and LMB shifted the fluorescence distribution for the I κ B- α test NES sequence, from a predominantly N~C labeling patterns to ~50% exclusively N pattern (Fig. 4). In both cases, the effect of CHX and LMB was partial; not all of the cells showed an exclusively N labeling pattern.

Finally, the Rev(1.4)-GFP construct contains no NES; therefore, it should not be sensitive to LMB. Consistent with this notion, CHX and LMB did not shift the fluorescence distribution of the Rev(1.4)-GFP fusion protein in favor of the N labeling pattern (Fig. 4).

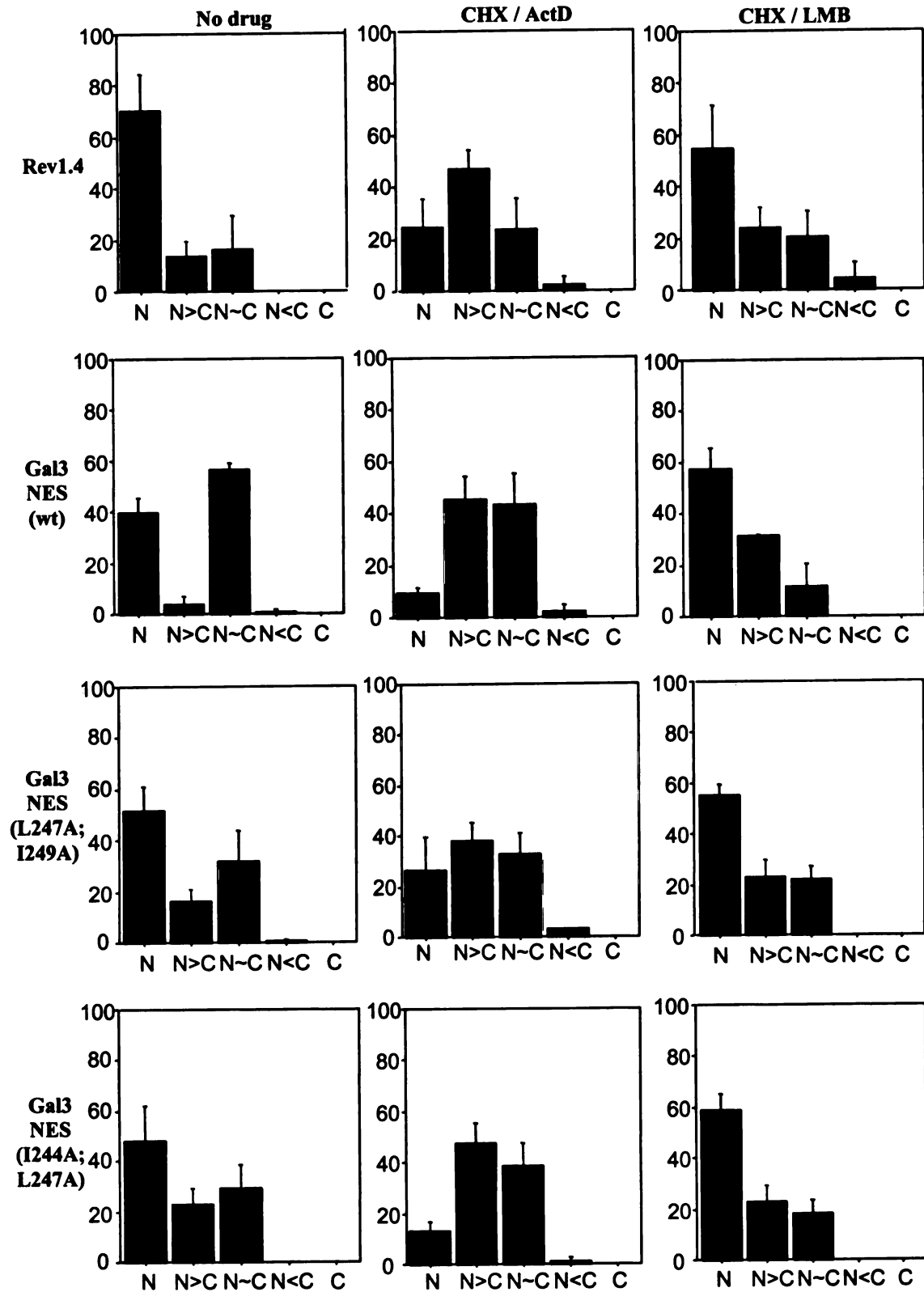
Site-directed mutagenesis of the Gal3 NES

Site-directed mutagenesis was carried out to generate Gal3 NES (L247A; I249A), the two positions corresponding to critical residues in the leucine-rich NES of PKI (11). In parallel, the Gal3 NES (I244A; L247A) mutant was also generated. The fluorescence distributions of Gal3 NES (I244A; L247A) and Gal3 NES (WT) were very similar (Fig. 5), particularly in terms of the effects of CHX and ActD ($p=0.1183$), and CHX and LMB ($p=0.0505$). Addition of CHX and ActD shifted the distribution histogram to the right, at the expense of exclusively nuclear (N) pattern. In the presence of CHX and LMB, the predominant labeling pattern was exclusively nuclear (N).

Figure 5. A comparison of the histogram distributions of the percent of cells with various fluorescence patterns for Gal3 NES (WT), Gal3 NES (I244A; L247A), and Gal3 NES (L247A; I249A).

The constructs used for each transfection are indicated at the left-hand side of each row. Transfected cells were incubated in the absence of drugs (No Drug), the presence of CHX (10 µg/ml) and ActD (5 µg/ml) (CHX / ActD), or the presence of CHX (10 µg/ml) and LMB (5.4 ng/ml) (CHX / LMB). The data represent the averages of triplicate determinations with standard deviation.

Figure 5



The fluorescence distributions shown in Figure 5 were compared using a Chi-squared test. Comparisons were made across all rows (e.g. Gal3 NES (WT) No Drug vs. Gal3 NES (WT) CHX/ActD, $p<0.0001$; Gal3 NES (WT) No Drug vs. Gal3 NES (WT) CHX/LMB), $p<0.0001$; Gal3 NES (WT) CHX/ActD vs. Gal3 NES (WT) CHX/LMB, $p<0.0001$) and across all columns (e.g. Rev(1.4) CHX/ActD vs. Gal3 NES (WT) CHX/ActD, $p<0.0001$; Rev(1.4) CHX/ActD vs. Gal3 NES (L247A;I249A) CHX/ActD, $p=0.0157$; Rev(1.4) CHX/ActD vs. Gal3 NES (I244A;L247A) CHX/ActD, $p<0.0001$; Gal3 NES (WT) CHX/ActD vs. Gal3 NES (L247A;I249A) CHX/ActD, $p<0.0001$; Gal3 NES (WT) CHX/ActD vs. Gal3 NES (I244A;L249A) CHX/ActD, $p=0.1183$; Gal3 NES (L247A;I249A) CHX/ActD vs. Gal3 NES (I244A;L247A) CHX/ActD, $p=0.001$).

The histograms of Gal3 NES (L247; I249A) generally resembled those of Rev(1.4), which does not carry a NES (Fig. 5). In the absence of drugs, the distributions of Gal3 NES (L247A;I249A) and Rev(1.4) were not statistically similar ($p<0.0001$), although both exhibited predominantly N fluorescence distribution, compared to the 40%-60% split between N and N~C labeling pattern observed in Gal3 NES (WT). In contrast, Rev(1.4) and Gal3 NES (L247A;I249A) responded very similarly to treatment with CHX and ActD ($p=0.0157$), as well as CHX and LMB ($p=0.003$). If the leucine-rich NES were disrupted by the L247A and I249A mutations, one would not expect a shift toward more cytoplasmic fluorescence upon reduction of nuclear import by ActD, nor would one expect a shift toward more nuclear fluorescence upon LMB inhibition of CRM1.

DISCUSSION

The nuclear versus cytoplasmic distribution of Gal3 depends on the cell type. In BHK (baby hamster kidney) and MDCK (Madin-Darby canine kidney) cells, the protein is cytoplasmic (14, 15). This cytoplasmic localization was observed both for the endogenous protein as well as for the protein over-expressed in the same cells transfected with a cDNA construct encoding the hamster polypeptide. Over-expression of the same cDNA in mouse 3T3 fibroblasts, however, resulted in a predominantly nuclear localization (15). The distribution of Gal3 between the nuclear and cytoplasmic compartments in a single cell type is also dependent on the proliferative state of the culture under analysis. For example, quiescent cultures of fibroblasts (serum starved or density inhibited) exhibit a predominantly cytoplasmic localization whereas proliferative cultures of the same cells (serum stimulated or low density cultures) show nuclear accumulation (16).

It should be noted that observations of an exclusively cytoplasmic localization of a protein in cells do not necessarily mean that it does not enter the nucleus. It may simply reflect a dynamic situation in which the rate of nuclear export far exceeds nuclear import such that in any steady state observation, the protein is apparently found only in the cytoplasm. For example, the ubiquitin-protein ligase (E3), hRPF1/Nedd4, is a key component of the ubiquitin proteasome pathway. Immunofluorescence analysis showed a cytoplasmic localization, due to the presence of a Rev-like "strong" NES. Incubation of cells in the presence of LMB, however, showed nuclear localization of the same protein and a nuclear speckle protein, hPRTB (human proline-rich transcript, brain-expressed), has been identified as a substrate of hRPF1/Nedd4 in the nucleus (17). Similar

observations regarding LMB-induced conversion from cytoplasmic to nuclear localization have also been demonstrated for the mitogen activated protein kinase interacting kinase Mnk1, as well as several protein translation factors, which shuttle between the nucleus and the cytoplasm (18, 19). Incubation of cells with LMB resulted in shifting Mnk1 from an exclusively cytoplasmic to nuclear localization.

Indeed, the intracellular traffic and distribution of Gal3 are similar to those of Mnk1. Gal3 shuttles between the nucleus and cytoplasm (3) and it has also been documented that incubation of human and mouse fibroblasts with LMB accumulates the protein in the nuclear compartment (4, 5). Thus, there must be specific and regulated balance between the four key parameters that govern nuclear versus cytoplasmic distribution of Gal3: (a) cytoplasmic anchorage; (b) nuclear import; (c) nuclear retention; and (d) nuclear export.

Henderson and Eleftheriou (8) developed the Rev(1.4)-GFP reporter system for testing potential NES sequences. Each putative NES sequence is challenged to overcome the active NLS of the HIV-1 Rev protein such that the fusion protein localizes to the cytoplasm. Such an NES, classified as "strong," was found in proteins such as PKI, the mitogen activated protein kinase kinase (MAPKK), and the c-Abl oncogene (8). Some test NES sequences display "weak" nuclear export activity. These can partially neutralize the NLS of the Rev(1.4)-GFP reporter, resulting in nuclear and cytoplasmic localization of the fusion protein. In the presence of ActD, which decreases the NLS activity in the Rev(1.4)-GFP reporter, the fusion containing a "weak" NES shifts further to the cytoplasm in the majority of the cells. "Very weak" NESs cannot normally overcome the rate of Rev NLS-mediated nuclear import in the absence of ActD but are able to shift the

GFP fluorescence partially to the cytoplasm in 20-50% of the cells when import is decreased by ActD. The tumor suppressor p53 and its hdm2 regulator each has an NES that fits this latter category.

This notion of ranking of NES strengths has received strong support from an entirely independent line of investigation. Using microinjection of defined recombinant export substrates, Heger *et al.* (20) showed that different leucine-rich NESs varied dramatically in determining the kinetics of export in intact cells. Thus, the NES of PKI, classified as a "strong" NES by the pRev(1.4)-GFP assay (8), was found to export its protein very "fast" (5-10 minutes) (20). On the other hand, p53 was found to contain a "very weak" NES by the Rev(1.4)-GFP reporter assay (8) and, indeed, it turned out to be "very slow" (> 10 hours) in the kinetic assay of Heger *et al.* (20). More interestingly, the latter study also reported that co-transfection experiments revealed that proteins containing a "fast" NES inhibited the export and biological activity *in vivo* of proteins harboring a "slower" NES (20). Thus, the export of a protein harboring a leucine-rich NES could also depend what other export substrates are present in competition for transport receptors/cofactors.

By the criteria established in the development of the Rev(1.4)-GFP test vector (8), the NES of Gal3 (residues 240-255 tested) would fall in the "weak" category. This weak NES activity may be important for the nuclear function of the protein. A strong NES might result in futile shuttling of Gal3 between the nucleus and cytoplasm while a weak NES would allow longer residence in the nucleus so that the protein can accumulate to sufficient concentrations to assemble into the SMN complex for pre-mRNA splicing. This notion was first advanced to explain the very low affinity observed between I κ B- α

and the CRM1 exportin (21), which appears to be consistent with our own observation that its NES exhibits "weak" nuclear export activity in the Rev(1.4)-GFP assay system.

In this connection, it may be useful to note that, in the study of Lee and Hannink (21), the addition of LMB only shifted the cytoplasmic localization of I κ B- α to a nuclear and cytoplasmic (N+C) pattern, rather than the exclusively nuclear (N) pattern. This corresponds well with our present results, in which there were appreciable percentages of cells showing the N~C pattern in the presence of LMB for all NESs tested in the Rev(1.4)-GFP fusion constructs (Fig. 4). Similarly, the nuclear accumulation of GFP-I κ B- α (22), GFP-MalE-Gal3(1-263) (see Chapter 3), and endogenous Gal3 (4, 5) was increased by LMB addition but there were still appreciable levels of the respective proteins remaining in the cytoplasm.

We had generated the double mutant, L247A and I249A, in the GFP-MalE-Gal3 system to test whether the putative leucine-rich NES of Gal3 was functional. The exclusively cytoplasmic localization of GFP-MalE-Gal3(1-263; L247A, I249A) indicated, however, that the mutations may have disrupted the NLS. This, in turn, implies that the NLS and NES overlap in this segment of the Gal3 polypeptide. The M9, KNS, and HNS sequences represent other examples of overlapping signals, in which the same stretch of amino acid sequence is capable of mediating both nuclear import and nuclear export (23-25). The M9 signal, a stretch of ~38 amino acids with critical glycine and proline residues, was identified on hnRNP A1 protein, responsible for its shuttling property between the nucleus and the cytoplasm. The 39-residue KNS shuttling signal was identified on hnRNP K protein. For nuclear export, the critical residues include negatively charge acidic amino acids. Finally, Fan and Steitz (25) identified a 33-residue

sequence, designated HNS, responsible for the shuttling activity of HuR, an RNA-binding protein that can stabilize labile mRNAs containing AU-rich elements in their 3'-untranslated regions.

The purpose of exporting Gal3 from the nucleus and, more generally, of shuttling the protein between the nucleus and the cytoplasm remains to be elucidated. In studying nuclear export of Gal3 using a permeabilized cell system, it was found that in the transported fraction, Gal3 is associated with high molecular weight complexes of ~650 kD (4). On the basis of our previous documentation that Gal3 is involved in pre-mRNA splicing (26, 27) and that its detection in the nucleus is sensitive to ribonuclease (28, 29), the possibility is raised that Gal3 is exported from the nucleus in the form of a ribonucleoprotein complex (RNP) along with the processed mRNA. The intriguing question then is whether Gal3 plays a role in determining the stability of the mRNA or in targeting it to ribosomes for translation.

REFERENCES

1. Patterson, R.J., Wang, W., and Wang, J.L. (2004) *Glycoconjugate J.* **19**: 499-506.
2. Wang, J.L., Gray, R.M., Haudek, K.C., and Patterson, R.J. (2004) *Biochim. Biophys. Acta* **1673**: 75-93.
3. Davidson, P.J., Davis, M.J., Patterson, R.J., Ripoché, M.-A., Poirier, F., and Wang, J.L. (2002) *Glycobiology* **12**: 329-337.
4. Tsay, Y.-G., Lin, N.Y., Voss, P.G., Patterson, R.J., and Wang, J.L. (1999) *Exp. Cell Res.* **252**: 250-261.
5. Openo, K.P., Kadrofske, M.M., Patterson, R.J., and Wang, J.L. (2000) *Exp. Cell Res.* **255**: 278-290.
6. Ossareh-Nazari, B., Bachelier, F., and Dargemont, C. (1997) *Science* **278**: 141-144.
7. Kudo, N., Wolff, B., Sekimoto, T., Schreiner, E.P., Yoneda, Y., Yanagida, M., Horinouchi, S., and Yoshida, M. (1998) *Exp. Cell Res.* **242**: 540-547.
8. Henderson, B.R., and Eleftheriou, A. (2000) *Exp. Cell Res.* **256**: 213-224.
9. Laemmli, U.K. (1970) *Nature* **227**: 680-685.
10. Agrwal, N., Sun, Q., Wang, S.-Y., and Wang, J.L. (1993) *J. Biol. Chem.* **268**: 14931-14939.
11. Wen, W., Meinkoth, J.L., Tsien, R.Y., and Taylor, S.S. (1995) *Cell* **82**: 463-473.
12. Meyer, B.E. and Malim, M.H. (1994) *Genes Dev.* **8**: 1538-1547.
13. Kalland, K.H., Szilvay, A.M., Brokstad, K.A., Seatrevik, W., and Haukenes, G. (1994) *Mol. Cell. Biol.* **14**: 7436-7444.
14. Sato, S., Burdett, J., and Hughes, R.C. (1993) *Exp. Cell Res.* **207**: 8-18.
15. Gaudin, J.-C., Mehul, B., and Hughes, R.C. (2000) *Biol. Cell* **92**: 49-58.
16. Moutsatsos, I.K., Wade, M., Schindler, M., and Wang, J.L. (1987) *Proc. Natl. Acad. Sci. U.S.A.* **84**: 6452-6456.
17. Hamilton, M.H., Tcherepanova, I., Huibregtse, J.M., and McDonnell, D.P. (2001) *J. Biol. Chem.* **276**: 26324-26331.

18. Parra-Palau, J.L., Scheper, G.C., Wilson, M.L., and Proud, C.G. (2003) *J. Biol. Chem.* **278**: 44197-44204.
19. Bohnsack, M.T., Regener, K., Schwappach, B., Saffrich, R., Paraskeva, E., Hartmann, E., and Gorlich, D. (2002) *EMBO J.* **21**: 6205-6215.
20. Heger, P., Lohmaier, J., Schneider, G., Schweimer, K., and Stauber, R.H. (2001) *Traffic* **2**: 544-555.
21. Lee, S.-H. and Hannink, M., *J. Biol. Chem.* **276**: 23599-23606 (2001).
22. Huang, T.T., Kudo, N, Yoshida, M., and Miyamoto, S. (2000) *Proc. Natl. Acad. Sci. U.S.A.* **97**: 1914-1019.
23. Michael, W.M., Choi, M., and Dreyfuss, G. (1995) *Cell* **83**: 415-422.
24. Michael, W.M., Eder, P.S., and Dreyfuss, G. (1997) *EMBO J.* **16**: 3587-3598.
25. Fan, X.C. and Steitz, J.A. (1998) *Proc. Natl. Acad. Sci. U.S.A.* **95**: 15293-15298.
26. Dagher, S.F., Wang, J.L., and Patterson, R.J. (1995) *Proc. Natl. Acad. Sci. U.S.A.* **92**: 1213-1217.
27. Park, J.W., Voss, P.G., Grabski, S., Wang, J.L., and Patterson, R.J. (2001) *Nucleic Acids Res.* **27**: 3595-3602.
28. Laing, J.G., and Wang, J.L. (1988) *Biochemistry* **27**: 5329-5334.
29. Hubert, M., Wang, S.-Y., Wang, J.L., Seve, A.-P., and Hubert, J. (1995) *Exp. Cell Res.* **220**: 397-406.

Chapter 5

Concluding Statements

Concluding Statements

Prior to this study, localization of galectin-3 to the nuclear and cytoplasmic compartments had been reported in a variety of cell types. Moreover, the localization of galectin-3 was also known to be sensitive to a variety of cellular conditions or cues, including malignant transformation, serum starvation or stimulation, and proliferative status. Several lines of evidence suggested two key points: (a) galectin-3 might traffic between the nucleus and cytoplasm; and (b) galectin-3 could be exported from the nucleus via a putative leucine-rich nuclear export signal. However, the subcellular trafficking of galectin-3, as well as the mechanism of its movement between the nuclear and cytoplasmic compartments, had not been rigorously examined.

This study focused on three points: (a) documenting the trafficking of galectin-3 between the nuclear and cytoplasmic compartments (nucleocytoplasmic shuttling); (b) identifying the signal(s) required for nuclear import; and (c) testing the activity of the putative leucine-rich nuclear export signal in galectin-3. These projects, and the data derived from them, are descriptive in nature. Subcellular trafficking assays carried out in heterodikaryons revealed that galectin-3 shuttles between the nuclear and cytoplasmic compartments, a region of galectin-3 which is sufficient to specify nuclear import was identified, and the activity of the leucine-rich nuclear export signal was verified.

These descriptive studies now serve as a foundation for more detailed, mechanistic studies of the subcellular trafficking of galectin-3. At the biochemical level, for example, the receptor(s) that mediate nuclear import of galectin-3 can be identified, possibly by using the putative nuclear localization signal to identify interacting partners. In addition, the activity of the leucine-rich export signal in galectin-3 suggests that the

protein might be exported by CRM1, and interaction between the two proteins should be tested for.

The description of galectin-3 trafficking also opens avenues for biophysical investigations of galectin-3 dynamics within different subcellular compartments, as well as between compartments. For example, photobleaching studies could be employed to determine the diffusion constant of galectin-3 in the cytoplasm and nucleoplasm. A difference in mobility might indicate constraint of galectin-3 in one compartment, indicating an interaction (or multiple interactions) that impede mobility. Alternatively, mobility studies between compartments could provide valuable insight into the rate of nuclear import and export of galectin-3. For example, a lower rate of galectin-3 nuclear import than export might indicate a less avid association of galectin-3 with the nuclear import machinery, a larger complex of machinery to be translocated through the nuclear pore, or retention of galectin-3 in the cytoplasm via some other interaction.

MICHIGAN STATE UNIVERSITY LIBRARIES



3 1293 02736 2817